Technical Report Documentation Page

1. Report No.	2. Government Accession No.	3. Recipient's Catalog No.
FHWA/TX-08/0-6100-2		

4. Title and Subtitle	5. Report Date
DEVELOPMENT OF A PRECAST BRIDGE DECK OVERHANG SYSTEM FOR THE ROCK CREEK BRIDGE	Published: December 2008
	6. Performing Organization Code

7. Author(s)	8. Performing Organization Report No.
David Trejo, Monique Hite, John Mander, Thomas Mander, Mathew Henley, Reece Scott, Tyler Ley, and Siddharth Patil	Report 0-6100-2

9. Performing Organization Name and Address	10. Work Unit No. (TRAIS)
Texas Transportation Institute The Texas A&M University System College Station, Texas 77843-3135	11. Contract or Grant No. Project 0-6100

12. Sponsoring Agency Name and Address	13. Type of Report and Period Covered
Texas Department of Transportation Research and Technology Implementation Office P. O. Box 5080 Austin, Texas 78763-5080	Technical Report: October 2007 – June 2008
	14. Sponsoring Agency Code

15. Supplementary Notes

Project performed in cooperation with the Texas Department of Transportation and the Federal Highway Administration.
Project Title: Development of a Precast Bridge Deck Overhang
URL: http://tti.tamu.edu/documents/0-6100-2.pdf

16. Abstract

Precast, prestressed panels are commonly used at interior beams for bridges in Texas. The use of these panels provides ease of construction, sufficient capacity, and good economy for the construction of bridges in Texas. Current practice for the overhang deck sections requires that formwork be constructed. The cost of constructing the bridge overhang is significantly higher than that of the interior sections where precast panels are used. The development of a precast overhang system has the potential to improve economy and safety in bridge construction. This research investigated the overhang and shear capacity of a precast overhang system for potential use in the Rock Creek Bridge in Parker County, Texas. Grout material characteristics for the haunch and constructability issues were also addressed. Results indicate that the capacity of the precast overhang system is sufficient to carry factored AASHTO loads with no or very limited cracking. Results from the shear study indicate that the shear capacity of threaded rods and threaded rods with couplers is lower than the conventional R-bar system. However, modifications of the initial design and layout for the end panels should provide sufficient capacity. A commercial grout has been identified for use in the haunch zone. A recommendation for the haunch form system for use on the bridge is also provided.

17. Key Words	18. Distribution Statement
Precast, Prestressed, Bridge Overhang, Grout, Constructability, Bridge Deck Panel	No restrictions. This document is available to the public through NTIS: National Technical Information Service Springfield, Virginia 22161 http://www.ntis.gov

19. Security Classif.(of this report)	20. Security Classif.(of this page)	21. No. of Pages	22. Price
Unclassified	Unclassified	132	

Form DOT F 1700.7 (8-72) **Reproduction of completed page authorized**

DEVELOPMENT OF A PRECAST BRIDGE DECK OVERHANG SYSTEM FOR THE ROCK CREEK BRIDGE

by

David Trejo
Associate Professor

Monique Hite
Assistant Professor

John Mander
Zachry Professor in Design and Construction Integration I

Thomas J. Mander, Mathew Henley, and Reece Scott
Graduate Student Researchers

Zachry Department of Civil Engineering
Texas A&M University

Tyler Ley
Assistant Professor

Siddharth Patil
Graduate Student Researcher

Department of Civil and Environmental Engineering
Oklahoma State University

Report 0-6100-2
Project 0-6100
Project Title: Development of a Precast Bridge Deck Overhang

Performed in cooperation with the
Texas Department of Transportation
and the
Federal Highway Administration

Published: December 2008

TEXAS TRANSPORTATION INSTITUTE
The Texas A&M University System
College Station, Texas 77843-3135

DISCLAIMER

The contents of this report reflect the views of the authors, who are responsible for the facts and accuracy of the data herein. The contents do not necessarily reflect the official view or policies of the Federal Highway Administration (FHWA) or the Texas Department of Transportation (TxDOT). This report does not constitute a standard, specification, or regulation. The researcher in charge was David Trejo.

The United States Government and the State of Texas do not endorse products or manufacturers. Trade or manufacturers' names appear herein solely because they are considered essential to the objective of this report.

ACKNOWLEDGMENTS

This project was conducted in cooperation with TxDOT and FHWA. The researchers would like to gratefully acknowledge the assistance provided by TxDOT officials, in particular, the following:

- Ricardo Gonzalez
- Ralph Browne
- Graham Bettis
- Loyl Bussell
- German Claros
- Lewis Gamboa
- John Holt
- Manuel Padron
- Jason Tucker
- Alfredo Valles

TABLE OF CONTENTS

Page

LIST OF FIGURES ..... **x**
LIST OF TABLES ..... **xiii**
EXECUTIVE SUMMARY ..... **xv**
CHAPTER 1. INTRODUCTION **1**
CHAPTER 2. BRIDGE OVERHANG SYSTEM **3**
2.1 Double-panel Testing 3
2.1.1 Experimental Plan 5
2.1.2 Specimen Layout and Reinforcing Details 6
2.1.3 Materials 8
2.1.4 Instrumentation for Double-panel Specimens 11
2.1.5 Specimen Loading Plan for Double-panel Specimens 12
2.1.5.1 Specimen 1 12
2.1.5.2 Specimen 2 14
2.1.6 Experimental Results 14
2.1.6.1 As-Received Precast Panels 14
2.1.6.2 AASHTO Overhang Seam Load (Double-panel Specimens) 16
2.1.6.3 AASHTO Overhang Mid-panel (Quarter-point) Loads 17
2.1.6.4 Overhang Failure Loads (Double-panel Specimens) 17
2.1.6.5 Interior Loads 21
2.1.6.6 Additional Measured Strains (Double-panel Specimens) 23
2.1.7 Summary for Double-panel Specimens 25
2.2 Single-Panel Testing 26
2.2.1 Experimental Plan 26
2.2.2 Materials 29
2.2.3 Results and Analysis 30
2.2.4 Discussion 35
2.2.5 Summary of Single-panel Tests 36
2.3 Summary for Overhang Panel Test 36
CHAPTER 3. SHEAR CONNECTIONS **37**
3.1 Experimental Plan 37
3.2 Design of Experiment 39
3.3 Construction Process and Testing Procedure 41
3.4 Materials 46
3.5 General Results 48

3.6 Analysis of Interface shear for the Two Forms of Construction 53
3.6.1 Conventional Construction with R-bars 53
3.6.2 Threaded Rod in Pocket Shear Connectors 54
3.7 Discussion of Sliding Friction Performance 56
3.8 Redesign of the Pocket Requirements Based on Imposed Live Load Plus Impact 57
3.9 Effect of Haunch Height: 2-in. (50 mm) versus 3.5-in. (89 mm) 58
3.10 Discussion on the Problem of Beam Failure 60
3.11 Summary 62
CHAPTER 4. MATERIALS 63
4.1 Haunch Grout Material 63
4.1.1 Experimental Plan 63
4.1.1.1 Mixing Variables 63
4.1.1.2 Design Considerations and Testing 64
4.1.1.3 Flowability 64
4.1.1.4 Segregation 66
4.1.1.5 Bleeding 67
4.1.1.6 Expansion/Subsidence 68
4.1.1.7 Fresh Density 68
4.1.1.8 Strength 68
4.1.2 Materials 69
4.1.2.1 SikaGrout™ 212 High Performance Grout 69
4.1.2.2 Sand 69
4.1.3 Results & Analysis 70
4.1.3.1 Flowability 70
4.1.3.2 Bleeding 72
4.1.3.3 Expansion/Subsidence 73
4.1.3.4 Strength 74
4.1.3.5 Comparisons 75
4.1.4 Constructability and Proposed Special Specifications 76
4.1.4.1 Construction Sequence for Haunch of the Partial Full-Depth Precast Overhang System 77
4.1.4.2 Special Specification 80
4.1.5 Summary of Grout Testing 81
4.2 Haunch Form Materials 82
4.2.1 Experimental Plan 82
4.2.1.1 Lateral Pressure 83
4.2.1.2 Tension 85
4.2.1.3 Tension and Lateral Pressure 86
4.2.2 Materials 87
4.2.3 Results and Analysis 88
4.2.4 Discussion 89
4.2.5 Summary for Haunch Form Materials 90

CHAPTER 5. CONCLUSIONS AND RECOMMENDATIONS 91
REFERENCES 95
APPENDICES 97

LIST OF FIGURES

Figure 2.1 (a) Full-scale bridge construction showing precast overhang (left) and conventional overhang (right); (b) Full-scale experimental set-up showing precast overhang (left) and conventional overhang (right). 4

Figure 2.2 Photograph of the bridge deck in the laboratory. 5

Figure 2.3 Dimensions and steel layout for Specimen 1. 7

Figure 2.4 Various views and layout of Specimen 2. 8

Figure 2.5 Stress-strain curves for steel reinforcement in panels (CIP = reinforcement embedded in cast-in-place concrete; Precast = reinforcement embedded in precast panels). 10

Figure 2.6 (a) Loading positions for Specimen 1. Load cases 1.1, 1.2, 1.4 and 1.5 were loaded up to 60 kips (267 kN). Load case 1.7 was loaded to 120 kips (534 kN) per wheel load. All other load cases were loaded to failure; (b) Loading positions for Specimen 2. Loads 2.1, 2.2, 2.5 and 2.6 were loaded up to 60 kips (267 kN). All other load cases were loaded to failure. 13

Figure 2.7 Photographs showing cracking in between concrete lifts and good consolidation between concrete lifts. 15

Figure 2.8 Reinforcing details of precast overhang panels. 15

Figure 2.9 Force-deformation for the vertical load plate 2 ft. (0.6 m) from overhang edge (AASHTO load) for (a) on seam for Load 1.1 (conventional mid-specimen), Load 1.6 (precast overhang Specimen 1), Load 2.1 (precast overhang Specimen 2) and Load 2.5 (lab-cast overhang Specimen 2); (b) specimen quarter point for Load 1.2 (conventional overhang Specimen 1), Load 1.5 (precast overhang Specimen 1), Load 2.2 (precast overhang Specimen 2) and Load 2.6 (lab-cast overhang Specimen 2). 16

Figure 2.10 Crack mapping of overhang failure loads. Numbers are vertical pauses in kips (1 kip = 4.448 kN) where cracks were marked. 18

Figure 2.11 Observed failure cracks of overhangs. 19

Figure 2.12 Force-deformation for overhang failure; Load 1.3 (Specimen 1 conventional mid-specimen), Load 1.6 (Specimen 1 precast overhang seam load), Load 2.3 (Specimen 2 precast overhang trailing wheel load) and Load 2.7 (Specimen 2 lab-cast seam load). 20

Figure 2.13 Specimen 2: Crack mapping of interior trailing axle load. Numbers are vertical load pauses in kips (1 kip = 4.448 kN) where cracks were marked. 22

Figure 2.14 Interior loading failures. 22

Figure 2.15 *Force-deformation for interior quarter-point and midpoint failure; Load 1.7 precast and Load 1.7 conventional (Specimen 1 trailing axle load), Load 1.8 precast and conventional (Specimen 1 trailing axle load), Load 2.4 (Specimen 2 trailing wheel load single panel loaded), Load 2.8 (Specimen 2 trailing wheel load straddling lab-cast seam). NOTE: Load 1.7 conventional underlies Load 1.7 precast.* 23

Figure 2.16 Shear connector stress for Specimen 1 overhang failure load case 1.6. 24

Figure 2.17 Transverse bar strains in precast overhang. 25

Figure 2.18 Typical layout of a test specimen. 27

Figure 2.19 The intended and actual detail used in Specimens 3 and 4. 28
Figure 2.20 The load points investigated for Specimens 3 and 4. 29
Figure 2.21 Locations of materials used in Specimens 3 and 4. 30
Figure 2.22 Crack pattern for the conventional and precast systems for the midspan loading investigated in Specimen 3. The surface strain locations are shown with two points connected by a line. 31
Figure 2.23 Crack pattern for the conventional and precast systems for the corner loading investigated in Specimen 2. The surface strain location is shown by two points connected by a line. 32
Figure 2.24 The load versus surface strain for the precast and conventional overhangs for the midspan loading of Specimen 3. 32
Figure 2.25 The load versus load point deflection for the precast and conventional overhangs for the midspan loading of Specimen 3. 33
Figure 2.26 The load versus surface strain for the precast and conventional overhangs for the corner loading of Specimen 4. 33
Figure 2.27 The load versus load point deflection for the precast and conventional overhangs for the corner loading of Specimen 4. 34
Figure 3.1 Specimen alias designation key. 38
Figure 3.2 Experimental test setup: (a) Photograph from laboratory floor; (b) Photograph from laboratory balcony; (c) Side elevation. 40
Figure 3.3 Beam cross sectional views of shear connectors and photographs of the T.R. shear connections tested. 41
Figure 3.4 CIP details of beam-to-slab shear connections. 42
Figure 3.5 Reinforcing details for shear test beams. Clockwise from top-left: 2-in. (50 mm) haunch CIP, 2-in. (50 mm) haunch precast, 3.5-in. (89 mm) haunch precast, and 3.5-in. (89 mm) CIP. 43
Figure 3.6 Reinforcement layout of the precast shear deck specimens. 44
Figure 3.7 Photograph of reinforcing of a CIP shear test specimen. 45
Figure 3.8 Photograph of LVDTs and string potentiometers connected to a shear test specimen. 46
Figure 3.9 Stress-strain curve from tensile test of one high-strength threaded rod (ASTM A193 B7). 47
Figure 3.10 Lateral force versus relative displacement for all 13 shear specimens. 49
Figure 3.12 Normalized lateral force versus relative displacement: Specimens with R-bar shear connection. 53
Figure 3.13 Normalized lateral force versus relative displacement for all shear specimens with the threaded-rod shear connection. Note that after initial breakaway (and slip), the normalized lateral force is indicative of the coefficient of sliding friction. 55
Figure 3.14 Lateral force versus relative displacement of all tests with a 2-in. (50 mm) haunch. 58
Figure 3.15 Lateral force versus relative displacement of all tests with a 3.5-in. (89 mm) haunch. 59
Figure 3.16 Strut-and-tie mechanism within the beams tested. 60
Figure 3.17 Hoopsets grouped on either side of the fasteners. 61
Figure 4.2 Testing procedure for flow cone test. 66

Figure 4.3 Examples of good and bad flow cone tests. 67
Figure 4.5 Influence of time and sand content on efflux time. 71
Figure 4.6 Efflux time and flow cone results. 72
Figure 4.7 (a) Bleed water percentages for increasing sand contents; (b) Expansion/Subsidence profile of Sika mixtures. 73
Figure 4.8 Volume change profiles of mixes with varying sand percentages. 74
Figure 4.9 Strength development curves for different w/p. 75
Figure 4.10 Comparison of strength vs efflux time. 76
Figure 4.13 Experimental setup for the tension test. 86

LIST OF TABLES

Table 2.1 Compression and splitting tensile results. 9
Table 2.2 Stress and strain values for steel reinforcement. 10
Table 2.3 Peak loads and factors of safety for tested double-panel bridge deck system. 25
Table 2.4 Summary of the average material properties and standard deviations of the mixtures used in Specimens 3 and 4. 30
Table 2.5 The cracking load, maximum load, and safety factor for Specimens 3 and 4. 31
Table 3.1 Matrix of 2-in. (50 mm) haunch and 3.5-in. (89 mm) haunch (italicized) shear specimens tested. 39
Table 3.2 Matrix of compressive strengths for shear test haunch, deck, pocket, and beam. 48
Table 3.3 Raw experimental data for 2-in. (50 mm) and 3.5-in. (89 mm) haunch (italicized) specimens. 51
Table 3.4 Analysis of data for 2-in. (50 mm) and 3.5-in. (89 mm) haunch (italicized) specimens. 51
Table 4.1 Test matrix of Sika mix designs. 64
Table 4.2 Characteristics of sand. 69
Table 4.3 Grout placement procedure. 77
Table 4.3 (continued) Grout placement procedure. 78
Table 4.4 Summary of the manufacturer reported foam properties. 87
Table 4.5 Summary of the testing for the foams and adhesives investigated. 88

EXECUTIVE SUMMARY

This report contains a summary of the testing completed through June 30, 2008, under TxDOT project 6100, "Development of a Precast Bridge Deck Overhang System," with specific recommendations for the application of this precast overhang system for the bridge over Rock Creek in Parker County, Texas. The design for the precast overhang panels for the Rock Creek Bridge presented in this report was shown to perform satisfactorily in all of the testing conducted for the loading specified by the AASHTO LRFD 2007 Bridge Design Specifications. The testing investigated in this report includes: the structural capacity of the precast overhang system and the corresponding deck joints; the interface shear capacity of the connectors, grout materials, and performance parameters; and the development of a haunch form system. Girder and rail performance were not evaluated.

In review of the test results and recommendations contained in this report, it is the authors' opinion that the precast overhang system will provide a system with comparable structural performance to a bridge deck system using the conventional reinforced overhang details typically used by TxDOT. Furthermore, it appears that this system will provide large improvements in safety, constructability, and economy over the conventional overhang system.

Insofar as the interface shear is concerned between the precast, prestressed full-depth deck panels that are seated on a grout bed connected by threaded-rods in concrete filled pockets, the performance did not meet the requirements assumed in the initial design. The interface roughness between the deck-haunch-beam-system is critical in providing shear resistance once the breakaway strength of the concrete is exceeded. The grout has a dependable friction coefficient of not more than 0.4. This is not sufficient, and special roughening of the girder top and panel bottom may be needed. Moreover, it is imperative that the threaded-rod shear connectors are appropriately anchored with sufficient beam hoop steel nearby to ensure distress to the prestressed concrete web of the girders does not occur. Notwithstanding these two issues of roughness and beam anchorage, an alternative solution was proposed based on the analysis of the test results to enable the construction of the Rock Creek Bridge to proceed. Nevertheless, additional research is needed to validate and further optimize the design and construction of the deck-haunch-beam system for general widespread use.

In conclusion, the research team supports the construction of the precast overhang system with the modified details, design procedures, and material recommendations contained in this report. This recommendation is based on testing results from the laboratory. It should be noted that this design procedure is likely not optimal and to achieve the economy, constructability, and safety capable of the system, additional research is needed.

CHAPTER 1. INTRODUCTION

The construction of bridges is costly. In addition, workers constructing these bridges can often be placed in unsafe conditions. Optimizing design and construction processes for accelerated bridge construction can provide significant benefits, including improved economy and safety. The state-of-the-art of accelerated bridge deck construction was reviewed in a recently published document (Badie et al. 2006). Research and case studies were presented in this document and a description of several methodologies for accelerated construction was provided. Guidance was also provided to overcome the following challenges with full-depth bridge deck construction:

- adjustment of precast panel grading to meet construction tolerances,
- methodologies to provide structural compatibility between the girders and bridge deck, and
- performance of different cementitious grouts needed for the accelerated bridge deck systems.

Some issues that received limited coverage in the document but still are in need of more research work include:

- ability to provide a durable design,
- ability to achieve an acceptable ride (smoothness),
- impact on safety,
- ability to provide a functioning form between the variable area between the beam and the deck panel (haunch),
- verification of composite action between the precast deck system and girder,
- comparison between accelerated and conventional methodologies to determine the impact on construction schedule and cost,
- validation testing of full-scale beams to observe the shear/flexure interaction of various system components subjected to field conditions, and
- resolution of potential challenges associated with proper seating of warped panels due to differential drying and shrinkage.

While the use of full-depth bridge decks have the ability to increase the speed of bridge deck construction, care should be taken to be sure that the above items have been addressed and that the resulting system provides benefits, both short- and long-term, not achieved with conventional construction techniques.

This research investigated precast, prestressed panels for bridge overhang systems. The research team investigated four specific areas, including:

- evaluation of precast, prestressed overhang capacity;
- evaluation of the performance and constructability of the shear connection details;
- evaluation of grout materials for the haunch; and
- assessment of constructability issues, including haunch forming and grout placement.

It should be noted that this research program was divided into two general phases. The first phase included the evaluation and reporting of the above listed items necessary for the Rock Creek Bridge in Parker County, Texas. The objective of this phase was to assess the system design, materials, and methods specifically for this bridge, not necessarily to optimize these issues but instead to identify systems, materials, and methods that could be used in the Rock Creek Bridge. The research team, in collaboration with engineers from the Texas Department of Transportation (TxDOT), identified potential systems and processes that could be used, and these were evaluated by the research group. Phase II of the research will focus more on the optimization of materials and design issues. A final report will be submitted after the conclusion of the Phase II research.

As a result of the very aggressive research schedule and need to deliver a report before the letting of the Rock Creek Bridge, researchers from the Texas Transportation Institute (TTI) teamed with researchers from Oklahoma State University (OSU). The TTI researchers focused their efforts on capacity testing of double-panel, overhang deck systems, shear capacity of shear connections, and grout performance. OSU researchers focused their efforts on capacity testing of a single overhang deck system and the development and testing of haunch forms. TTI and OSU researchers worked closely with TxDOT personnel on the preliminary design and testing plan for the research. Constructability issues were addressed at both research institutes.

This report is organized into five chapters: 1–Introduction; 2–Bridge Overhang System; 3–Shear Connections; 4–Materials for Precast Overhang Systems; and 5–Conclusions and Recommendations for the Rock Creek Bridge and for future research.

CHAPTER 2. BRIDGE OVERHANG SYSTEM

The research team and TxDOT personnel met on several occasions to develop and review designs options for precast, prestressed overhang panels for the Rock Creek Bridge. The design of the overhang panel system, with the shear design, is shown in Appendix A. Because of the accelerated nature of the research program, testing was performed at TTI and OSU laboratories. Researchers at TTI experimentally evaluated deck systems with double-panel specimens, with an emphasis on examining the panel-to-panel seams. Researchers at OSU evaluated single-panel systems.

Approximately 85 percent of new concrete bridge decks in the state of Texas use stay-in-place, precast, prestressed panels spanning between adjacent beams (Figure 2.1 [a]). These panels are nominally 4-in. (100 mm) thick and prestressed transversely to the direction of traffic flow. A second stage concrete pour of 4 in. (100 mm) in thickness is cast on top of the stay-in-place panels. One of the main difficulties with this system is forming the deck overhang to cast a full 8-in. (200 mm) thick deck section. Formwork has to be attached to the outside girder, making it a time-consuming and potentially unsafe operation. TxDOT has recently developed a precast, full-depth overhang system that potentially reduces the cost of construction and improves safety, long-term durability, and the speed of construction of the bridge.

2.1 Double-panel Testing

This section presents results from an investigation on the performance of full-depth, double-panel precast overhang systems, where the flexural capacity and failure modes of the panels were evaluated. In particular, the general capacity and the effect of the transverse seam between adjacent panels was assessed and compared with the conventional cast-in-place (CIP) system, which has continuous longitudinal reinforcement and no transverse seams. The set-up for experimental testing is shown in Figure 2.1 (b). This system consists of a standard TxDOT bridge overhang and the proposed precast, prestressed overhang system. The different construction methods only influence the first interior bay; hence, the transverse width of the setup is reduced to three beams.

The proposed precast overhang system is based on mimicking the conventional CIP deck, having the same reinforcing details throughout. The 8-ft. (2.4 m) wide panels were constructed in a two-stage casting process at a precast plant. The first stage concrete placement (4-in. [100 mm] thick) for the panels is performed in the same long-line stressing bed as conventional precast panels. The new overhang panels are prestressed along their length (transverse to the bridge axis) and reinforced longitudinally. After release of the strands, the second stage concrete placement (4-in. [100 mm] thick), reinforced with reinforcing steel in both directions, was cast on top of the first stage concrete. Over the panel width there were three full-depth rectangular pockets that provide a location for shear connectors between the panel and bridge girder.

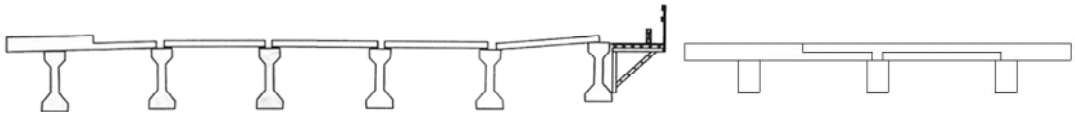

Figure 2.1 *(a) Full-scale bridge construction showing precast overhang (left) and conventional overhang (right); (b) Full-scale experimental set-up showing precast overhang (left) and conventional overhang (right).*

A bridge deck will exhibit both bending and shear forces simultaneously when subject to everyday traffic loads. In this research, flexural bending of the deck is uncoupled from the deck panel - girder interface shear. This was achieved by seating the concrete beams that support the deck panels directly on the laboratory strong floor so they exhibit no longitudinal bending. The full-scale test investigated the failure modes and the capacity of the new system compared to the conventional CIP overhang system. Two double-panel specimens were tested to evaluate load-deformation behavior, map crack formations, and to identify failure modes. Two single-panel systems were also tested and evaluated at OSU.

2.1.1 Experimental Plan

Two full-scale, double-panel specimens, representative of TxDOT precast concrete bridge decks, were tested to characterize resistance to factored wheel loads. Particular emphasis was placed on comparing performance of the proposed precast overhang with the conventional CIP overhang system. The setup consisted of two precast panels, 8-ft. (2.4 m) long by 8-ft. 9-in. (2.7 m) wide, cast adjacent to one another and placed on reinforced concrete beams that were supported continuously on the laboratory floor. The concrete beams were rectangular, 12-in. (300 mm) wide, representative of a TxDOT Type A girder top flange width. The beams were 16-in. (400 mm) deep, sufficient to place internal reinforcement and fasteners while providing adequate space to place instrumentation. Conventional precast panels spanned the center and one of the outside beams for the conventional overhang system. The overall experimental footprint measured 16 ft. (4.9 m) along the longitudinal bridge axis and 18 ft. (5.5 m) in the transverse direction. A photograph of the experimental setup looking across a transverse axis (along the seam of the two adjoining panels) is shown in Figure 2.2.

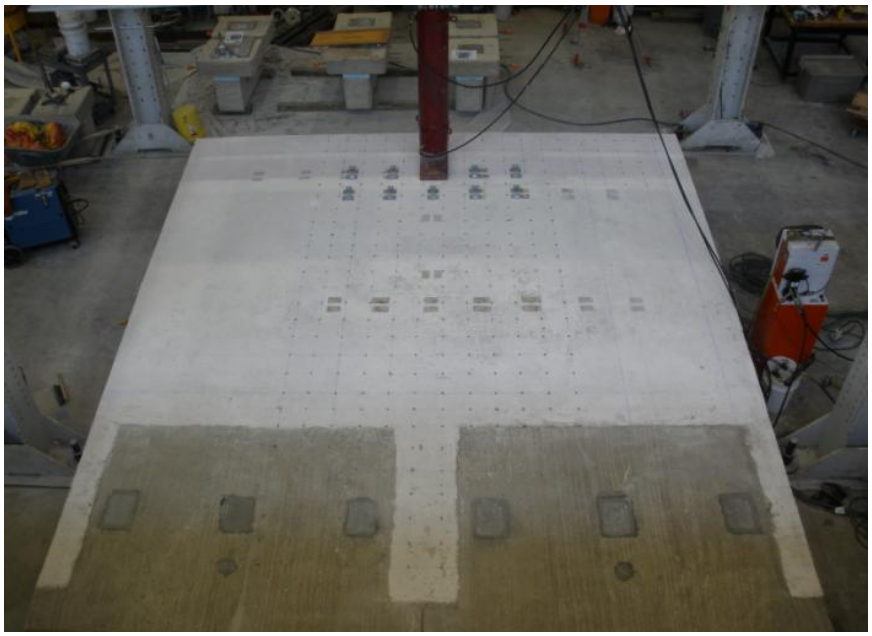

Figure 2.2 Photograph of the bridge deck in the laboratory.

2.1.2 Specimen Layout and Reinforcing Details

Specimen 1 was designed to provide a comparison between the performance of the precast overhang and the conventional CIP overhang systems. The main difference in the reinforcement details was the continuous prestress over the overhang in the precast panel, as well as the effect of the seam between the panels. To determine the effect of the seam between the precast overhang panels, the conventional overhang was constructed with bottom transverse #4 (#13M) mild steel reinforcing bars placed at 6-in. (150 mm) centers, rather than the maximum allowable spacing of 18 in. (450 mm). This reinforcement spacing was further justified, as the precast overhang panel design allows the option of #4 (#13M) mild steel to be used as the bottom transverse reinforcement in lieu of the prestressing strands. Figure 2.3 shows the overall dimensions and reinforcement details for Specimen 1. Note that the specimen consists of a conventional overhang and a precast overhang. Composite action was anticipated between the girder and precast overhang panel through the grout in the haunch and the threaded rod connectors at each pocket. Conversely, the conventional overhang had R-bar stirrups at 12-in. (300 mm) centers extending above the beam surface by 5.25 in. (133 mm).

Specimen 2 was designed and tested with the objectives of confirming the findings of the precast overhang system tested on Specimen 1 and of investigating an alternative approach for constructing full-depth overhang panels. The latter objective was achieved by constructing a conventional panel system with a "second stage" concrete placement to achieve a full-depth overhang panel. The reinforcement details for this system are similar to the precast overhang system, with the exception that the prestressing strands are replaced with conventional reinforcement in the "second stage" cast. As with the conventional overhang system, #4 (#13M) mild steel reinforcing bars were placed at 6-in. (150 mm) centers. The shear connections for this system were similar to the Specimen 1 connectors with the exception of the pockets, which were reduced from 10 x 7-in. (250 x 175 mm) pockets to 6-in. (150 mm) square pockets. Smaller composite pockets allowed for the main top steel over the cantilever portion to be spaced closer to 6-in. (150 mm) uniform spacing. It was anticipated that by evaluating the lab-cast panels, information could be obtained on the effect of the prestress in the bottom layer. The general layout for Specimen 2 is shown in Figure 2.4.

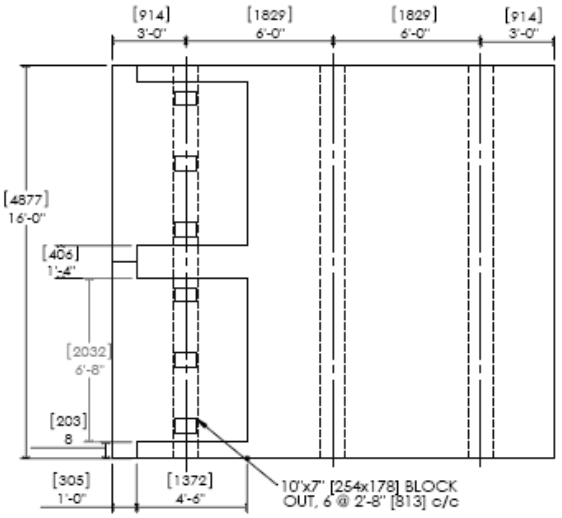

(a) Plan View Dimensions

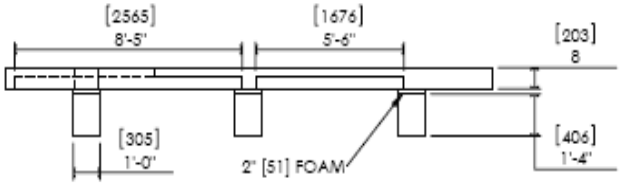

(b) Transverse cross section

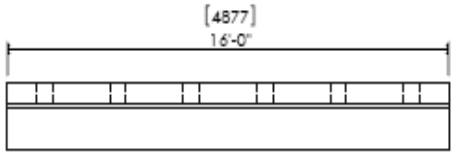

(c) Side Elevation

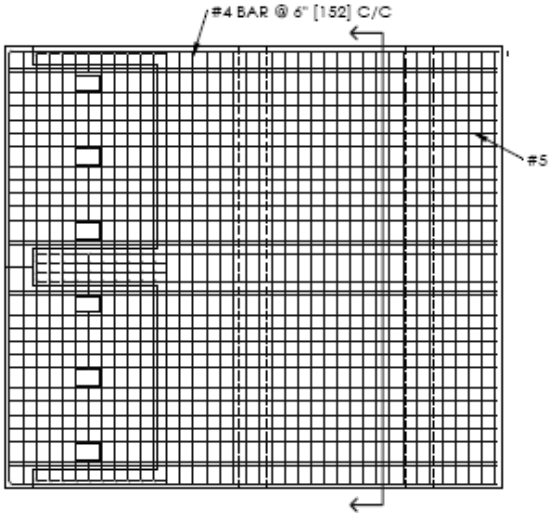

(d) Plan View top steel layout

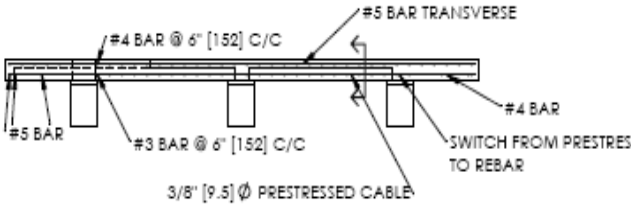

(e) Transverse cross section

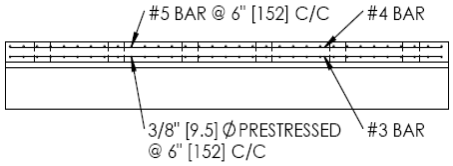

(f) Side elevation of steel

Figure 2.3 Dimensions and steel layout for Specimen 1.

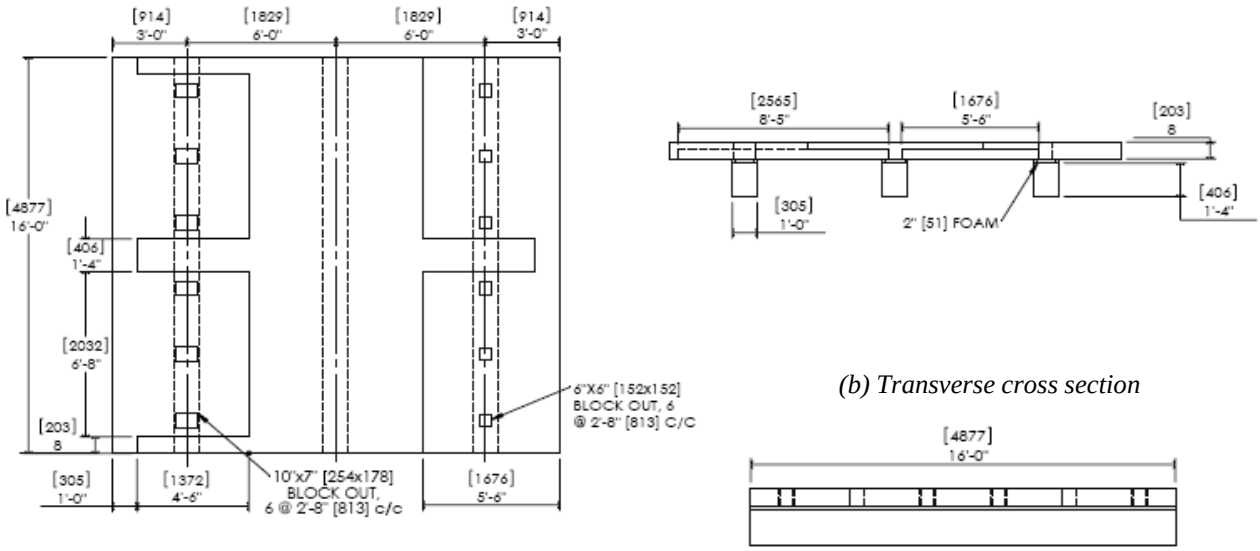

(a) Plan View Dimensions

(b) Transverse cross section

(c) Side Elevation

Figure 2.4 Various views and layout of Specimen 2.

2.1.3 Materials

All precast panels for the research program were fabricated at Austin Prestressed Co. Four full-depth overhang panels and four conventional precast, prestressed panels were used for the two double-panel tests conducted at TTI. All other bridge components were constructed in the High Bay Structural and Materials Laboratory (HBSML) at Texas A&M University.

All concrete placed in the laboratory was supplied by Transit Mix of Bryan, Texas, an approved TxDOT supplier. Type H concrete, with a specified target strength of 5000 psi (34 MPa), was used for the laboratory beams. Type S concrete, with a target strength of 4000 psi (28 MPa), was used for the deck. A slump of 4 in. (100 mm) was specified for all concrete mixtures. Cylinders were cast from each concrete batch in accordance with Tex-447-A, *Making and Curing Concrete Test Specimens*. Compression tests were conducted at 3, 7, and 28 days after casting and at the time of testing of the test specimens following Tex-418-A, *Compressive Strength of Cylindrical Concrete Specimens*. Splitting tensile tests were also conducted on the day of testing in accordance with Tex-421-A, *Splitting Tensile Strength of Cylindrical Concrete Specimens*. Table 2.1 shows the compressive strengths of the different concretes used in the

research at 3, 7, and 28 days after casting, and also the measured compressive strength on the day of each experiment. Splitting tensile strengths are also shown in the table.

Tensile tests were also conducted to characterize the mild steel and prestressing strands used in the panels and CIP decks. Figure 2.5 shows the stress-strain curves for the steel reinforcement used in the precast panels (this includes a wire mesh used in the panels) and the CIP deck. All steel met the 60 ksi (414 MPa) yield requirements of ASTM A615, Standard Specification for Deformed and Plain Carbon-Steel Bars for Concrete Reinforcement. Table 2.2 shows critical values from the tension tests.

Table 2.1 *Compression and splitting tensile results.*

Specimen No.	**Component**	**Cast Date**	**Compressive Strength, psi (MPa)**				**Tensile Strength, psi (MPa)**
			3-day	**7-day**	**28-day**	**Time of Test**	**Time of Test**
1	Stage I	2/5/08	4200 (29)	5880 (41)	8035 (55)	8450 (58)	870 (6.0)
1	Stage II	2/8/08	5960 (41)	7200 (50)	7680 (53)	9030 (62)	805 (5.5)
1	SIP Panel	2/12/08	4320 (30)	6600 (45)	7745 (53)	8990 (62)	890 (6.1)
1	Deck	3/28/08	3800 (26)	6565 (45)	8380 (58)	8515 (59)	805 (5.5)
2	Stage I	1/31/08	5340 (37)	6880 (47)	8770 (60)	9540 (66)	810 (5.6)
2	Stage II	2/5/08	4200 (29)	5880 (41)	6855 (47)	7560 (52)	750 (5.2)
2	SIP Panel	2/11/08	4900 (34)	6455 (45)	7000 (48)	7510 (52)	870 (6.0)
2	Lab cast overhang	4/14/08	4700 (32)	6600 (45)	7910 (55)	8345 (58)	675 (4.7)
2	Deck closure	5/19/08	2900 (20)	3550 (24)	4840 (33)	4500 (31)	465 (3.2)

Notes: Stage I is first stage pour of precast overhang panels) ; Stage II is second stage pour of precast overhang panels; SIP Panel = stay-in-place panel for interior bay.

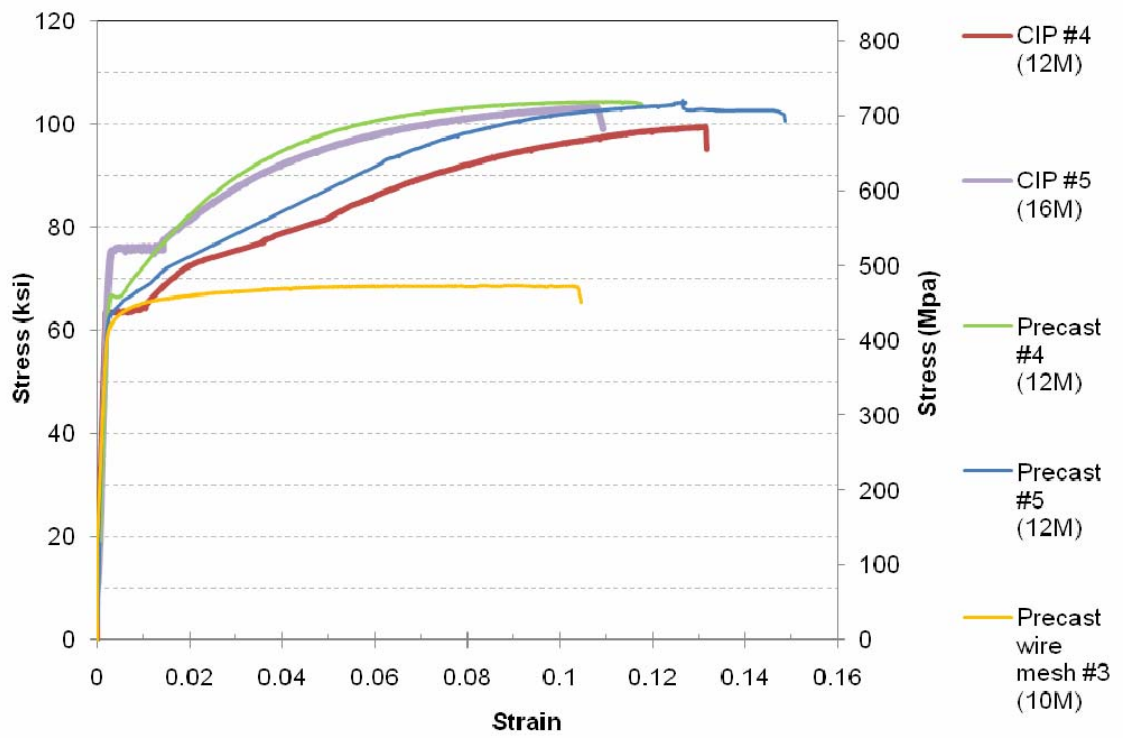

Figure 2.5 *Stress-strain curves for steel reinforcement in panels (CIP = reinforcement embedded in cast-in-place concrete; Precast = reinforcement embedded in precast panels).*

Table 2.2 Stress and strain values for steel reinforcement.

Specimen	Yield Stress, ksi (MPa)	Yield Strain	Strain at onset of strain-hardening
CIP #4 (#13M)	63 (434)	0.00185	0.0095
CIP #5 (#16M)	76 (524)	0.00255	0.014
Precast wire mesh	63 (434)	0.00215	0.0025
Precast #4 (#13M)	66 (455)	0.00250	0.0055
Precast #5 (#16M)	63 (434)	0.00230	0.0025

Specimens 1 and 2 had a 2-in. (50 mm) haunch. SikaGrout™ 212 was used to fill the haunch (a more comprehensive analysis of the grout material is provided in Chapter 4). A water-to-powder ratio (w/p) of 0.19 was used for all grouts placed in the haunch area. A grout with a w/p of 0.16 was used for the pockets in Specimen 1. Because subsidence cracks were observed after less than 12 hours after the grout placement in Specimen 1 around the pocket perimeter, Class S concrete was used in the pockets for Specimen 2. No visible cracks were observed when concrete was placed in the pockets in Specimen 2.

2.1.4 Instrumentation for Double-panel Specimens

Various types of instrumentation were installed on the overhang specimens to ensure that sufficient data were obtained to assess the performance of the specimens. In addition to the instrumentation, surface strains were measured with externally mounted strain gauges on the top deck surface. Surface cracks, when present, were mapped at various load levels. Loads were measured with a load cell, and displacements and strains were monitored and recorded with an electronic data acquisition system programmed to scan and record all channels at 3-second intervals.

A total of 24 string pots were used for Specimen 1, with a line of nine string pots placed along the longitudinal axis of the wheel load. Ten surface gauges were used, measuring transverse strains over the beam. The two shear connectors were instrumented with quarter-bridge strain gauges to determine the axial force acting on the shear connector while loading the overhang.

The instrumentation plan was altered for Specimen 2 to include six additional string pots and ten internal strain gauges. The number of string pots increased from 9 to 14 along the longitudinal direction beneath the wheel load. String pots were spaced at 15-in. (375 mm) centers, with a string pot on both sides of the seam. Transverse displacement profiles were also measured in the plane of the wheel load. There were six strain gauges placed on the #5 (#16M) transverse bars closest to the seam edge. These were spaced such that they were at the beam centerline and interior face for the exterior beams and both beam faces on the interior beam. An additional four gauges were placed on the middle longitudinal bar, at 4 and 24 in. (100 and 600 mm) on both sides of the seam.

2.1.5 Specimen Loading Plan for Double-panel Specimens

Hydraulic jacks were used to represent truck wheel loads over a rectangular tire footprint measuring 10-in. (250 mm) long by 20-in. (500 mm) wide. Steel load plates, 3-in. (75 mm) thick, were seated on a .5-in. (13 mm) thick neoprene pad (Shore 70, similar in hardness to a tire tread).

The loads that were placed on the concrete deck surface were positioned at various locations on the deck to represent the most adverse design scenarios required by the American Association of State Highway and Transportation Officials Load and Resistance Factor Design (AASHTO LRFD) Bridge Design Specification (2007). Specific aspects of the loading for each specimen are described next.

2.1.5.1 Specimen 1

Figure 2.6 (a) illustrates the load cases tested on Specimen 1. Load cases 1.1 and 1.2 are the required AASHTO factored load at the longitudinal midpoint (or seam), and the longitudinal quarter- point (center of a panel), respectively. For the overhang, this positioned the center of the load plate 6 in. (150 mm) off the beam face, resulting in 2 in. (50 mm) of the load plate bearing over the grout bed (haunch). This load location is referenced in Section 3.6.1.3 of the AASHTO LRFD Bridge Design Specifications (2007). Load case 1.3 is the edge failure load, where the wheel load edge is on the edge of the panel. This may be representative of a crash load, with an increased moment due to the overturning force from the barrier resistance. The shear force will be the same as the AASHTO required load point; however, a greater moment at the beam face makes it more critical. Load cases 1.3 and 1.4 are similar to 1.1 and 1.2, while load case 1.5 differs from load case 1.3, as it is on the seam edge. Load case 1.7 is an axle load at the midpoint of each panel. Load case 1.8 is the interior failure load for an axle. Axle wheel loads are spaced at 6-ft. (1.8 m) centers.

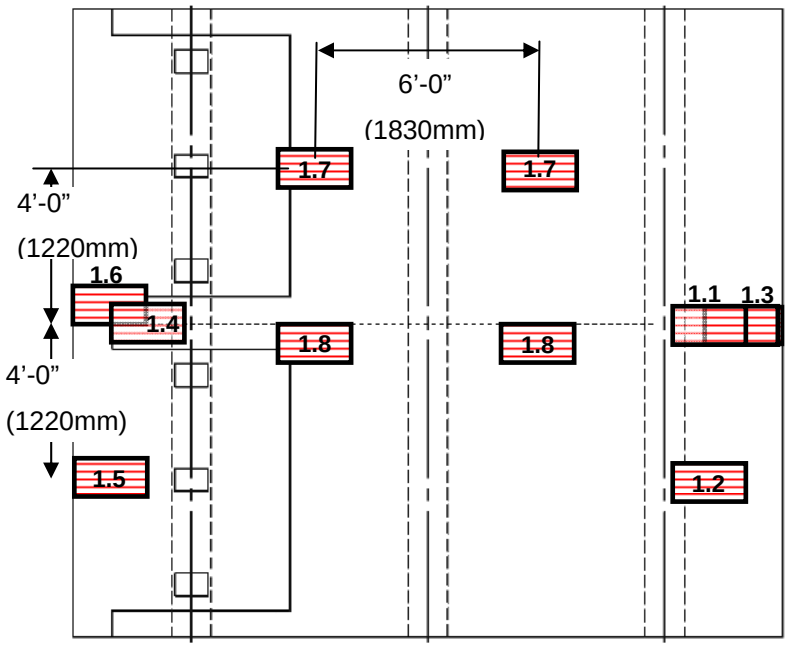

(a) Loading positions for Specimen 1

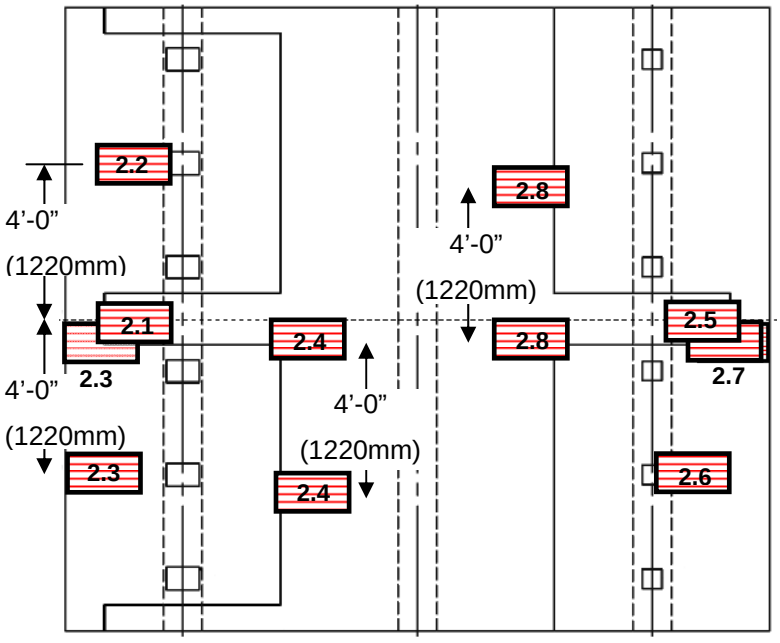

(b) Loading positions for Specimen 2

Figure 2.6 *(a) Loading positions for Specimen 1. Load cases 1.1, 1.2, 1.4 and 1.5 were loaded up to 60 kips (267 kN). Load case 1.7 was loaded to 120 kips (534 kN) per wheel load. All other load cases were loaded to failure; (b) Loading positions for Specimen 2. Loads 2.1, 2.2, 2.5 and 2.6 were loaded up to 60 kips (267 kN). All other load cases were loaded to failure.*

2.1.5.2 Specimen 2

Loading for Specimen 2 is shown in Figure 2.6 (b). The overhang loading on the lab-cast side was the same as Specimen 1 for the conventional and precast overhang to allow direct comparison of results. The failure load on the precast side was a trailing wheel load on the same panel as shown in Figure 2.8. Load case 2.4 was a trailing wheel load on one panel. Load 2.8 is similar; however, one wheel load is on the adjacent panel, closest to the seam. The trailing wheel load is 4 ft. (1.2 m), whereas in Specimen 1, load cases 1.7 and 1.8 represent a total axle load with the two wheel loads spaced 6 ft. (1.8 m) apart.

2.1.6 Experimental Results

For all sixteen loading conditions, force-displacement data were obtained based on the wheel load and the vertical displacement below the center of the load plate. String pots were placed along the beam face to obtain the true panel deflection by allowing for compression and "bedding in" of the beam to the strong floor.

2.1.6.1 As-Received Precast Panels

The precast panels were constructed with Class H concrete with a specified 28-day compressive strength of 5000 psi (34 MPa). Observations of the as-received panels indicated that the reinforcement may not have been placed per the drawings. This section will provide a description of the as-received panels.

As noted, the panels were constructed in two stages. Stage I concrete was broom-finished to provide enhanced friction between the Stage I and II interface. Delivered panels exhibited signs of cracking between the Stage I and II concrete placements, likely due to differential shrinkage or curling of the panels. Cracks propagated approximately 2 ft. (0.6 m) in both directions from the corner, as shown in Figure 2.7 (a). Figure 2.7 (b) shows that satisfactory compaction was achieved at other locations between the two concretes placed in the different stages.

Following the conclusion of the first experiment, a full-depth panel was carefully dissected to examine the steel layout. This was considered necessary, as it was earlier observed that the top longitudinal steel was placed above the transverse steel, instead of below it. Undamaged steel

samples were extracted from the dismantled specimen to characterize the tensile strengths of the steel used.

A longitudinal and transverse section of the dismantled overhang is shown in Figure 2.8 (a) and (b), respectively. The white box represents the typical undamaged cross section slab size, with the red bars showing the correct reinforcing that should have been cast. Welded wire mesh was continuously used for the bottom longitudinal reinforcement to the edge of the panel. The drawings specify three #5 (#16M) bars should have been used, spaced as shown in Figure 2.8 (a). Figure 2.8 (b) illustrates the correct layout of the top steel, with the longitudinal #4 (#13M) bars laying beneath the #5 (#16M) transverse bars with 2 in. (50 mm) clear cover to the top.

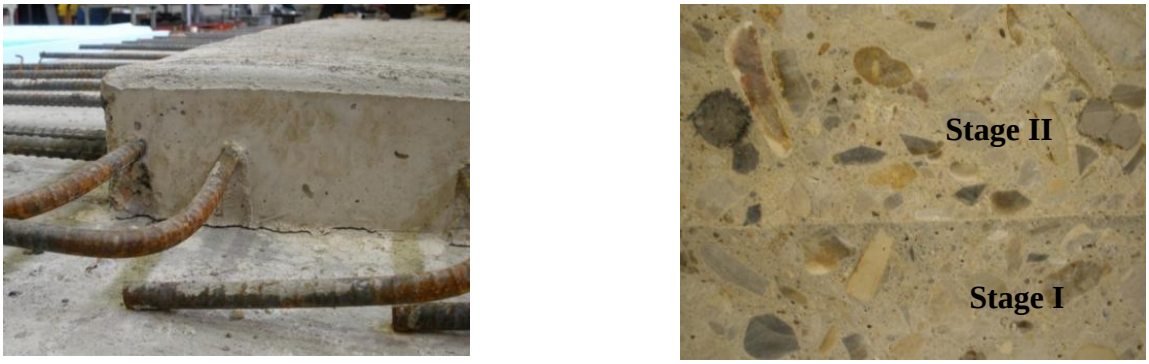

(a) Cracking between Stage I and II *(b) Cross section of Stage I and II concrete*

Figure 2.7 *Photographs showing cracking in between concrete lifts and good consolidation between concrete lifts.*

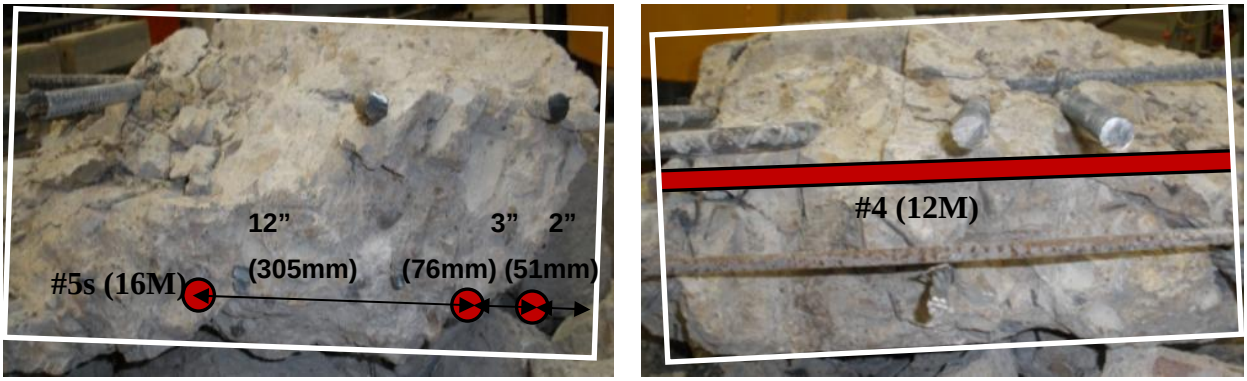

(a) Longitudinal cross section of overhang *(b) Longitudinal cross section of overhang*

Figure 2.8 *Reinforcing details of precast overhang panels.*

2.1.6.2 AASHTO Overhang Seam Load (Double-panel Specimens)

Both precast overhang panel setups and lab-cast panels behaved in a similar fashion. Some hairline cracks were only observed at loads of 60 kips (267 kN) between the seam above the exterior beam face. The conventional overhang had three cracks on the underside of the deck propagating from the beam face. The cracks were continuous to the overhang free edge. Top surface cracks were observed above the beam face and along the beam centerline.

Figure 2.9 (a) presents the results for the AASHTO overhang wheel load at the longitudinal midpoint of the bridge deck (the seam between precast panels). Vertical displacements obtained were small, with the largest displacement being approximately 0.012 in. (0.3 mm), corresponding to a slab transverse rotation of 0.002 radians at the beam face.

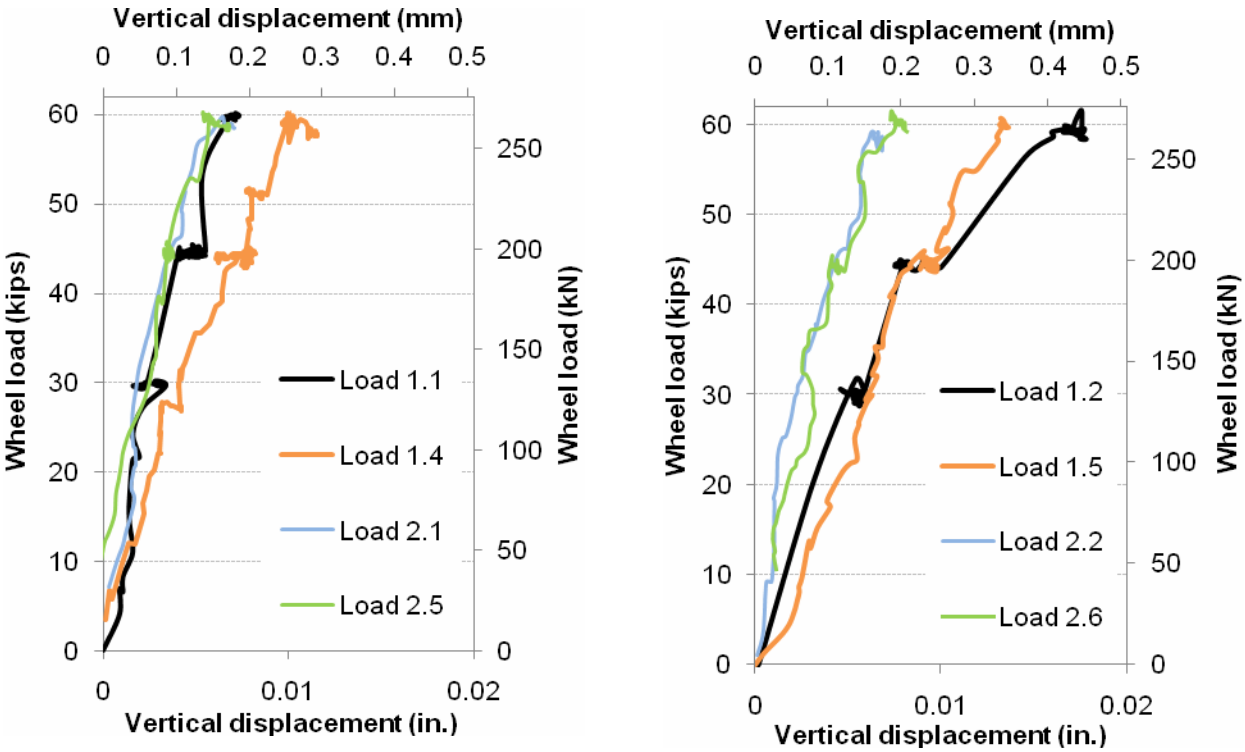

Seam (specimen mid point) *Specimen quarter-point*

Figure 2.9 *Force-deformation for the vertical load plate 2 ft. (0.6 m) from overhang edge (AASHTO load) for (a) on seam for Load 1.1 (conventional mid-specimen), Load 1.6 (precast overhang Specimen 1), Load 2.1 (precast overhang Specimen 2) and Load 2.5 (lab-cast overhang Specimen 2); (b) specimen quarter point for Load 1.2 (conventional overhang Specimen 1), Load 1.5 (precast overhang Specimen 1), Load 2.2 (precast overhang Specimen 2) and Load 2.6 (lab-cast overhang Specimen 2).*

2.1.6.3 AASHTO Overhang Mid-panel (Quarter-point) Loads

The design AASHTO loading was applied at the longitudinal quarter point of both specimens. For the precast overhang, this corresponded to the longitudinal midpoint of a precast panel.

The sole crack observed on the precast panel propagated from the PVC tubing hole that was cast in the full-depth section of the panel. The hole was cast in the panel to accommodate testing at OSU; hence, it does not provide any representation of the in-field panel construction. The conventional overhang had two hairline cracks on the underside of the deck in line with the load plate.

Load-displacement curves for these tests are presented in Figure 2.9 (b). In Specimen 1 the stiffness of the precast deck was similar to the stiffness of the conventional overhang. The stiffness values of the precast overhang panel and lab-cast of Specimen 2 were greater than that of Specimen 1. Both displayed no residual displacement or cracks in the deck.

2.1.6.4 Overhang Failure Loads (Double-panel Specimens)

A flexural failure mechanism in the overhang was achieved by moving the loading footprint to the edge of the deck. In Specimen 1, a singular wheel load was placed on the edge of the seam for the precast overhang (Load 1.4). The lab-cast overhang in Specimen 2 was loaded the same way (Load 2.7). This provides an indication of the staple bar strength between adjacent panels in comparison to the continuous reinforcement in the conventional panel failure load (Load 1.3). Specimen 2 uses a trailing wheel load applied over the same precast overhang panel (Load 2.3).

Cracks were mapped at selected loads based on the force-deformation data during the experiment. Figure 2.10 shows the cracks that were observed during the experiments on the top deck surface.

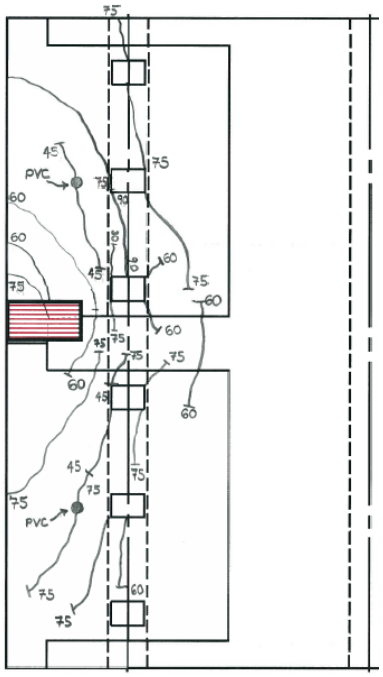

Precast Overhang Specimen 1

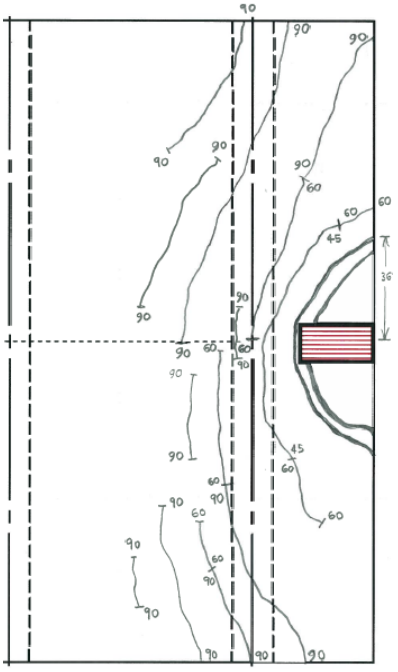

Conventional Overhang Specimen 1

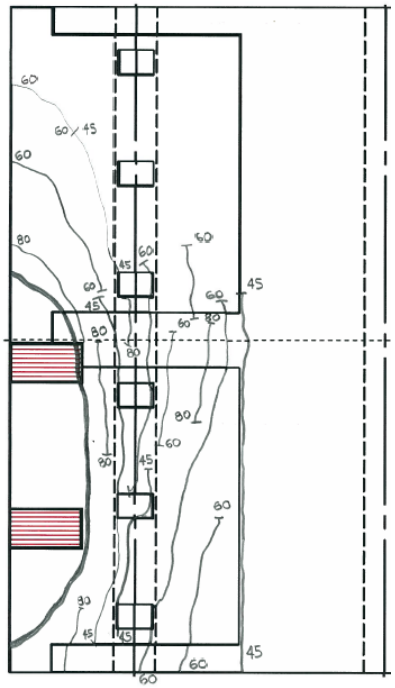

Precast Overhang Specimen 2

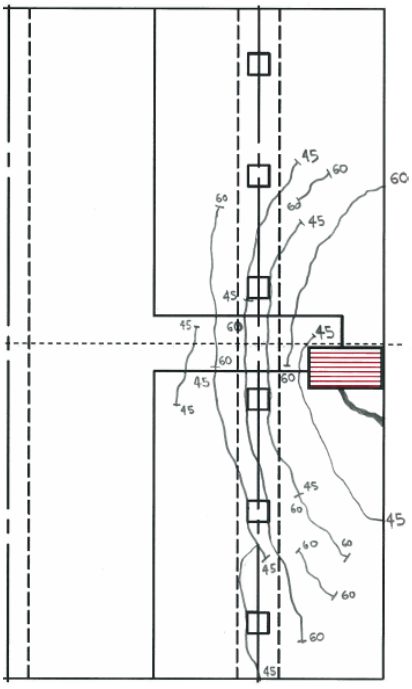

Lab-cast Specimen 2

Figure 2.10 *Crack mapping of overhang failure loads. Numbers are vertical pauses in kips (1 kip = 4.448 kN) where cracks were marked.*

Photographs taken at the time of failure are shown in Figure 2.11. The conventional overhang failure was close to symmetrical about the load plate. For the precast loads, cracks were observed in the panel adjacent to the panel loaded.

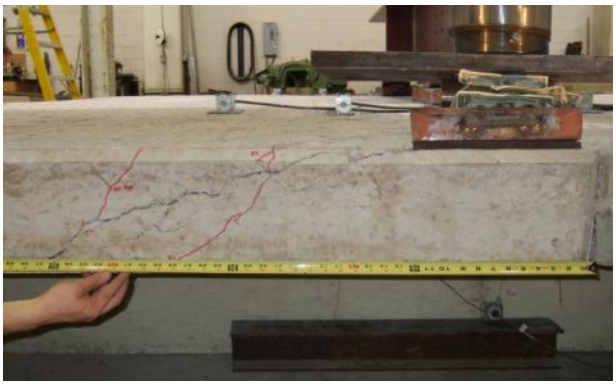

(a) Specimen 1 precast, prestressed overhang

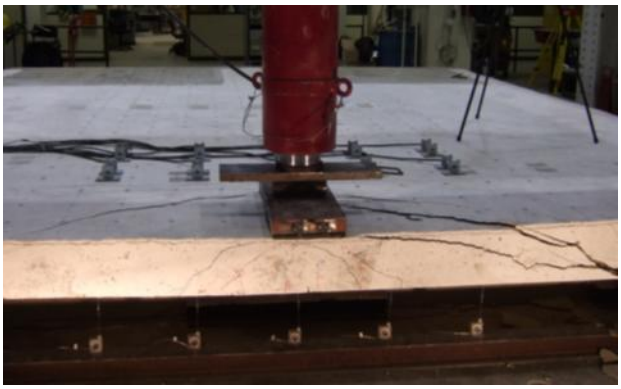

(b) Specimen 1 conventional overhang failure

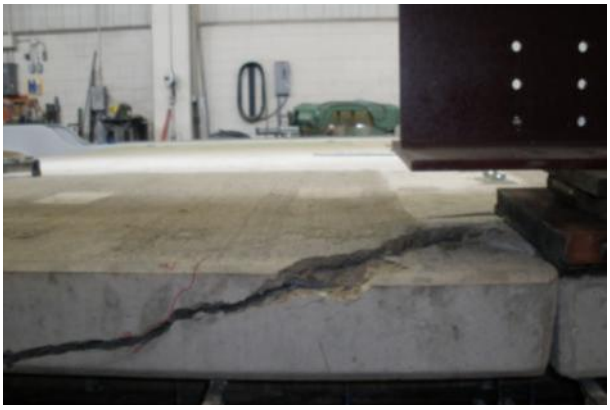

(c) Specimen 2 overhang trailing wheel load

(d) Specimen 2 lab-cast overhang failure load

Figure 2.11 *Observed failure cracks of overhangs.*

The force-displacement curves for load cases 1.3, 1.4, 2.3, and 2.7 are shown in Figure 2.12. The curves indicate that the initial stiffness is similar for the precast panels and CIP overhang with a single applied load up to approximately 30 kips (133 kN). Up to approximately 45 kips (200 kN) the force-deformation behavior is similar for the precast and conventional overhangs loaded at the seam. For Specimen 1, the ultimate load capacities were 99 kips (440 kN) and 84 kips (374 kN) for the CIP and precast overhangs, respectively. Thus, there is a reduction of 14 percent in load carrying capacity in the full-depth precast system. It should be noted that both

ultimate capacities significantly exceed the ASSHTO truck load. Although the introduction of the seam could be the reason for this reduction of capacity, it is necessary to examine the theoretical capacity to explain the difference.

First, it should be noted that although constructed to be similar, the material properties on the two overhangs were different. The yield stress of the CIP reinforcing bars was 76 ksi (524 MPa) compared to 63 ksi (434 MPa) in the precast side. Second, the precast system has a considerably smaller positive moment in the longitudinal direction at the seam (M_y= 5.76 kip-ft./ft. [25.6 kN] for precast and M_y = 18.39 kip-ft./ft. [81.8 kN] for CIP).

Greater ductility is observed in the precast overhang panel than the conventional panel and lab-cast systems. In terms of total loads on a panel, load case 2.7, which represented trailing wheels on a single panel, does not appear to adversely affect performance. Although the ultimate failure load is within 1 kip (4.5 kN) of the singular seam load, the stiffness was reduced for this load case. A folding mechanism along the beam face was observed, resulting in larger vertical displacements.

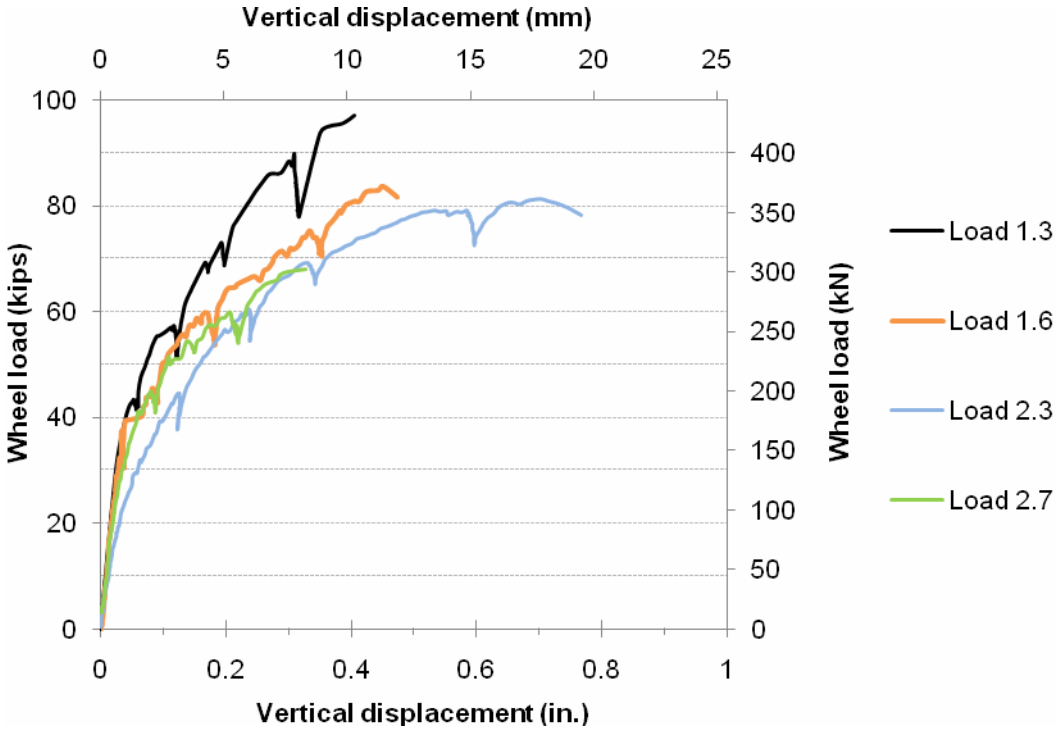

Figure 2.12 *Force-deformation for overhang failure; Load 1.3 (Specimen 1 conventional mid-specimen), Load 1.6 (Specimen 1 precast overhang seam load), Load 2.3 (Specimen 2 precast overhang trailing wheel load) and Load 2.7 (Specimen 2 lab-cast seam load).*

2.1.6.5 Interior Loads

Load cases 1.7 and 1.8 consisted of two simultaneously applied wheel loads via a spreader beam that represented a truck axle. One wheel pad was placed in each of the two interior bays of Specimen 1. In Specimen 2, load cases 2.4 and 2.8 also consisted of two simultaneously applied wheel loads, 4 ft. (1200 mm) apart to represent a trailing wheel load. These were applied along a midspan line parallel to the longitudinal axis of the bridge. In this way, the AASHTO trailing wheel condition for one bay (between beams) was represented. In load case 2.4 the two loads were placed within one panel, adjacent to the seam. In load case 2.8 the trailing loads were placed with one near the center of the panel and the other straddling the adjacent panel. The purpose of the comparison was to highlight the possibility of any difference in the imposition of bending and the possibility of shear stresses across the seam.

Specimen 1 had few surface cracks for both load cases, all of which were confined on the beam faces. Flexural-punching shear failure occurred on the interior beam of the precast side at 191 kips (850 kN). Figure 2.14 (left) shows the flexure/shear punching failure of the precast interior panel. Cracks are mapped for the trailing wheel loads in Figure 2.13.

Figure 2.15 provides the results of all interior failure loads (load case 1.8, 2.4, and 2.8) as well as quarter-point loads (load case 1.7). It is evident that load case 2.4 is the critical case in the trailing wheel load over a single panel. However, the initial stiffness in all load cases is comparable up to approximately 70 kips (311 kN) for loading near the seam. Note that this is in excess of the maximum factored AASHTO load (~45 kips [200 kN]). Behavior beyond 70 kips (311 kN) is still satisfactory, with a moderate degree of ductility (failure warning) exhibited. Figure 2.14 (right) shows the failure of the trailing wheel load over the adjacent panels.

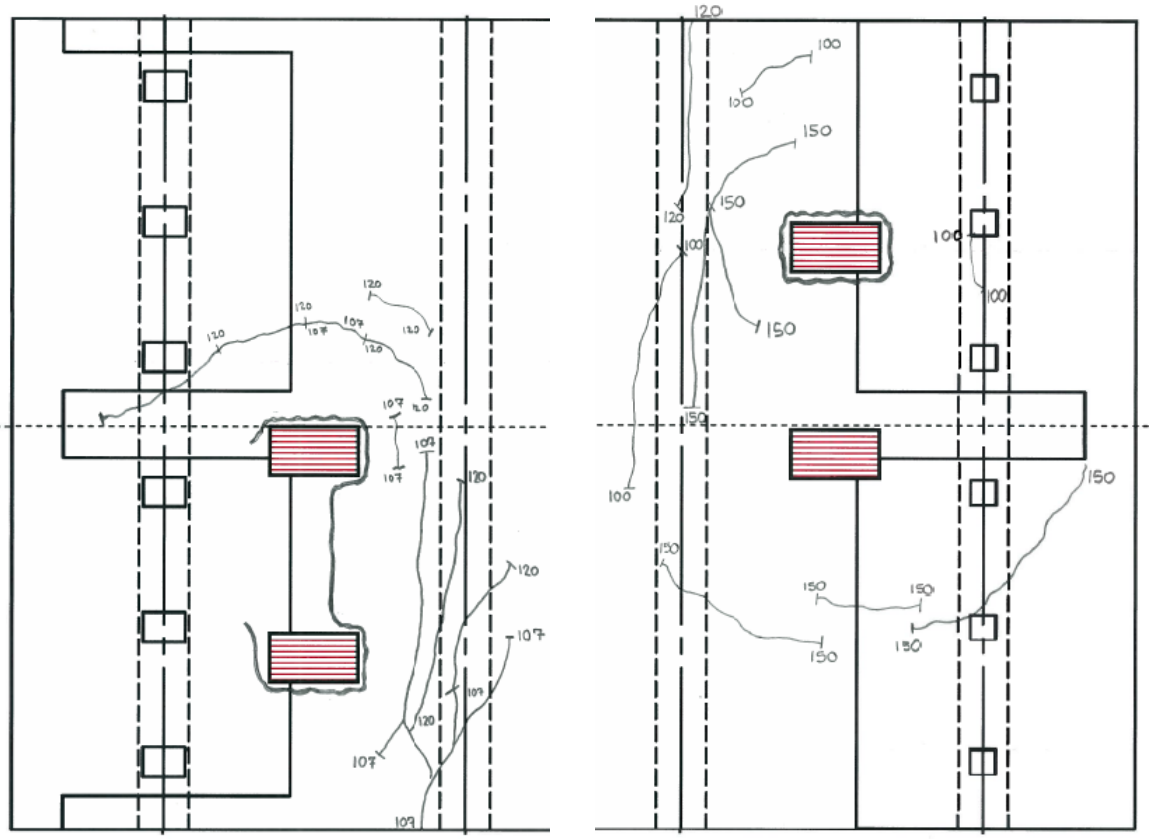

Seam precast panel loaded *Straddling seam of lab-cast*

Figure 2.13 *Specimen 2: Crack mapping of interior trailing axle load. Numbers are vertical load pauses in kips (1 kip = 4.448 kN) where cracks were marked.*

Midpoint (off-set to seam) axle load *Trailing wheel load over two panels*

Figure 2.14 *Interior loading failures.*

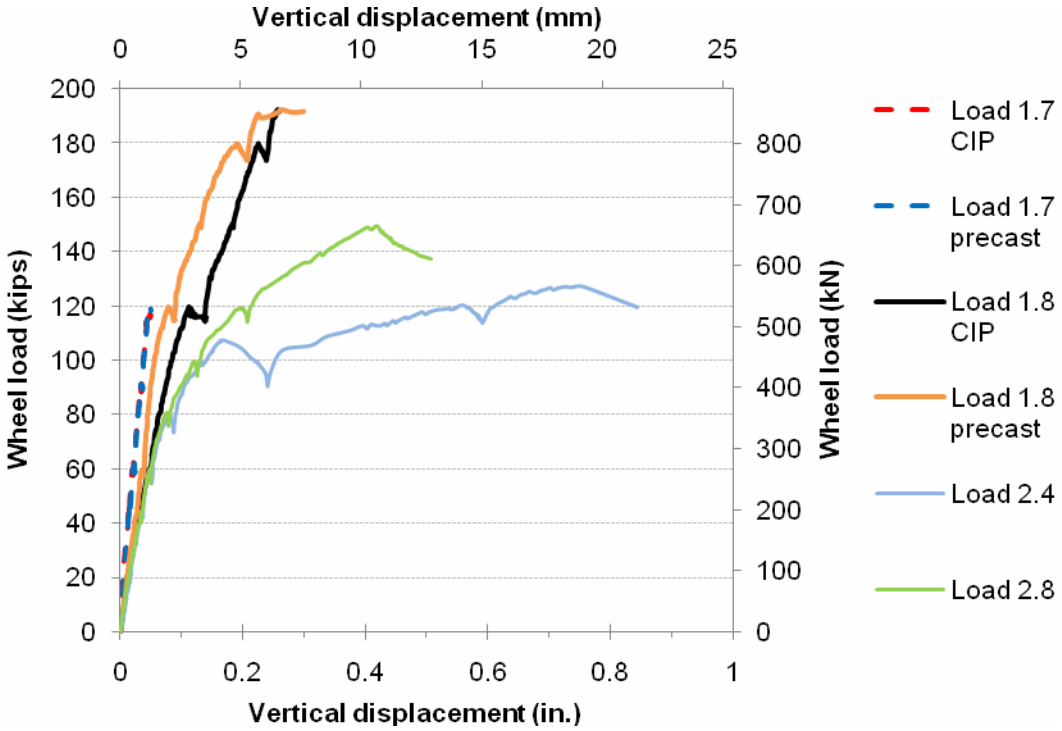

Figure 2.15 *Force-deformation for interior quarter-point and midpoint failure; Load 1.7 precast and Load 1.7 conventional (Specimen 1 trailing axle load), Load 1.8 precast and conventional (Specimen 1 trailing axle load), Load 2.4 (Specimen 2 trailing wheel load single panel loaded), Load 2.8 (Specimen 2 trailing wheel load straddling lab-cast seam). NOTE: Load 1.7 conventional underlies Load 1.7 precast*

2.1.6.6 Additional Measured Strains (Double-panel Specimens)

In the pocket closest to the seam, for both precast overhang panels, strains in one shear connector were recorded. The strains in the rod from the overhang load case 1.6 are presented in Figure 2.16. The maximum tensile stress recorded was 6.4 ksi (44 MPa), a minimal value for a rod with yield stress of 105 ksi (724 MPa).

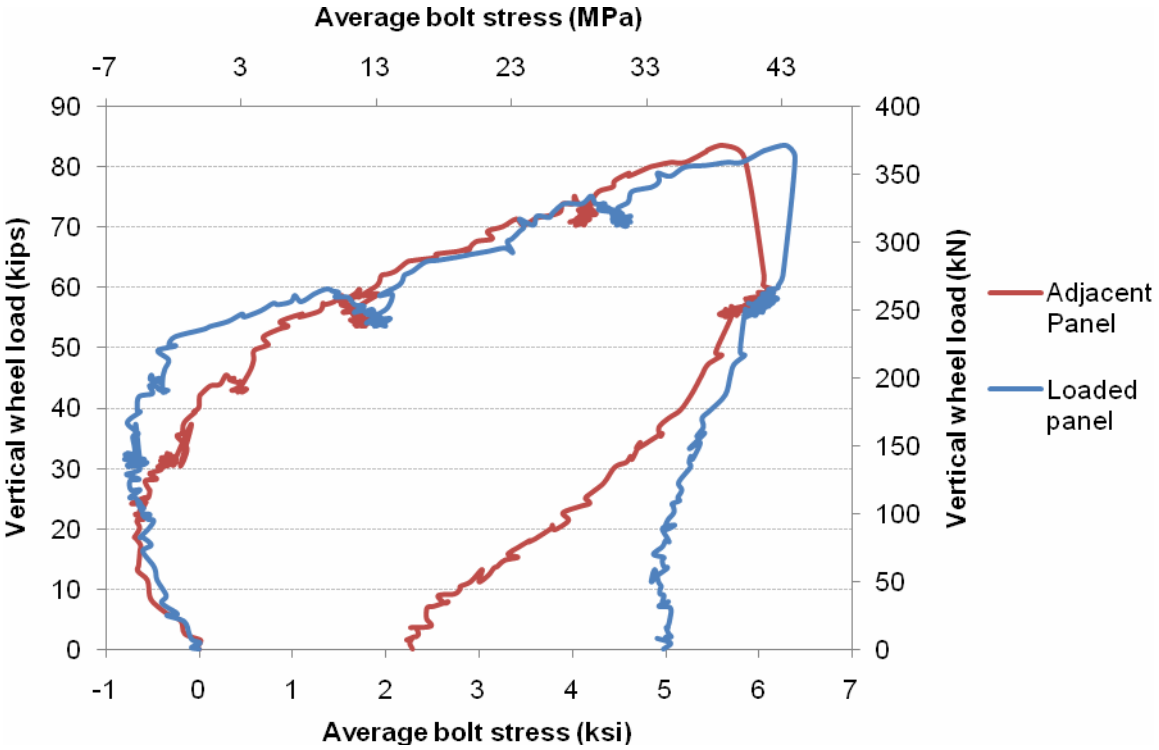

Figure 2.16 *Shear connector stress for Specimen 1 overhang failure load case 1.6.*

Figure 2.17 shows the strain observed on the #4 (#13M) top transverse reinforcement. The yield strain was 0.00217 in./in. (mm/mm). Hence, at the 60 kip (267 kN) load, the bars remained elastic (~55 percent of yield) over the beam centerline. The ultimate load yielded the bar from the beam centerline to approximately 15 in. (375 mm) beyond the interior beam face.

Based on an evaluation of the strains and load deformation behavior, it is apparent that a full failure mechanism did not form until the load reached approximately 78 kips (347 kN).

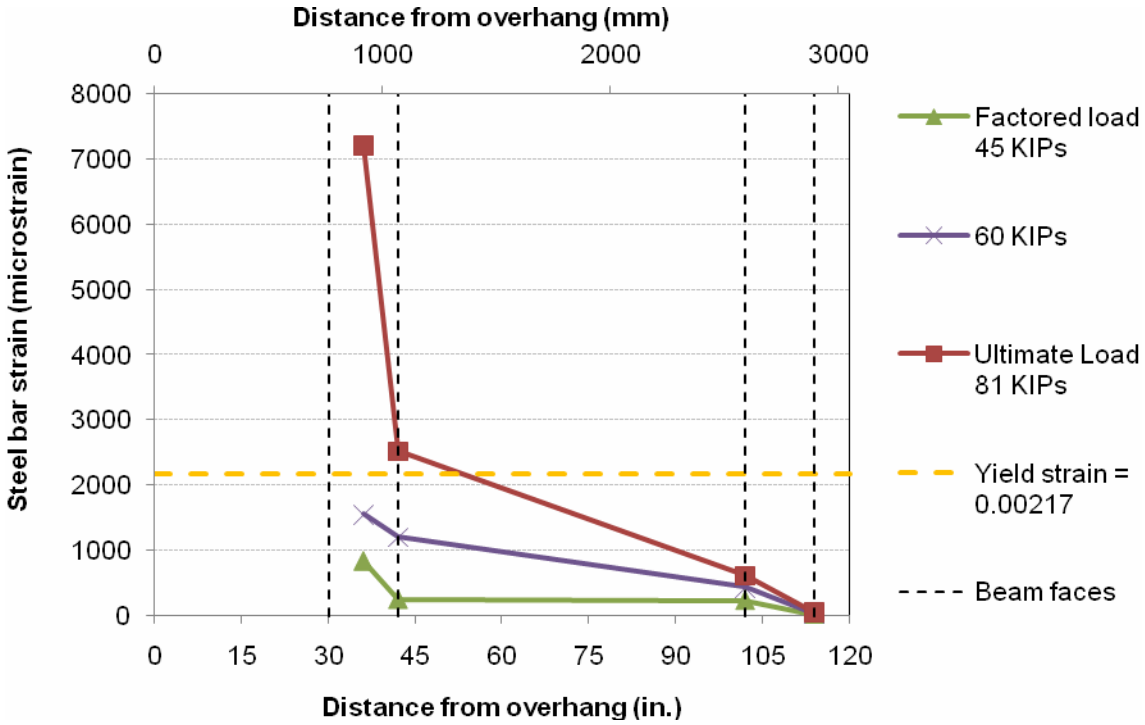

Figure 2.17 *Transverse bar strains in precast overhang.*

2.1.7 Summary for Double-panel Specimens

Results from the overhang tests indicate that the precast overhang system exhibits sufficient capacity for a 3-ft. (0.9 m) overhang. Table 2.3 shows the factors of safety obtained from the double-panel testing. Note that these are only for the capacity of the precast overhang system, not the bridge.

Table 2.3 *Peak loads and factors of safety for tested double-panel bridge deck system.*

Load Case	Peak Wheel Load kips (kN)	Factor of safety (ultimate/16 kips)
Conventional mid-specimen edge load	99 (440)	6.2
Precast overhang seam edge load	84 (374)	5.3
Interior trailing axle load mid-point	193 (859)	12.1
Precast overhang trailing wheel load	81 (360)	5.1
Precast interior trailing wheel single panel	127 (565)	7.9
Lab-cast overhang seam edge load	68 (302)	4.3
Lab-cast interior trailing wheel straddling seam	150 (667)	9.4

Based on the results from the two full-scale double-panel specimens, the following conclusions can be drawn:

- The concept of using conventional stay-in-place panels to construct a precast overhang was verified. Current TxDOT bridge capacities have sufficient reserve strength over the required AASHTO loads. The full depth precast panels also showed sufficient strength in both interior and exterior bays.
- The stiffness of the full-depth precast-prestressed panels was comparable to the conventional CIP deck. Overhang failure loads were made critical by loading at the edge of the panel and seam joint. It is evident that the introduction of the seam decreases the overall strength, but only the bottom longitudinal steel is discontinuous. Nevertheless, some positive (and negative) moment strength is still provided due to the CIP panel-to-panel joint that has a single layer of link bars. Although this is weaker than the full-depth overhang, overall the reduction of load carrying capacity is only in the order of 14 percent, and, based on this research, is considered safe for implementation.

2.2 Single-Panel Testing

The objective of this section is to compare the structural capacity of single-panel, precast overhang systems from midpoint and corner loadings with the structural capacity of conventional overhang systems used by TxDOT.

2.2.1 Experimental Plan

To satisfy the objectives of this task, single-panel bridge decks were constructed that used current TxDOT reinforcement details and materials specifications. These specimens consisted of a bridge deck that was 8 ft. (2.40 m) in the longitudinal direction and 18 ft. (5.4 m) in the transverse direction. A layout of the test specimen is shown in Figure 2.18. The bridge deck was constructed on 3 girders that had a 6-ft. (1.8 m) center-to-center spacing with 3-ft. (0.9 m) overhangs. The bridge decks investigated were 8.25-in. (206 mm) thick with 2.25 in. (56 mm) of cover from the bridge deck surface to the top reinforcing bar. One exterior span and cantilever was built with the new precast overhang panel being investigated in this project. The other side of the deck system was built using a 4-in. (100 mm) precast panel and a conventionally formed

8.25-in. (206 mm) overhang. By constructing the specimens in this manner it allowed the capacity of the two overhang systems to be compared using a single specimen.

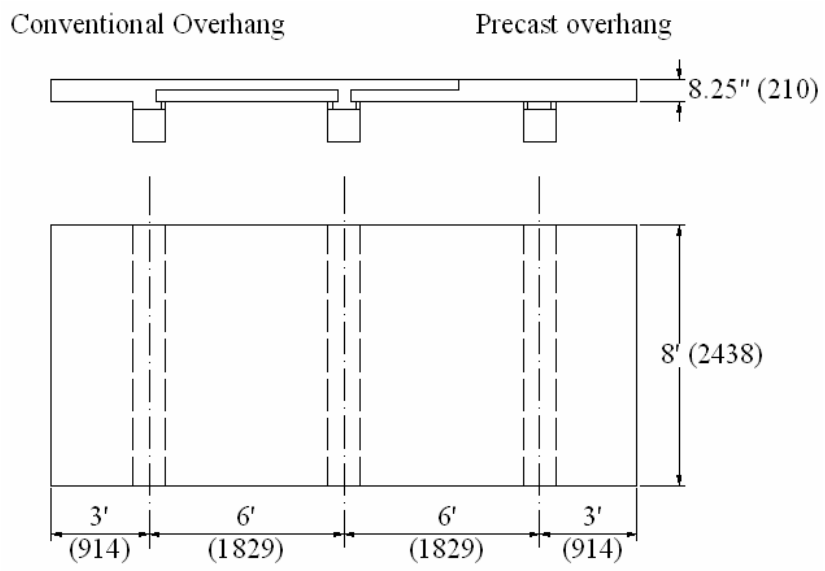

Figure 2.18 *Typical layout of a test specimen.*

The girders used in this testing had a top flange width of 12 in. (300 mm) and were 14 in. (350 mm) in height. As with the double-panel specimens, a top flange width of 12 in. (300 mm) was used to simulate a Texas Type A girder, the narrowest beam shape currently used by TxDOT.

The reinforcing details used for the precast overhang panel (Specimen 3) are shown Figure 2.19. The reinforcing details for Specimen 4 matched those typically used in TxDOT bridge decks. These consisted of #5 (#16M) bars at 6-in. (150 mm) spacings transversely and #4 (#13M) bars at 9 in. (175 mm) longitudinally in the top mat of steel. The partial depth precast panel reinforcing was typical of that used by TxDOT with 3/8-in. (10 mm) diameter prestressing strands at 6-in. (150 mm) centers in the transverse direction and 0.22 $in.^2$/ft. (0.001 mm^2/m) of reinforcing bar in the longitudinal direction. The bottom layer of steel in the conventional overhang consisted of #4 (#13M) bars at 18-in. (450-mm) centers for Specimen 4 and 6-in. (150

mm) centers for Specimen 3. It is not anticipated that this change will greatly alter the performance of the specimen.

During the construction of the precast overhang panels by Austin Prestressed Co., the reinforcing bars in the top of the slab were inadvertently switched for Specimens 3 and 4. After the error was discovered, it was decided, through conversations with TxDOT personnel, to use this same reinforcing detail throughout the top layer of reinforcing in Specimen 3 and 4. This change is shown in Figure 2.19. It is not anticipated that this change will have a significant impact on the test results and will be addressed later in the discussion section.

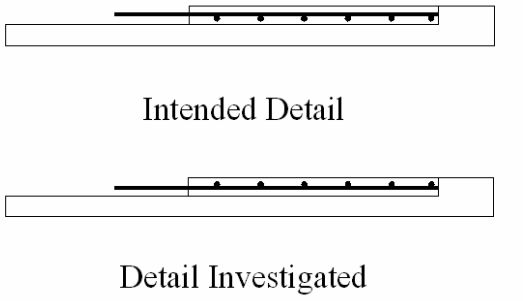

Figure 2.19 *The intended and actual detail used in Specimens 3 and 4.*

The loading points for Specimens 3 and 4 are shown in Figure 2.20. For each test a 10 x 20 in. (250 x 500 mm) steel plate was used to represent a 16 kip (71 kN) AASHTO HL 93 tire patch. As with the double-panel sections, the center of the tire patch was placed 1 ft. (300 mm) from the edge of the exterior beam. Two different load cases were investigated. In Specimen 3 a load at the midspan of the cantilever was applied, and in Specimen 4 the load was placed at the corner. This loading condition was chosen to simulate an HL 93 truck traveling at the very edge of the guard rail at midspan and at the location where a bridge deck terminates, such as at the approach slab.

While loading the midspan of Specimen 3, the AASHTO tire patch was inadvertently rotated 90^{o} in the loading for the conventional overhang section. The correct loading orientation was used for the precast overhang panel. This modification should be conservative and will be discussed further in the discussion section.

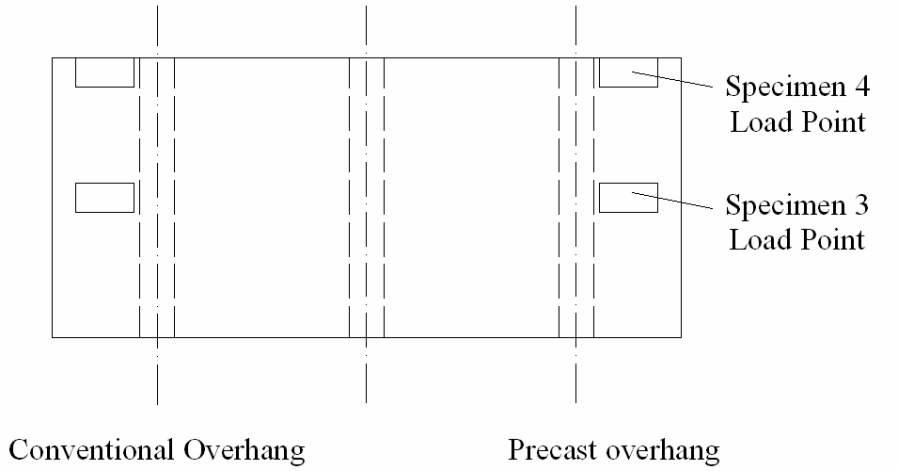

Figure 2.20 *The load points investigated for Specimens 3 and 4.*

The structural response of the specimens was evaluated with surface demec strain readings with 4.4-microstrain accuracy and by deflection measurements using Mituyo™ electronic dial gages (0.0005 in. [0.013 mm]) accuracy. These systems provided flexible and accurate methods to investigate the performance of the overhang systems.

2.2.2 Materials

A summary of the concrete and grout mixtures is provided in Table 2.4, along with the relevant material properties. All mixtures met the requirements for TxDOT 421 Class S concrete. The grout used in the haunch did not contain coarse aggregate and so did not meet the gradation requirements. The location where each mixture was used in the specimen is shown in Figure 2.21.

Table 2.4 *Summary of the average material properties and standard deviations of the mixtures used in Specimens 3 and 4.*

Specimen	Test	CIP	Stage I	Stage II	Grout	Pocket Concrete	Partial Depth Panel
3	Compression, psi (MPa)	6976 (48)	9098 (63)	7096 (49)	8137 (56)	4085 (28)	8475 (58)
	Tension, psi (MPa)	660 (5)	729 (5)	620 (4)	544 (4)	524 (4)	693 (5)
4	Compression, psi (MPa)	5371 (37)	9151 (63)	6857 (47)	6287 (43)	4881 (34)	8475 (58)
	Tension, psi (MPa)	514 (4)	774 (5)	550 (4)	600 (4)	458 (3)	693 (5)

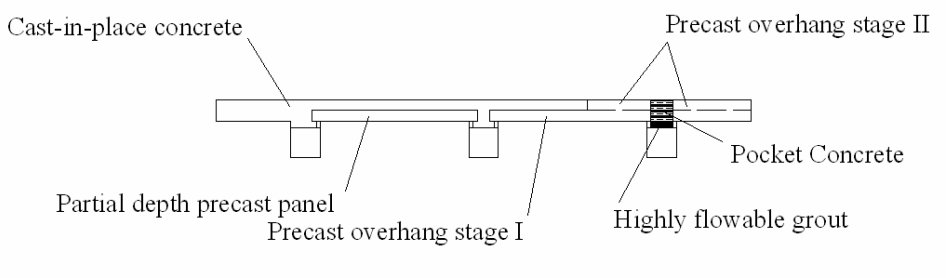

Figure 2.21 *Locations of materials used in Specimens 3 and 4.*

The reinforcing used in Specimens 3 and 4 was reported to meet TxDOT 440 and ASTM A 615 grade 60 requirements. Actual values will be determined with testing for the final report.

2.2.3 Results and Analysis

Table 2.5 provides a summary of the failure and cracking loads and the safety factor for Specimens 3 and 4. The crack patterns for these specimens are shown in Figures 2.22 and 2.23. The surface strain measurements and deflection response at the load point are shown in Figures 2.24, 2.25, 2.26, and 2.27. The conventional and precast overhang information is shown side by side so that performance of the different single-panel systems can be compared. The cracking load is also shown for comparison.

Table 2.5 *The cracking load, maximum load, and safety factor for Specimens 3 and 4.*

Specimen	Type	Cracking Load, kips (kN)	Maximum Load, kips (kN)	Safety Factor (max load/16 kips)
3	Precast	41 (181)	73 (325)*	4.6*
	Conventional	56 (249)	104 (463)*	6.5*
4	Precast	40 (178)	72 (320)	4.5
	Conventional	40 (178)	56 (249)	3.5

**The maximum loads for these specimens were limited by the loading equipment and do not reflect the actual strength of the specimen.*

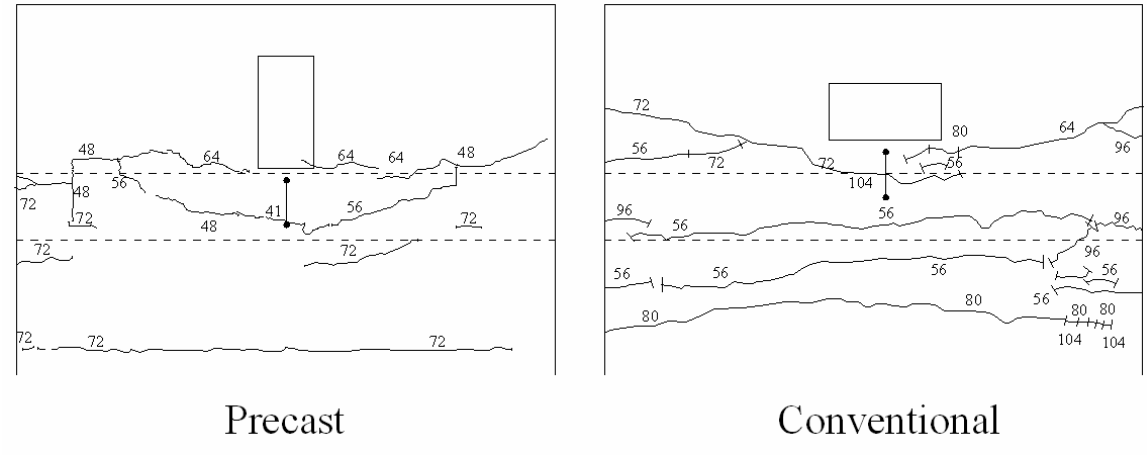

Figure 2.22 *Crack pattern for the conventional and precast systems for the midspan loading investigated in Specimen 3. The surface strain locations are shown with two points connected by a line.*

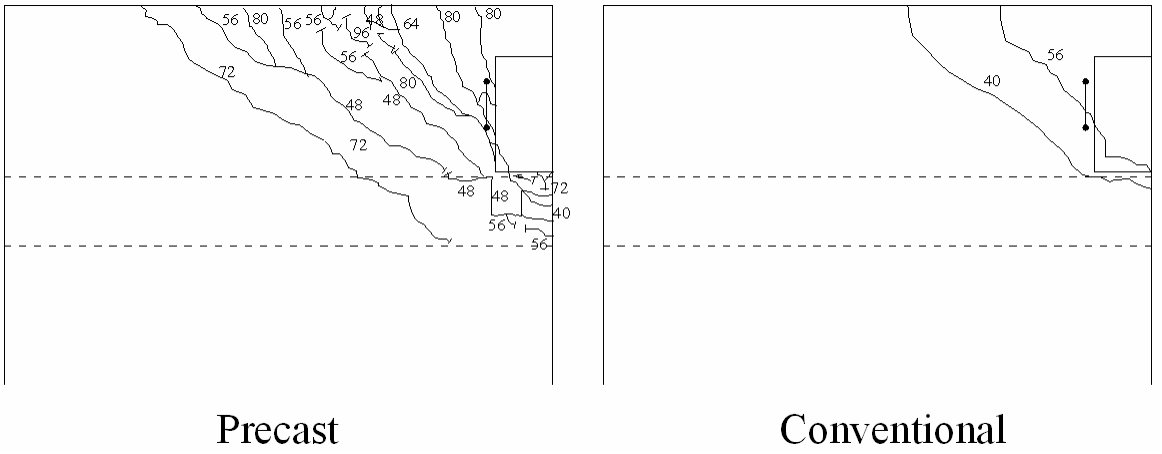

Figure 2.23 *Crack pattern for the conventional and precast systems for the corner loading investigated in Specimen 2. The surface strain location is shown by two points connected by a line.*

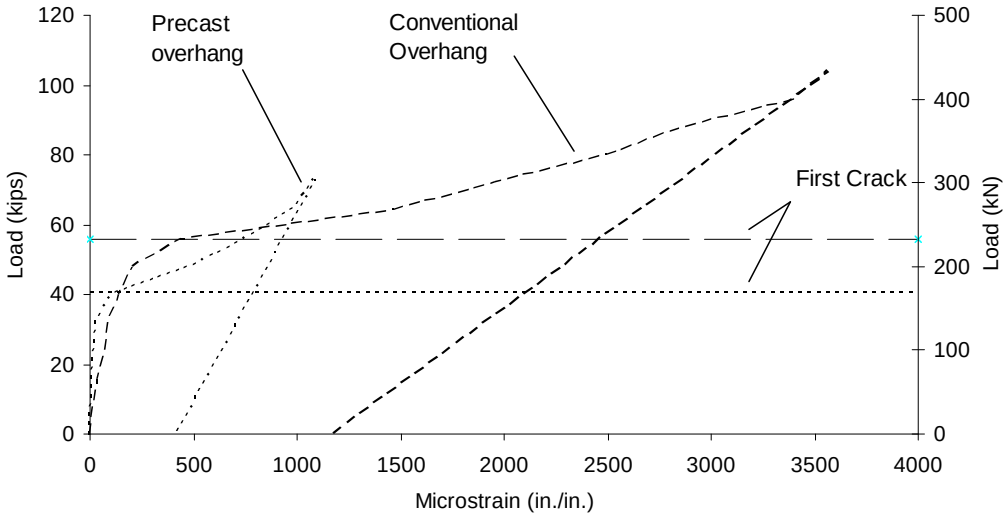

Figure 2.24 *The load versus surface strain for the precast and conventional overhangs for the midspan loading of Specimen 3.*

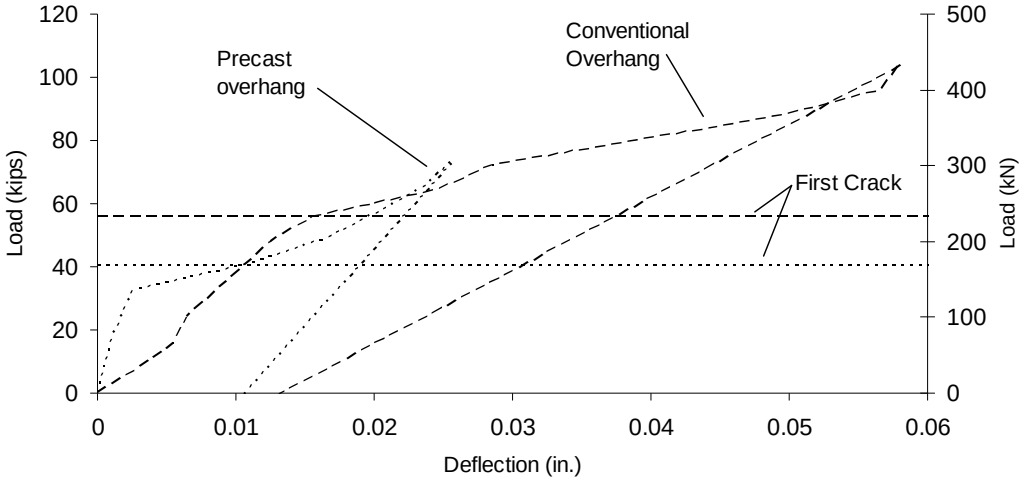

Figure 2.25 *The load versus load point deflection for the precast and conventional overhangs for the midspan loading of Specimen 3.*

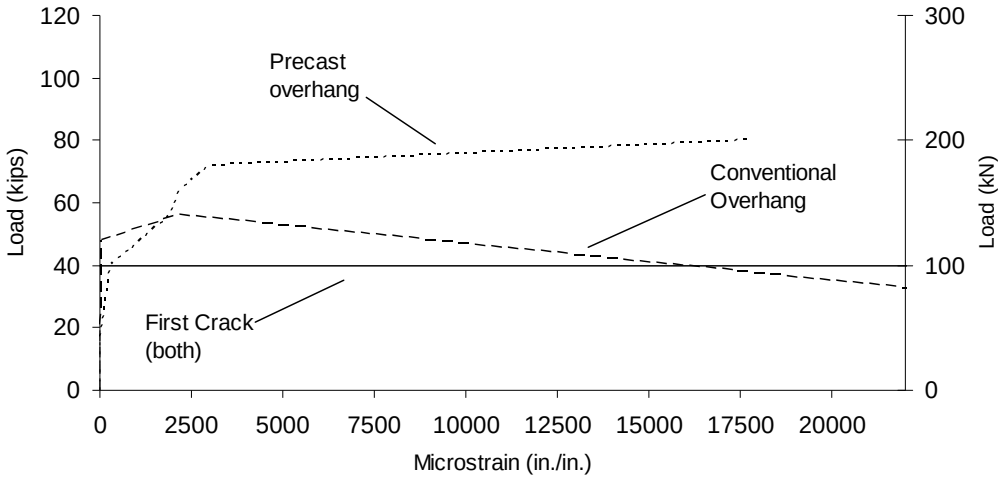

Figure 2.26 *The load versus surface strain for the precast and conventional overhangs for the corner loading of Specimen 4.*

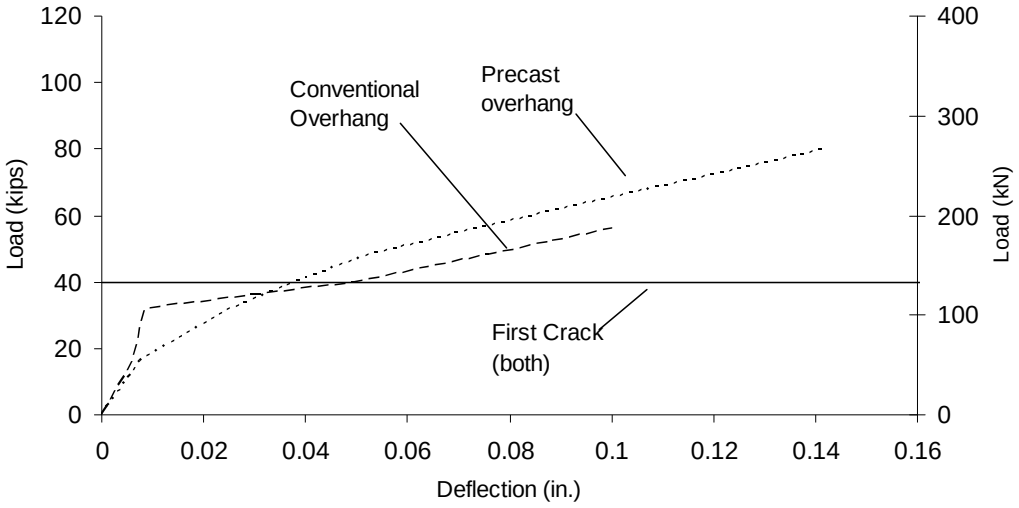

Figure 2.27 *The load versus load point deflection for the precast and conventional overhangs for the corner loading of Specimen 4.*

2.2.4 Discussion

As is shown in Table 2.5, all of the single-panel systems evaluated provide a satisfactory capacity well beyond the design load. When comparing the capacities of the systems through corner loading, as in the case of Specimen 4, the precast system exhibited a safety factor of 4.5 versus a safety factor of 3.5 for the conventional overhang. This implies that the precast system had a measurable increase in capacity over the conventional overhang.

In Figures 2.24 through 2.27, both systems are shown to provide the ability to strain significantly after the initial cracking of the system. This is a performance that is consistent with the ductile behavior of structures.

Three inadvertent details were introduced into the testing, including rotation of the conventional overhang load point by 90^{o} for Specimen 3, increased amount of compression steel in the conventional overhang in Specimen 3, and the modification of the top layer of reinforcing. In all three cases these modifications are thought to have minimal impact on the measured performance of the final structure. These will be discussed next.

While the load point was rotated by 90^{o}, the centroid of the load point did not change, so the equivalent moment and results between the conventional and precast overhang should be comparable.

It was realized while casting Specimen 4 that excessive compression steel was used in the conventional overhang tested in Specimen 3. While this additional steel would definitely have an impact on the capacity if it was on the tension face of the specimen it should have little impact on the performance of the system because it is in the compression face. The addition of compression steel has very little increase in the capacity of a reinforced concrete member. More information will be provided in the final report.

Upon delivery of the precast overhang panels from Austin Prestressed Co., it was realized that the longitudinal and transverse reinforcing in stage II had been switched. This change in the reinforcing layout should have a reduction in the capacity of the system by approximately 10percent. This is caused because the effective depth of the main reinforcing bars (transverse #5 [#16M] bars at 6-in. [150 mm] spacings) would have been reduced because they were placed under the longitudinal reinforcing. More information will be provided in the final report.

2.2.5 Summary of Single-panel Tests

The single-panel precast overhang system investigated was found to provide comparable strength, stiffness, and ductility when compared with the conventional overhang system. Furthermore, the precast overhang system had a sufficient safety factor of 4.5 above the design load of 16 kips (71 kN) in the corner loading of Specimen 4. A safety factor above 4.6 was found for the midspan loading investigated in Specimen 3. During the testing of both specimens there were no signs of cracking in the precast overhang system until a load of 40 kips (178 kN), 2.5 times the design load. While fatigue testing was not completed on this project, the large factor of safety encountered indicates that the service level stresses are expected to be low, which would indicate satisfactory fatigue performance for the system in service. The conventional overhangs were also found to provide satisfactory strength and cracking performance in this testing.

2.3 Summary for Overhang Panel Test

Testing performed in this research program of both single- and double-panel overhang specimens indicate that the prestressed overhang panels provide reasonably similar performance to conventional CIP overhang systems. Testing indicated that the capacity of the precast overhang system is sufficient to resist significant cracking for AASHTO factored loads and can provide reasonably high factors of safety.

CHAPTER 3. SHEAR CONNECTIONS

Prior to the development of the precast bridge deck overhang system investigated herein, composite action between the stay-in-place precast panels was achieved through girder reinforcement extended beyond the top surface. This reinforcement commonly consisted of inverted U-shaped bars, referred to in TxDOT drawings as R-bars. Continuity was established from a second stage concrete pour, thereby linking a second layer of continuous reinforcement to the existing reinforcement located between the panels at the deck-girder interface. Due to the inherent nature of having a precast overhang, options are needed to achieve precast deck panel to concrete girder composite action through the use of shear pockets within the panels. However, AASTHO LRFD (2007) does not address this design consideration for interface shear transfer (shear friction) in full-depth panels. More specifically, AASHTO LRFD C5.8.4.1 states, "composite section design utilizing full-depth precast deck panels is not addressed by these provisions. Design specifications for such systems should be established by, or coordinated with, the Owner." Therefore, the connection detail of these shear pockets needs to be examined in terms of both force-deformation performance and constructability, and compared to conventional construction to ensure the new precast system is not inferior.

To evaluate the performance and constructability of the shear connection detail, an investigation was conducted on push-off tests of coupon specimens mimicking the proposed design for a bridge replacement project on FM 1885 at Rock Creek, Parker County, Texas. The purpose of the push-off (interface shear) tests was twofold:

1) to determine the initial breakaway shear strength, post-breakaway resistance in terms of the implied coefficient of friction, and ultimate displacement limits of various connectors; and
2) to compare the performance of these connectors to current standard construction practice for cast-in-place deck overhangs.

3.1 Experimental Plan

Several testing combinations were conducted to study the effectiveness of the grout, number of connectors, effects of clustering, and various connection types as shown in the testing matrix

in Table 3.1. These two connector types could provide the Rock Creek Bridge contractor for the full-depth precast panels with two options when using a 1-in. (25 mm) high-strength threaded rod with a nut:

- Option 1 utilizes a coupler that is precast flat with the top of the girder with a bottom anchoring rod extending into the girder and a second top rod that is inserted during the construction process.
- Option 2 uses a continuous rod through the top of the girder, thus simplifying the casting process but reducing flexibility of the construction process.

Therefore, six different shear configurations were tested for validation: threaded rods with a coupler, threaded rods without a coupler, and the CIP control—all with a 2-in. (50 mm) and 3.5-in. (89 mm) haunch. Each of the six connections was tested with two separate specimens, and an additional specimen with two R-bars grouted in a precast pocket was tested to provide additional data—a total of 13 test specimens.

The nomenclature for the test specimens was based on the number of connectors within a specimen, connector type, test number reference, and whether or not the specimen was cast with a 2-in. (50 mm) or 3.5-in. (89 mm) haunch. To assist with some of the abbreviations, a summary of the abbreviations follows:

CIP—specimen is cast-in-place as a monolithic member

T.R.—1-in. (25 mm) diameter high-strength threaded rod (ASTM A193 B7)

Figure 3.1 presents a key to show the designation of the specimen alias. An "A" following the alias indicates that the specimen was cast with a 2-in. (50 mm) haunch, and "B" means that the specimen was cast with a 3.5-in. (89 mm) haunch.

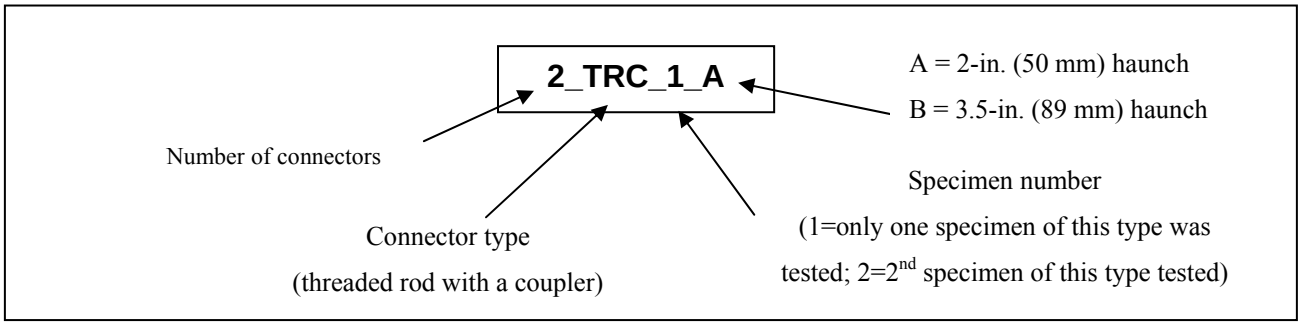

Figure 3.1 *Specimen alias designation key.*

Table 3.1 *Matrix of 2-in. (50 mm) haunch and 3.5-in. (89 mm) haunch (italicized) shear specimens tested.*

Test #	Haunch height	Shear test beam detail	No. of connectors	Connector diameter	Type	f'c for grout or (concrete) in haunch	Specimen alias
1	2-in. (50-mm)	CIP	2	0.5 in. (13 mm)	2-#4 R-bars	9091 psi (62.68 MPa)	4_CIP_1_A
2	2-in. (50-mm)	CIP	2	0.5 in. (13 mm)	2-#4 R-bars	9091 psi (62.68 MPa)	4_CIP_2_A
3	2-in. (50-mm)	T.R. w/coupler	2	1 in. (25 mm)	T.R. w/nut	7023 psi (48.42 MPa)	2_TRC_1_A
4	2-in. (50-mm)	Bolt w/coupler	2	1 in. (25 mm)	T.R. w/nut	6059 psi (41.78 MPa)	2_TRC_2_A
5	2-in. (50-mm)	T.R.	2	1 in. (25 mm)	Nut on T.R.	6059 psi (41.78 MPa)	2_TR_1_A
6	2-in. (50-mm)	T.R.	2	1 in. (25 mm)	Nut on T.R.	6059 psi (41.78 MPa)	2_TR_2_A
7	*3.5 in. (89 mm)*	*T.R. w/coupler*	*2*	*1 in. (25 mm)*	*T.R. w/nut*	*6132 psi (42.28 MPa)*	*2_TRC_1_B*
8	*3.5 in. (89 mm)*	*T.R. w/coupler*	*2*	*1 in. (25 mm)*	*T.R. w/nut*	*6132 psi (42.28 MPa)*	*2_TRC_2_B*
9	2-in. (50-mm)	2 R-bars w/ grout	2	0.5 in. (13 mm)	2-#4 R-bars	7377 psi (50.86 MPa)	4_R_A
10	*3.5 in. (89 mm)*	*T.R.*	*2*	*1 in. (25 mm)*	*Nut on T.R.*	*6200 psi (42.75 MPa)*	*2_TR_1_B*
11	*3.5 in. (89 mm)*	*T.R.*	*2*	*1 in. (25 mm)*	*Nut on T.R.*	*6200 psi (42.75 MPa)*	*2_TR_2_B*
12	*3.5 in. (89 mm)*	*CIP*	*2*	*0.5 in. (13 mm)*	*2-#4 R-bars*	*5706 psi (39.34 MPa)*	*4_CIP_1_B*
13	*3.5 in. (89 mm)*	*CIP*	*2*	*0.5 in. (13 mm)*	*2-#4 R-bars*	*5706 psi (39.34 MPa)*	*4_CIP_2_B*

3.2 Design of Experiment

The design of the shear test specimens was developed in conjunction with the design and casting of the full-scale testing components to maximize efficiency and minimize experimental differences. To accommodate the two 8-ft. (2.4 m) full-depth precast panels, 16-ft. (4.9 m) girders were cast for use in the full-scale test; the same 16-ft. (4.9 m) design was made into 4-ft. (1.2 m) quarter-beams for the purposes of the shear testing. Full-depth deck specimens for the shear tests were cast with a thickness of 8 in. (200 mm) and 7- x 10-in. (175 x 250 mm) pockets to match the design of the full-depth precast panels. The shear test panels were cast nominally 2-ft. (0.6 m) square to allow for two specimens to be tested on each 4-ft. (1.2 m) beam.

Photographs and a schematic of the experimental test setup are shown below in Figure 3.2. A 600-k (2670 kN) actuator pushes off a column that is prestressed to the laboratory strong floor

to produce the shear force, which is transferred to the deck portion of the specimen via two W14x109 spreader beams via four high-strength tension rods. The shear test beam is anchored down to the strong floor of the laboratory with high-strength prestressing threadbar; this is to minimize slip and beam uplift. A wood reaction block between the shear test beam and the column provides additional lateral reaction to inhibit specimen sliding.

(a)

(b)

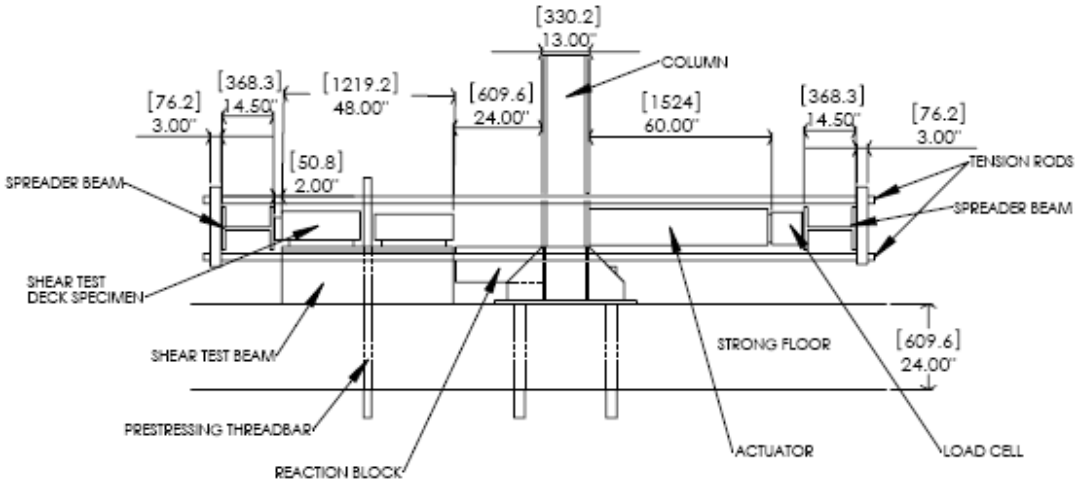

(c)

Figure 3.2 *Experimental test setup: (a) Photograph from laboratory floor; (b) Photograph from laboratory balcony; (c) Side elevation.*

3.3 Construction Process and Testing Procedure

During the construction process of the prototype Rock Creek bridge, girder curvature and deck grading are expected to vary along the haunch depth from 2 in. (50 mm) to 3.5 in. (89 mm); therefore, the shear tests investigated the connection strength of both 2-in. (50 mm) and 3.5-in. (89 mm) haunch specimens. Per TxDOT's standard bridge drawings, an extension of the shear stirrups was added for the CIP specimens when the haunch height was greater than or equal to 3 in. (75 mm). For the precast shear specimens, #4 [#13M] longitudinal bars are expected to be added on the outside of the threaded rod, similar to an existing detail for casting additional concrete atop precast girders in TxDOT standard bridge drawings. Figure 3.3 shows the details of the T.R. shear connections for the 2-in. (50-mm) and 3.5-in. (89-mm) haunch, and Figure 3.4 shows the same for the CIP specimens.

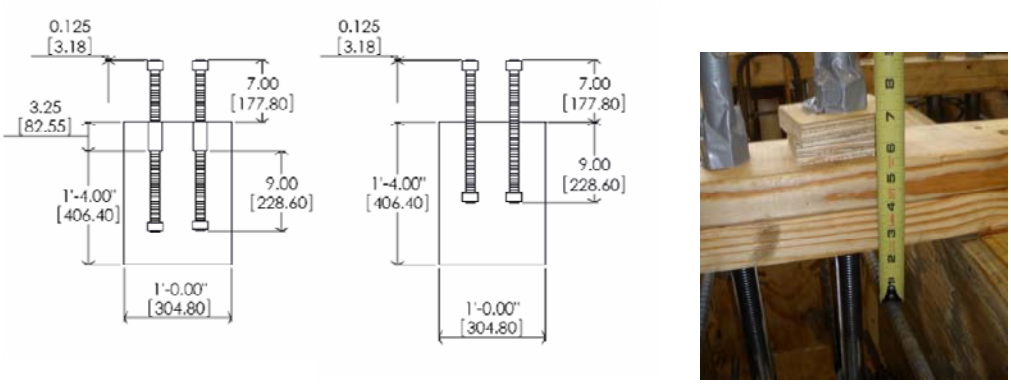

Option 1 **Option 2**

(a) Shear connectors for 2-in. (50 mm) haunch

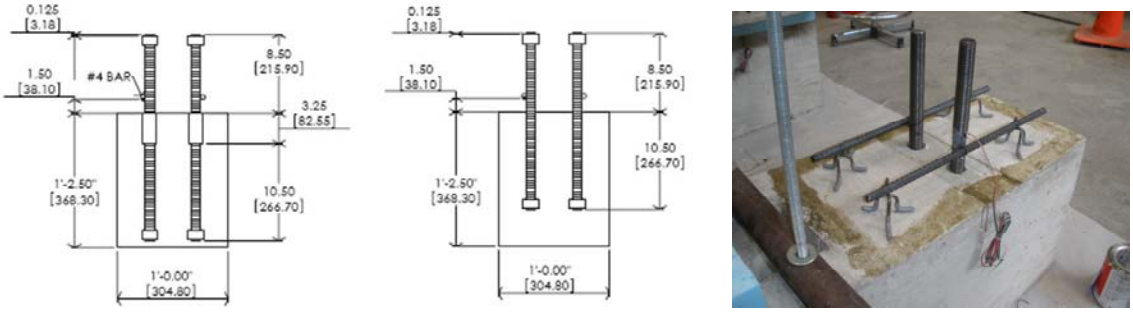

Option 1 **Option 2**

(b) Shear connectors for 3.5-in. (89 mm) haunch

Figure 3.3 *Beam cross sectional views of shear connectors and photographs of the T.R. shear connections tested.*

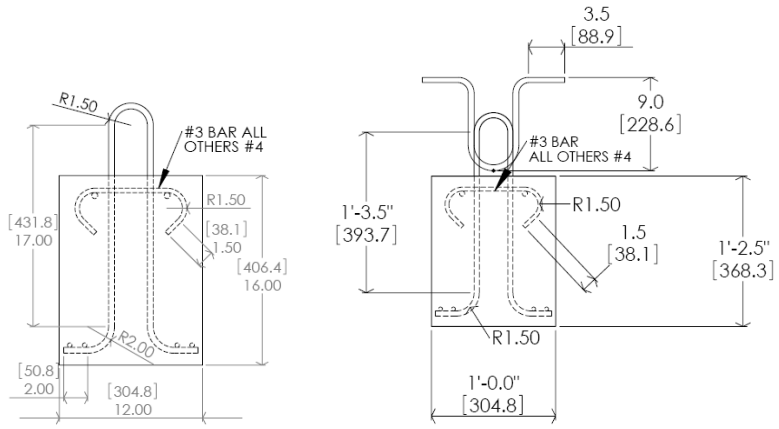

(a) 2-in. (50 mm) haunch *(b) 3.5-in. (89 mm) haunch*

Figure 3.4 *CIP details of beam-to-slab shear connections.*

Four different reinforcing details were used for the construction of the shear test beams in order to account for different shear connections and haunch heights. The shear beams for the 3.5-in. (89 mm) haunch specimens were cast 1.5-in. (38 mm) shorter than those for the 2-in. (50 mm) haunch specimens so that the assembled specimens all placed the shear test deck at the same height, permitting use of the same test setup without modifying the height of the line of action. The same reinforcement was used in the shear test beams for both of the precast (threaded rod) options for each of the haunch heights, so four different shear test beam reinforcement details were utilized, as shown below in Figure 3.5.

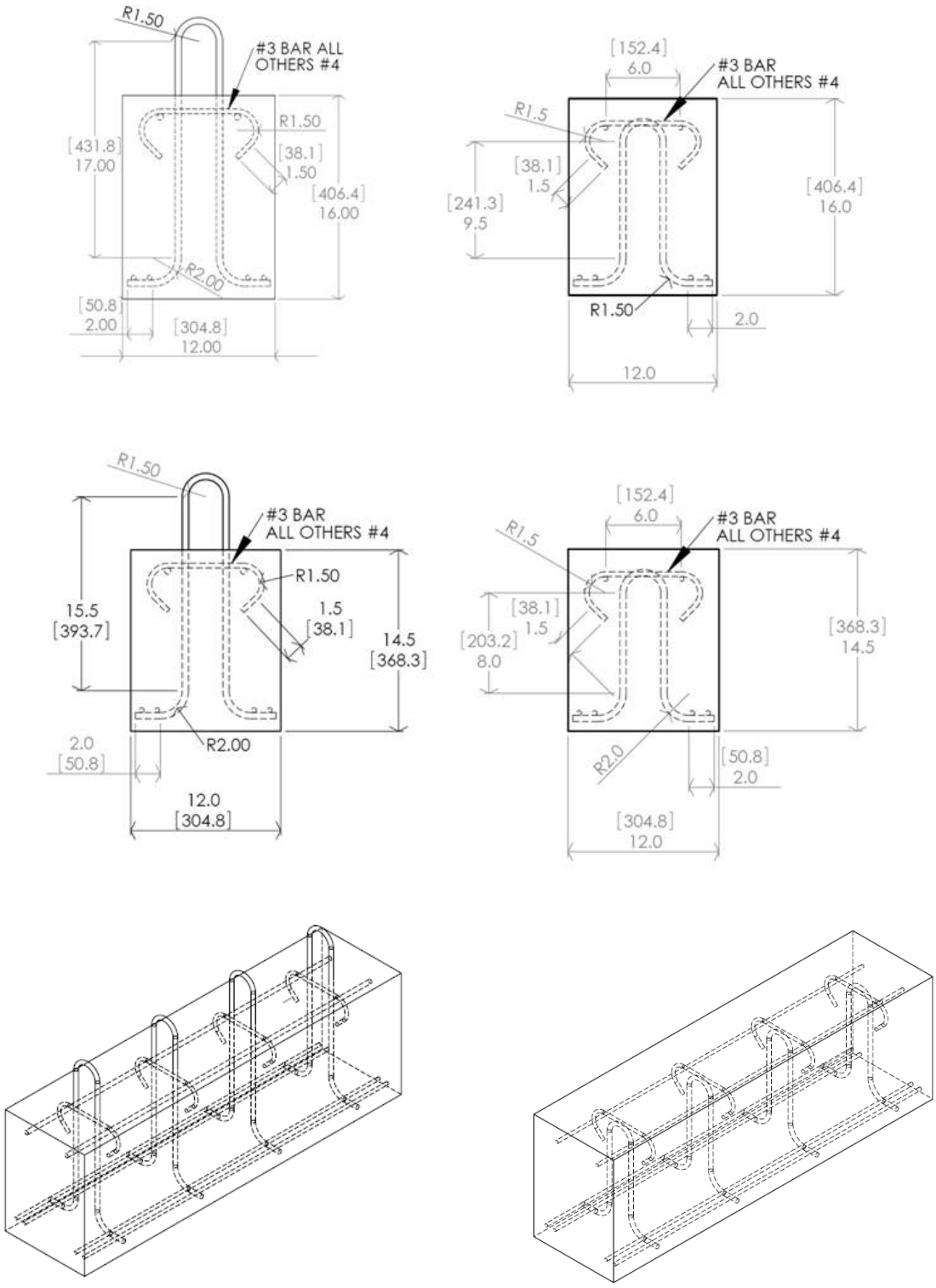

Figure 3.5 *Reinforcing details for shear test beams. Clockwise from top-left: 2-in. (50 mm) haunch CIP, 2-in. (50 mm) haunch precast, 3.5-in. (89 mm) haunch precast, and 3.5-in. (89 mm) CIP.*

The reinforcing of the precast shear deck specimens (shown in Figure 3.6) matches the details of the precast full-depth overhang panels, utilizing #4 (#13M) bars in place of the #3 (#10M) prestressing strands as prescribed.

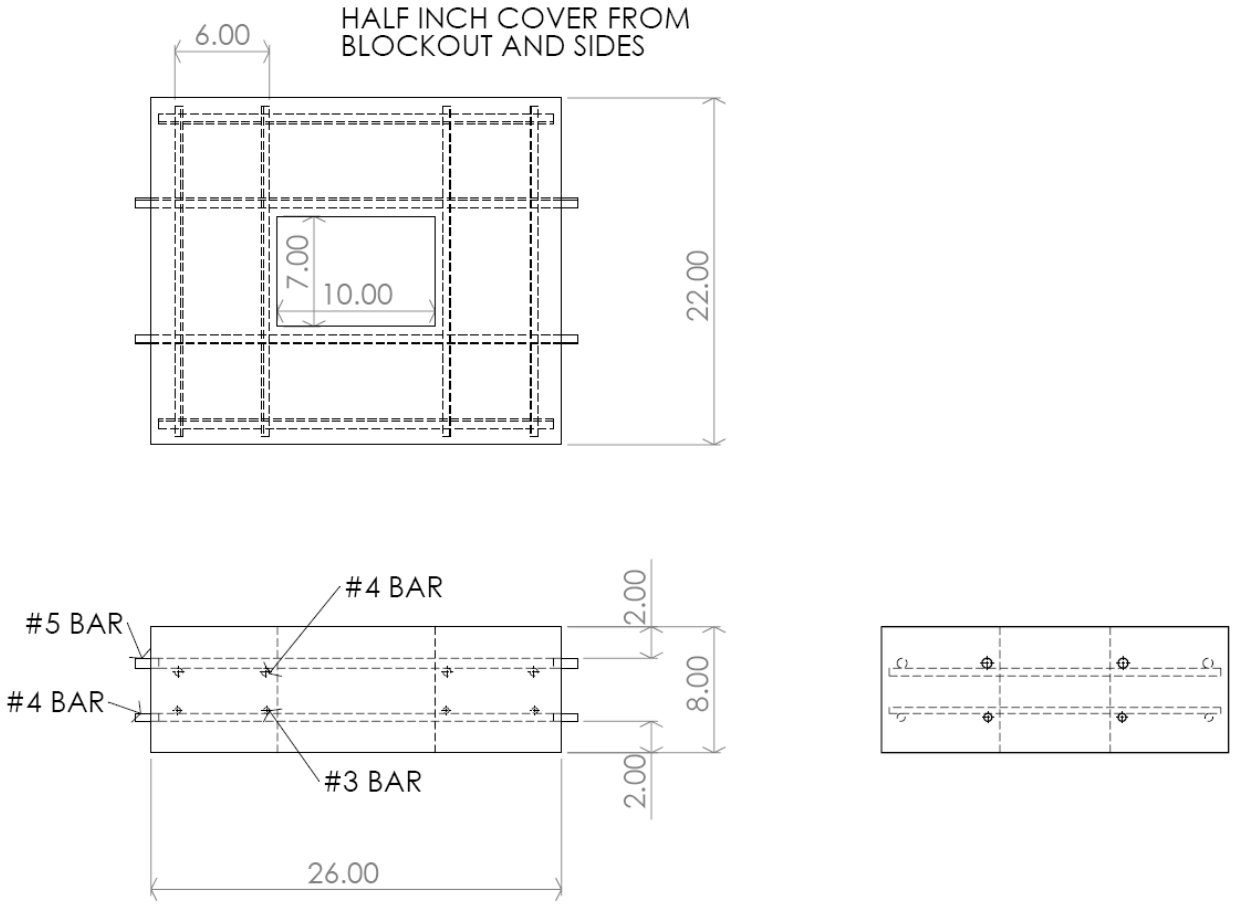

Figure 3.6 *Reinforcement layout of the precast shear deck specimens.*

The reinforcing of the CIP shear deck specimens (shown below in Figure 3.7) matches that of the full-scale specimen at the interior beam. It is similar to the precast shear deck specimen, but all of the bars are evenly spaced since there is no pocket to accommodate, and the bottom transverse steel is not continuous, simulating the edges of the two partial-depth precast panels resting on the girder.

Figure 3.7 *Photograph of reinforcing of a CIP shear test specimen..*

The construction process and testing procedure are outlined as follows:

1. Cast shear test beams and decks.
2. Grout/cast completed test specimens (two per shear test beam).
3. Assemble shear test frame.
4. Insert a fully constructed test specimen into the shear test frame.
5. Load test frame to 10 k (45 kN) to close any gaps, and then remove load.
6. Post-tension the tie-down high-strength prestressing threadbar. This is located at the center of each shear test beam. Apply a force of 120 k (530 kN) (before anchorage losses) using a center-hole jack system.
7. Load test frame continuously at approximately 0.15 kips/s (0.67 kN), quasi-statically, until specimen failure or approximately 1-in. (25 mm) deformation (clearance limit).
8. Unload test frame and shear test beam center anchor.
9. Turn shear test beam 180° for second specimen and repeat 5-8.
10. Repeat 4-9 for testing remaining shear specimens.

The key measurement that must be acquired from the shear tests is the displacement of the shear test deck specimen relative to the shear test beam. This is accomplished with a linear variable differential transducer (LVDT) mounted on each longitudinal face of the shear test beam pushing against a reaction angle mounted to the bottom of the shear test deck specimen and aligned with its transverse centerline. By utilizing an LVDT on each side, the amount of skew that the shear test deck specimen experiences during loading can be assessed. Two string potentiometers were attached to the vertical face of the shear test beam and attached to the side

of the beam, and connected to the soffit of the deck panel unit under test. These potentiometers indicate the degree of uplift and rotation of the deck panel unit with respect to the support beam. A photograph of the instrumentation on the specimen is shown in Figure 3.8.

Figure 3.8 *Photograph of LVDTs and string potentiometers connected to a shear test specimen.*

A 2000-kip (8900-kN) capacity load cell was attached in series to the actuator to provide accurate measure of the actual load applied to the shear test frame and shear test specimen. Half-bridge strain gauges were attached to one of the threaded rods or stirrup legs to provide information on the strain and tension the shear connector experienced during the test.

3.4 Materials

The shear test concrete specimen components were cast simultaneously with the full-scale test specimen whenever possible to maximize efficiency. Concrete was provided by Transit Mix (Bryan, Texas), with a mix designed for 4-in. (102 mm) slump specified 28-day strength of 4000 psi (28 MPa). More information about the compressive strengths of the concrete used in the different test specimens can be found in Chapter 2, *Bridge Overhang System*. Standard grade 60 rebar was used throughout reinforced concrete components, with #3 (#10M), #4 (#13M), and #5 (#16M) bars used as shown in the reinforcing details. For the precast shear connectors, 1-in. (25-

mm) high-strength T.R. (ASTM A193 B7) were used with high-strength (2H) nuts. This threaded rod has a specified minimum yield and ultimate tensile strengths of 105 and 125 ksi (724 and 862 MPa), respectively. Tensile tests were conducted to verify the tensile capacity of both the rebar and threaded rods used for the validation tests. The measured yield and tensile strengths of the #4 (#13M) rebar stirrups were 63 and 100 ksi (434 and 689 MPa), respectively. The measured yield and tensile strengths of the T.R. were 120 and 137 ksi (827 and 945 MPa), respectively, with a complete stress-strain curve shown in Figure 3.9. The shear connection specimens per "Option 1" were followed in accordance with the initial *Prestressed Concrete I-Beam Details External Beams* that were prescribed with 3.5-in. (89-mm) couplers.

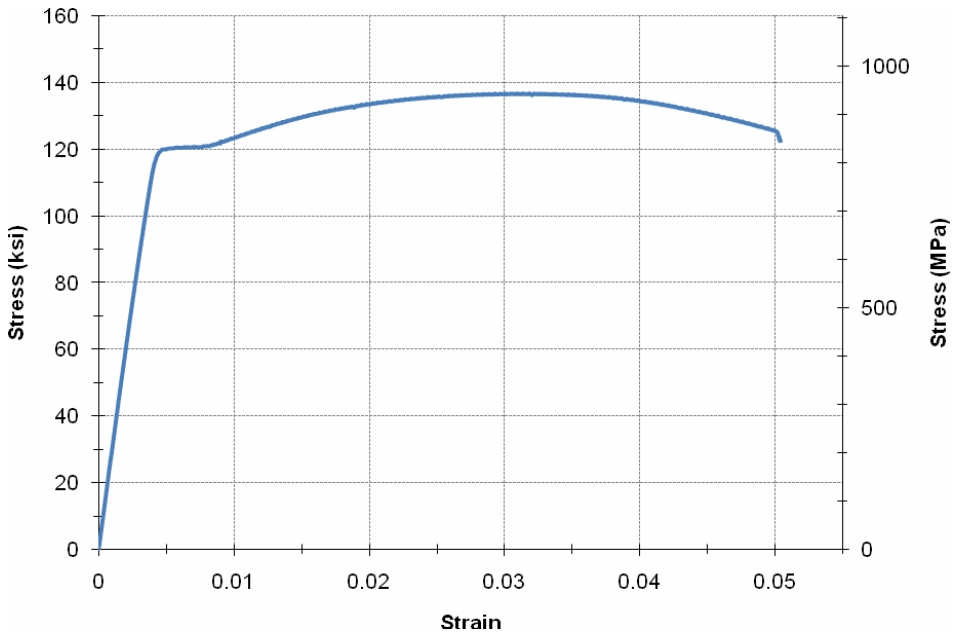

Figure 3.9 *Stress-strain curve from tensile test of one high-strength threaded rod (ASTM A193 B7).*

A proprietary grout (SikaGrout™ 212) was used for the assembly of the shear test specimen components. A 0.19 w/p was used for filling the haunch for its maximum strength while providing minimum flow characteristics to fill the haunch. To fill the pockets of the shear test specimens, a 0.16 w/p was initially used, but issues with subsidence cracking and the relative expense of the grout led to later specimens' pockets being filled with deck concrete from another pour. Table 3.2 shows the details for the compressive strengths achieved at the time of testing for

the shear test deck, beam, and haunch. More information about the grout used and material properties of the concrete used can be found in Chapter 4, *Materials,* Section 4.1.

Regardless of the pocket filling material, the shear test specimens were assembled in the same manner. A 2-in. (50 mm) wide strip of stiff foam (Dow 40) was bonded to the shear test beam using a plastic adhesive (3M Scotch-Grip 4693). Another coating of the adhesive was applied to the top of the foam, and the shear test deck was placed on top. After 20 to 30 minutes of curing, the haunch grout was mixed and poured into the haunches through the pockets up to a level of approximately 1 in. (25 mm) above the bottom of the shear test deck to ensure the haunch was completely filled. After the haunch grout had reached initial set (approximately 5 hours), the pocket grout/concrete was added and the specimen's surface was finished to as smooth a surface as possible.

Table 3.2 *Matrix of compressive strengths for shear test haunch, deck, pocket, and beam.*

Test #	Specimen alias	Haunch		Shear test deck		Shear test beam	
		Height Inches (mm)	f'c [psi] for grout (concrete)	f'c [psi] for deck	f'c [psi] for grout (concrete) in pocket	Connection type	f'c [psi] for concrete beam
1	4_CIP_1_A	2-in. (50-mm)	(9091)	9091	(9091)	CIP	6236
2	4_CIP_2_A	2-in. (50-mm)	(9091)	9091	(9091)	CIP	6236
3	2_TRC_1_A	2-in. (50-mm)	7023	7023	8314	T.R. w/coupler	5938
4	2_TRC_2_A	2-in. (50-mm)	6059	6059	(5354)	Bolt w/coupler	7340
5	2_TR_1_A	2-in. (50-mm)	6059	6059	(5354)	T.R.	6129
6	2_TR_2_A	2-in. (50-mm)	6059	6059	(5354)	T.R.	6129
7	*2_TRC_1_B*	*3.5 in. (89 mm)*	*6132*	*6132*	(5354)	*T.R. w/coupler*	*6129*
8	*2_TRC_2_B*	*3.5 in. (89 mm)*	*6132*	*6132*	(5354)	*T.R. w/coupler*	*6129*
9	4_R_A	2-in. (50-mm)	7377	7377	8314	2 R-bars w/ grout	7340
10	*2_TR_1_B*	*3.5 in. (89 mm)*	*6200*	*6200*	*(5354)*	*T.R.*	*6129*
11	*2_TR_2_B*	*3.5 in. (89 mm)*	*6200*	*6200*	*(5354)*	*T.R.*	*6129*
12	*4_CIP_1_B*	*3.5 in. (89 mm)*	*(5706)*	*5706*	*(5706)*	*CIP*	*6129*
13	*4_CIP_2_B*	*3.5 in. (89 mm)*	*(5706)*	*5706*	*(5706)*	*CIP*	*6129*

3.5 General Results

The results from the present interface shear tests are intended to demonstrate the efficacy of the deck-haunch-beam system working as a composite system. From the data collected, plots of

the applied lateral load versus relative displacement of the deck to the beam of the 13 shear specimens tested are shown in Figure 3.10.

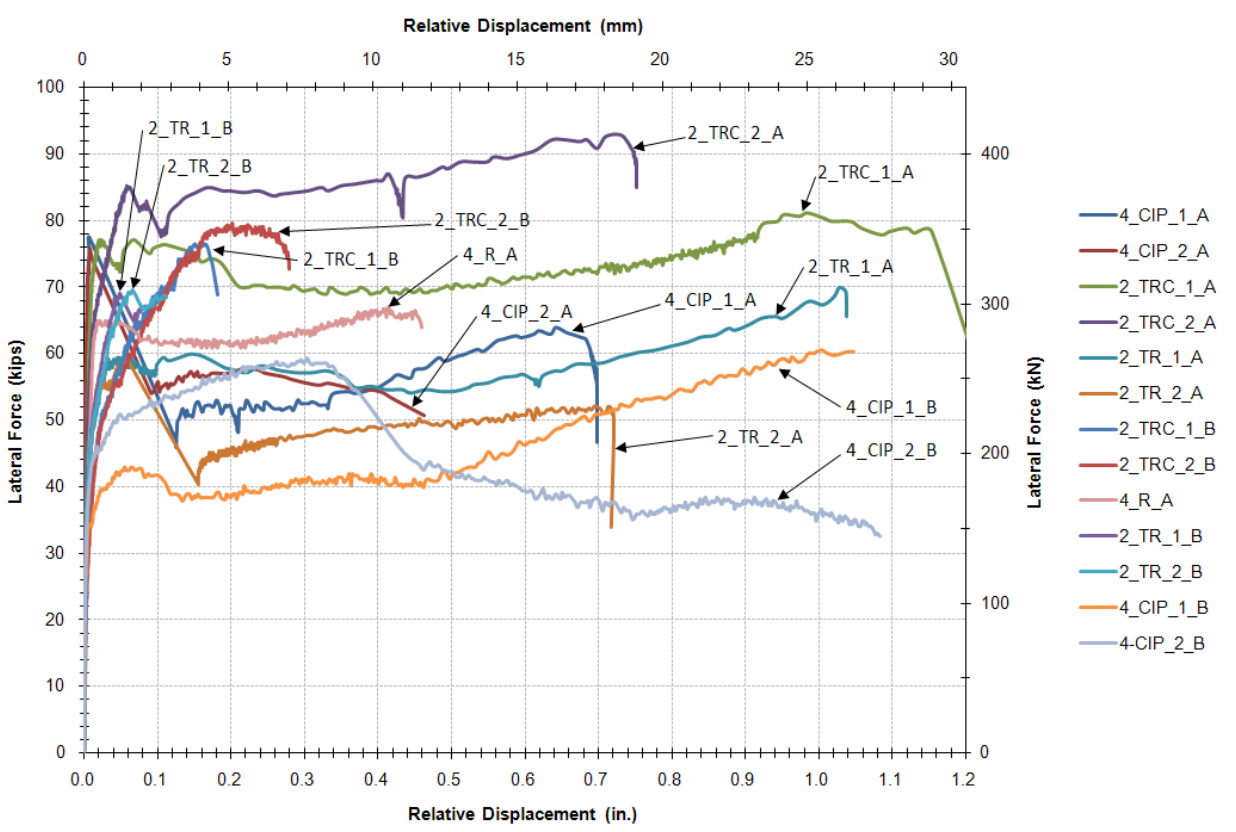

Figure 3.10 *Lateral force versus relative displacement for all 13 shear specimens.*

In general, there are five stages of behavior that are exhibited, as follows:

1. Initially, resistance is provided by the bond of the grout (or concrete in the case of conventional construction) between the precast deck panels and concrete beam. This stiff system is sustained until the bond between the grout and panels (or shear test beam) suddenly breaks. Results indicate that the initial breakaway force occurs at a displacement of approximately 0.01 to 0.06 in. (0.25 to 1.5 mm) at an approximate shear stress on the haunch of $6\sqrt{f'c}$ [psi] ($0.5\sqrt{f'c}$ [MPa]).
2. Following breakaway, there is often a sudden drop off in resistance until the shear connectors (or R-bars in the case of the conventional construction) engage in tension and direct shear. This may not occur until the displacement has reached 0.1 to 0.16-in. (2.5 to 4 mm).
3. As the lateral displacement increases, the deck panel uplifts in the vicinity of the fasteners, which in turn, elongate and provide a tie-down restraint force. This force is in turn resisted by a normal concrete beam-to-grout-to-panel

compression nearby. The horizontal component of this compression force is a frictional force that resists the applied lateral load. Thus, a frictional sliding deck panel-to-beam mechanism results. This tends to stabilize from displacements ranging from 0.2 in. (5 mm) to 0.6 in. (15 mm). This stable force appears to result from yielded connectors.

4. As the displacements become large, the resistance increases slightly, which is attributed to strain-hardening of the connectors.
5. Failure of a well-performing system tends to take place when the displacements exceed approximately 0.7 in. (18 mm). Failure may result from the following:
    - grout crushing
    - beam anchorage/shear failure
    - R-bar pull-out from deck panel (cone failure), and/or
    - shear failure of the connector.

To verify this, two opposing strain gauges were attached to one connector within each test specimen. The data captured by the string potentiometers and LVDTs provided the numerical values for the relative displacements both horizontally and vertically, and enabled computations for the axial tension and implied coefficient of friction. The vertical tie-down force (axial tension) was calculated and is shown in Table 3.3. The raw experimental data for all of the specimens with a 2-in. (50 mm) and 3.5-in. (89 mm) haunch is shown in Table 3.4.

The data were analyzed and calculations were made to determine the concrete shear stress at the breakaway resistance and implied friction coefficient, and to identify the failure mode per specimen. From the data, the concrete shear stress at the breakaway force is computed and normalized to determine the mean modulus of rupture of the concrete, which is 6.4 $\sqrt{f'c}$. As a lower bound for strength calculations, it would be reasonable to use $6\sqrt{f'c}$ for design or assessment calculations. As expected, the CIP specimens exhibit a larger coefficient of friction. Depending on the roughness of the interface surface, the coefficient of friction can vary. The dependable coefficient of friction from these tests at 0.2 in. (5 mm) and 0.5 in. is approximately 0.4.

Table 3.3 *Raw experimental data for 2-in. (50 mm) and 3.5-in. (89 mm) haunch (italicized) specimens.*

Test #	Specimen alias	Initial peak displacement, in. (mm) (a)	Initial peak force, kips (kN) (a)	Force @ 0.2 in. (50 mm), kips (kN) (b)	Peak load (past initial) [kips (kN)] (c)	Ultimate displacement [in. (mm)] (d)	Vertical tie-down force [kips (kN)]	
							@ Yield	@ Ultimate
1	4_CIP_1_A	0.008 (0.203)	77 (342)	51 (227)	64 (285)	0.70 (17.8)	50 (222)	79 (351)
2	4_CIP_2_A	0.008 (0.203)	76 (338)	58 (258)	58 (258)	1.18 (30.0)	50 (222)	79 (351)
3	2_TRC_1_A	0.066 (1.67)	77 (342)	70 (311)	81 (360)	1.57 (39.9)	125 (556)	142 (632)
4	2_TRC_2_A	0.058 (1.47)	85 (378)	84 (374)	93 (414)	0.75 (19.1)	125 (556)	142 (632)
5	2_TR_1_A	0.130 (3.30)	59 (262)	58 (258)	70 (311)	1.04 (26.4)	125 (556)	142 (632)
6	2_TR_2_A	0.056 (1.42)	59 (262)	45 (200)	52 (231)	0.72 (18.3)	125 (556)	142 (632)
7	*2_TRC_1_B*	*0.164 (4.16)*	*76 (338)*	*64 (285)*	*76 (338)*	*0.41 (10.4)*	*125 (556)*	*142 (632)*
8	*2_TRC_2_B*	*0.201 (5.11)*	*80 (356)*	*79 (351)*	*80 (356)*	*0.35 (8.89)*	*125 (556)*	*142 (632)*
9	4_R_A	0.034 (0.864)	65 (289)	61 (271)	67 (298)	1.03 (26.2)	50 (222)	79 (351)
10	*2_TR_1_B*	*0.048 (1.22)*	*69(307)*	*NA*	*67 (298)*	*0.08 (2.03)*	*50 (222)*	*79 (351)*
11	*2_TR_2_B*	*0.067 (1.70)*	*69 (307)*	*NA*	*69 (307)*	*0.11 (2.79)*	*125 (556)*	*142 (632)*
12	*4_CIP_1_B*	*0.055 (1.40)*	*43 (191)*	*39 (173)*	*61 (271)*	*1.37 (34.8)*	*50 (222)*	*79 (351)*
13	*4_CIP_2_B*	*0.014 (0.356)*	*45 (200)*	*57 (254)*	*58 (258)*	*1.16 (29.5)*	*50 (222)*	*79 (351)*

Note: NA = not achieved

Table 3.4 *Analysis of data for 2-in. (50 mm) and 3.5-in. (89 mm) haunch (italicized) specimens.*

Test #	Specimen alias	v_{ui} [ksi (MPa)]	$v_u/\sqrt{f'_c}$	$V/(A_{sv}f_y)$		Observed failure mode
				@ 0.2-in (5 mm)	@ 0.5-in (13 mm)	
1	4_CIP_1_A	0.435 (3.00)	6.9	1.04	1.2	Sliding shear – R-bar
2	4_CIP_2_A	0.431 (2.97)	7.0	1.16	0.95	Sliding shear
3	2_TRC_1_A	0.438 (3.02)	6.1	0.56	0.56	Sliding shear – beam failure
4	2_TRC_2_A	0.484 (3.34)	5.1	0.67	0.51	Sliding shear
5	2_TR_1_A	0.337 (2.33)	7.3	0.46	0.43	Sliding shear – cone failure
6	2_TR_2_A	0.337 (2.33)	7.3	0.36	0.51	Sliding shear
7	*2_TRC_1_B*	*0.435 (3.00)*	*5.7*	*0.02*	-	*Sliding shear*
8	*2_TRC_2_B*	*0.435 (3.00)*	*5.7*	*0.63*	-	*Sliding shear*
9	4_R_A	0.369 (2.55)	7.4	0.49	-	Sliding shear
10	*2_TR_1_B*	*0.392 (2.71)*	*6.4*	*NA*	-	*Brittle shear – beam failure*
11	*2_TR_2_B*	*0.395 (2.73)*	*6.3*	*NA*	-	*Brittle shear – beam failure*
12	*4_CIP_1_B*	*0.244 (1.68)*	*9.8*	*0.79*	*0.85*	*Sliding shear*
13	*4_CIP_2_B*	*0.255 (1.76)*	*9.4*	*1.16*	*0.85*	*Sliding shear*

NA = not achieved

Note: v_{ui} = shear stress at initial breakaway, $v_u/\sqrt{f'_c}$ = normalized shear stress, V = lateral force, A_{sv} = combined connector area, and f_y = connector yield force.

The plots of the lateral force versus relative displacement also reveal the ductility of the connector. Continuous threaded rods exhibited the least amount of ductility for satisfactory performance given a 3.5-in. (88 mm) haunch due to large forces that were transmitted that the shear test beam could not handle, resulting in a brittle shear failure of the beam. However, the continuous threaded rod within the 2-in. (50 mm) haunch seemed to reveal reasonable ductility. Figure 3.11 shows an interpretive schematic to classify the performance of the connector based on its ductility. Connectors experiencing ultimate displacements less than 0.2 in. (5 mm) can be considered as brittle with unsatisfactory ductility. Ultimate displacements in the range of 0.2 in. (5 mm) to 0.5 in. (13 mm) can be considered having satisfactory ductility, and connectors with displacements greater than 0.5 in. (13 mm) can be considered as ductile with above-satisfactory ductility.

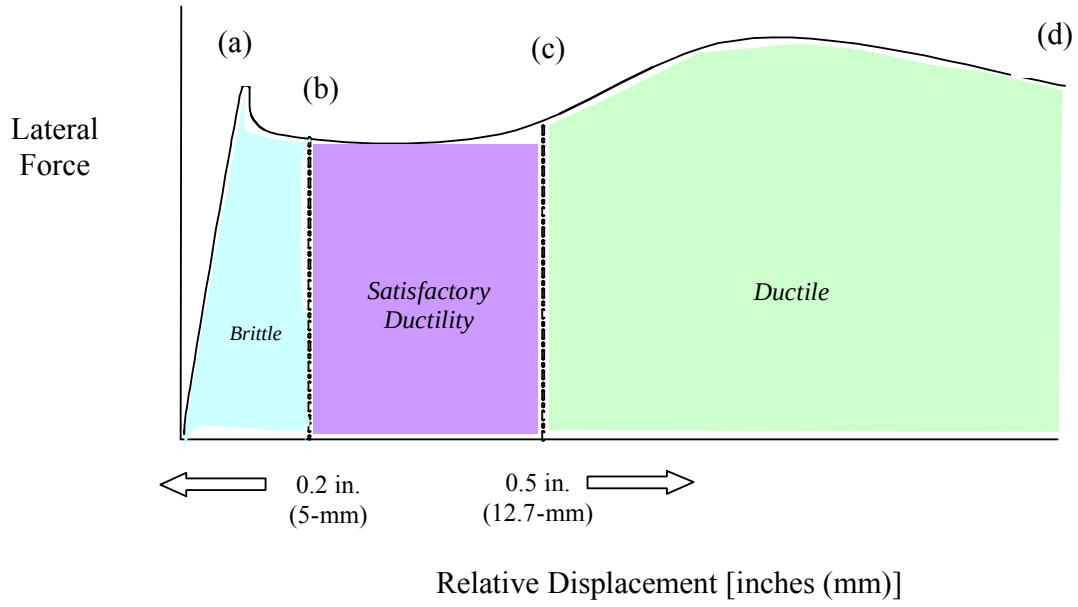

Figure 3.11 *Typical plot of lateral force versus relative displacement for shear specimens with critical parameters from Table 3.3 noted.*

3.6 Analysis of Interface shear for the Two Forms of Construction

3.6.1 Conventional Construction with R-bars

Figure 3.12 presents the normalized force-deformation behavior of conventional construction (reflective of present practice for both the 2-in. (50 mm) and 3.5-in. (89 mm) haunch. When the lateral relative displacements exceed 0.2 in. (5 mm), the R-bars have generally yielded. Also, in most cases the lateral force resistance increased when the displacements exceeded about 0.5 in. (13 mm). This is attributed to the increase in the R-bar tie-down force resulting from the strain-hardening of those bars. Consequently, the lateral resistance in this range of relative displacements is indicative of the coefficient of friction of the cracked concrete-concrete interface that develops between the beam and the deck.

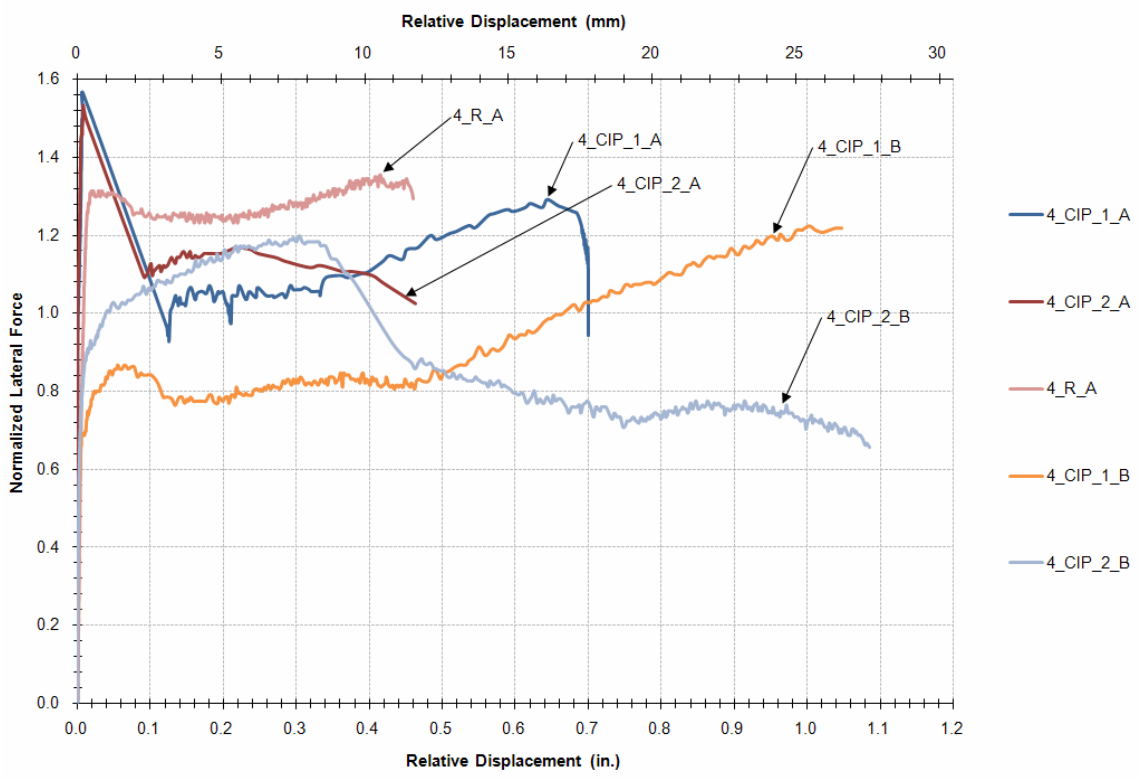

Figure 3.12 *Normalized lateral force versus relative displacement: Specimens with R-bar shear connection.*

Evidently, a dependable (i.e., conservative) value for the friction coefficient that can be assured for this class of construction is

$$\mu_c = 1 \tag{3.1}$$

Therefore, the interface shear, per unit length, provided by the R-bars is given by

$$V_{in} = \mu_c \frac{A_{sh} f_{yh}}{s} \tag{3.2}$$

where A_{sh} = area of R-Bars (hoops) in one hoopset; f_{yh} = yield stress of the R-bars/hoops; s = center-to-center spacing of the hoopsets; and μ_c = dependable coefficient of friction at the sliding interface shear surface.

From the results presented in Figure 3.12, it is also evident that for new or alternate shear systems a target (dependable) displacement limit should be set at 0.5 in. (12 mm). For this class of precast concrete slab-on-girder bridge, this 0.5-in. (12 mm) target deformability capability is considered sufficient, given that full composite deck-to-girder action is to be expected.

If alternative interface shear anchorage systems are to be introduced with equivalence to the standard R-bar system, then applying (3.1) and (3.2), the number of shear-connectors required to restrain one panel is found from

$$n \geq \frac{\mu_c A_{sh} f_{yh} / s}{\mu_g A_{sf} f_{yf}} \cdot l_p \tag{3.3}$$

where l_p = length of the precast deck panels, typically 8 ft. (2.4-m); A_{sf} = area of one threaded rod connector; f_{yf} = yield stress of the fasteners; and μ_g = coefficient of friction of the infill grout-to-panel soffit concrete interface. Note that a displacement capability > 0.5 in. (127 mm) should also be attained.

3.6.2 Threaded Rod in Pocket Shear Connectors

Although the initial breakaway behavior of the proposed system with threaded rod shear connectors was similar to those conventional specimens with R-bars, as shown in Fig 3.12, the post-breakaway behavior is somewhat different. Figure 3.13 presents the normalized lateral force applied to the specimens versus the relative lateral displacement. As mentioned above, providing the fastener has yielded, which appears to be the case when the displacements reach

approximately 0.2 in. (5 mm), the horizontal lines on the graphs are indicative of the sliding friction coefficient. Clearly this response is uniformly inferior to the R-bar specimens, not because of the connectors *per se*, but rather due to the presence of a different infill grout material. There are two reasons for this:

1. different frictional sliding performance, and
2. different displacement limits due to the high concentration of forces anchored in the beams.

These features are discussed next.

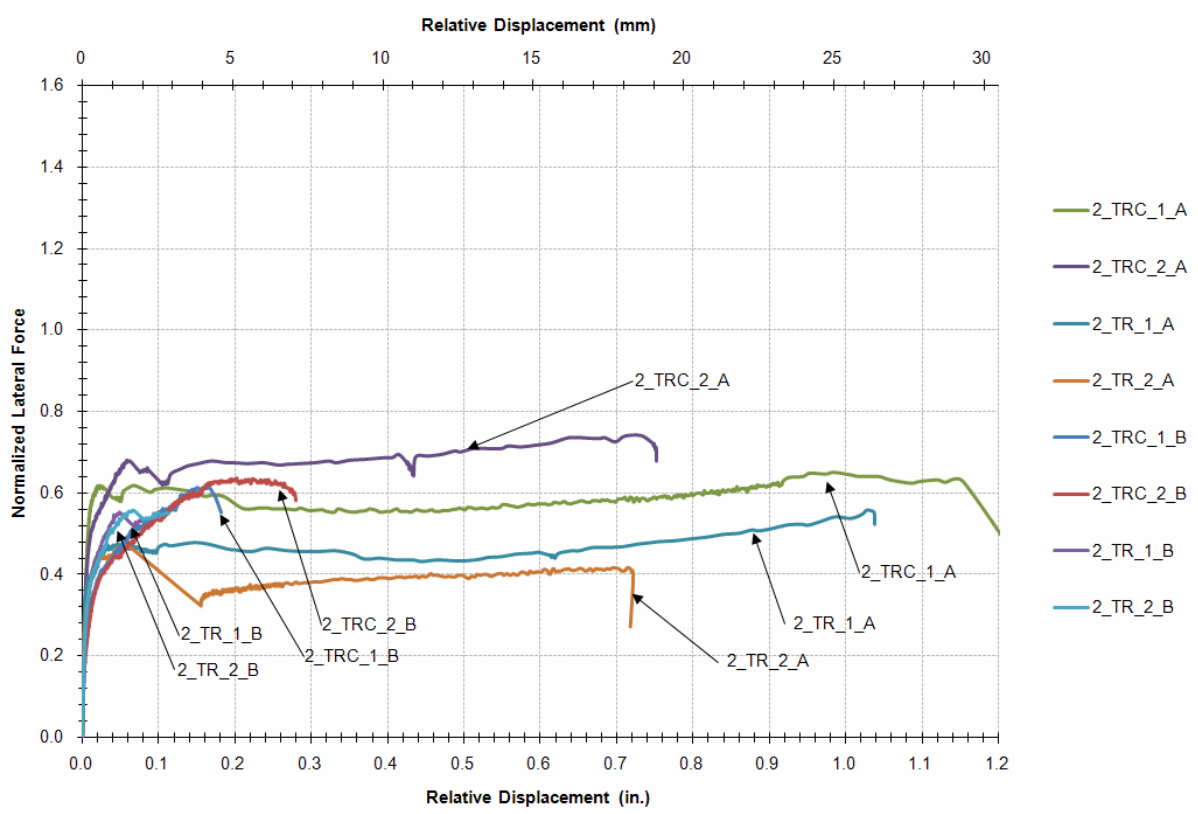

Figure 3.13 *Normalized lateral force versus relative displacement for all shear specimens with the threaded-rod shear connection. Note that after initial breakaway (and slip), the normalized lateral force is indicative of the coefficient of sliding friction.*

3.7 Discussion of Sliding Friction Performance

From Figure 3.13 it is evident that a dependable friction coefficient for the proprietary group used (SikaGrout™ 212 with w/p = 0.19) should be taken as $\mu_g = 0.4$. To obtain equivalence for the maximum R-bar spacing (2-legs #4 [#13M] @ 12-in. (300 mm) centers, $A_{sh} = 0.393$ in^2/ft. [0.002 mm^2/m]), the number of shear connectors required per 8-ft. (2.4 m) precast deck panel is:

$$n \geq \frac{(1)(0.393)(60/12)}{(0.4)(0.52)(105)} \times (96) = 8.6 \qquad (3.4)$$

As the initial design calls for three pockets with *two* 1-in. (25 mm) threaded-rod shear connectors per pocket, a total of six threaded-rod connectors are required per panel. The initial design details for the Rock Creek Bridge provide insufficient capacity to meet design equivalence of matching R-bar capacity. In the case of the end panel, where the present design calls for R-bars at 4-in. (100 mm) centers ($A_{sh} = 1.18$ in.^{2}/ft. [0.006 mm^2/m]), the number of fasteners needed per 8-ft. (2.4 mm) panel is:

$$n \geq \frac{\mu_c \, A_{sh} \, f_{yh} / s}{\mu_g \, A_{sf} \, f_{su}} \cdot l_p = \frac{(1)(0.393)(60/4)}{(0.4)(0.52)(105)} \cdot (96) = 25.9 \qquad (3.5)$$

The present design calls for three pockets and *four* threaded-rod connectors per pocket, a total of 12 threaded rods per panel.

Clearly, based on early assumed values, the present design for the Rock Creek Bridge is unable to match equivalent R-bar performance in terms of interface shear capacity. To remedy this shortfall in capacity, three possible solutions may be considered:

1. Use more threaded-rod connectors in each of the three pockets proposed in the present design, or
2. Increase the number of pockets in the panel, or
3. Increase both the number of pockets and the number of shear connectors.

Due to the unknown influence of using multiple fasteners in a pocket, option (ii) above is preferable at this time. However, at most, 7 pockets could be placed in an 8-ft. panel. That is, each pocket would be 5-in. (125 mm) wide and fit between alternate tendons that are spaced at 6 in. (150-mm). As the efficacy of using more than two threaded-rod connectors at this time is unknown, it is recommended that each pocket be limited to two threaded-rod connectors. Moreover, any solution that will require *three or more* fasteners per pocket is considered difficult

to construct. Therefore, based on the a maximum of seven pockets per panel, with two fasteners per pocket, the maximum interface shear transferable is

$$V_{in} = n\mu_g \frac{A_{sf} f_{yf}}{l_p} = (2 \times 7) \times 0.4 \frac{0.52 \times 105}{96} = 3.19 k/in = 0.56 kN/mm \quad (3.6)$$

In summary, the present design based on matching R-bar capacity is not achievable; an alternative approach to matching R-bar capacity is necessary. One alternative, and perhaps a more rational approach, is to examine the actual interface shear demand imposed by traffic load plus impact.

3.8 Redesign of the Pocket Requirements Based on Imposed Live Load Plus Impact

The shear demand was reassessed based on considering the lane loading under live load plus impact for each edge girder. The shear stress in the haunch was then computed assuming uncracked section properties of the composite prestressed concrete slab-on-girder. From this analysis the following results were obtained for the interface shear demand:

- At the ends of the girder, q = 3.0 k/in =0.53 kN/mm.
- At the center of the girder, q = 1.0 k/in = 0.18 kN/mm.
- Between the above, a linear interpolation may be assumed.

In light of these demands, and using the foregoing capacity data, in particular the results from Equation 3.6, the following pocket layout is proposed (note each grouted pocket has ***two*** 1-in. (25 mm) threaded-rods:

- For the *three* panels at the end of the girders, use ***seven*** pockets. For these panels place the pockets between alternate tendons. The pockets are 5-in. (125 mm) long (with respect to the longitudinal axis of the bridge) by 8-in. (200 mm) wide.
- Use ***four*** pockets for all other panels (in the central region of the span). The pockets are 5-in. (125 mm) long (with respect to the longitudinal axis of the bridge) by 8-in. (200 mm) wide and are to be placed between tendons 2 and 3, 6 and 7, 10 and 11, and 14 and15.

3.9 Effect of Haunch Height: 2-in. (50 mm) versus 3.5-in. (89 mm)

Tests conducted with the 2-in. (50 mm) haunch revealed adequate ductility, where the specimens with threaded rods and couplers revealed the largest breakaway resistance, peak load, and ultimate displacement, as shown in Figure 3.14. The results shown from the varying haunch height are inconclusive at the time of writing this report because the data from the 3.5-in. (89 mm) were clouded by poor beam performance (brittle beam failure), thereby limiting displacements to less than 0.2 in. (5 mm) (Figure 3.15). Additional testing is necessary to verify the effect of the haunch height on the deck-haunch-beam system. However, it is known that a larger overturning moment is inherently induced given a taller haunch.

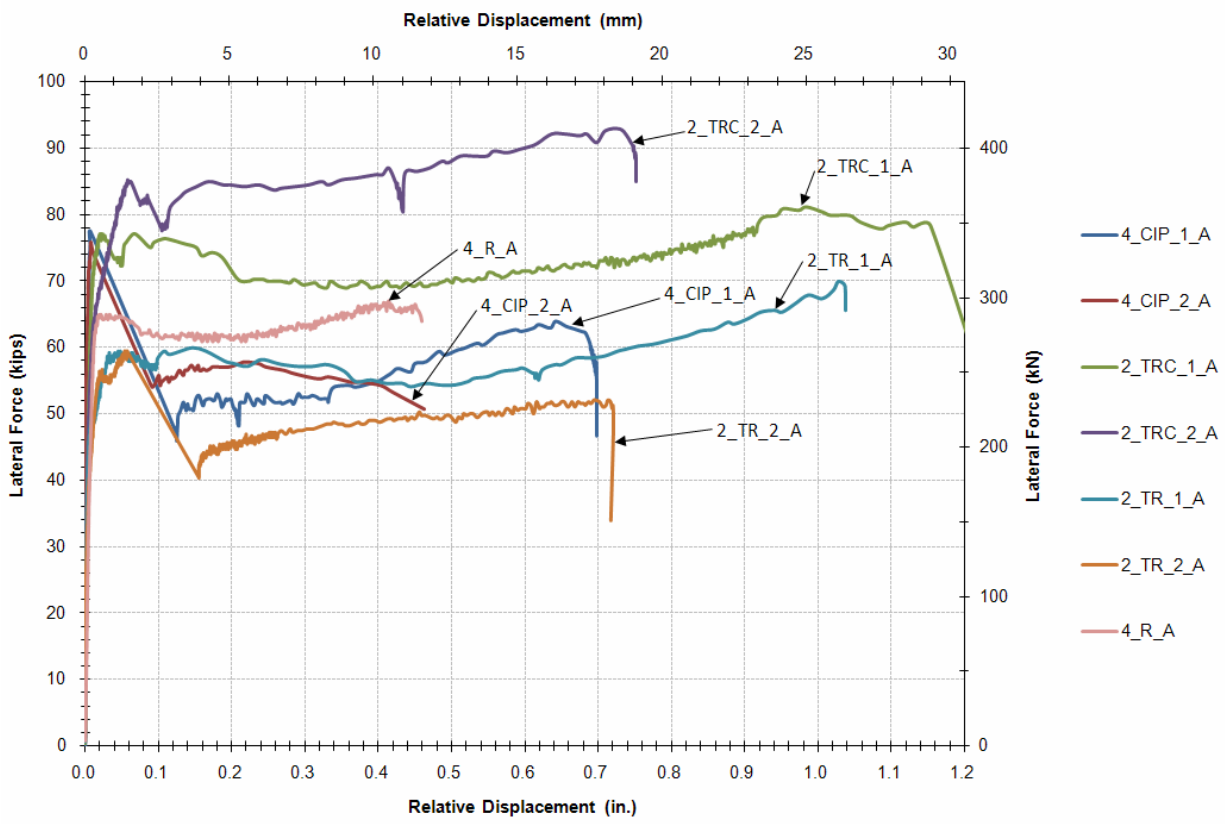

Figure 3.14 *Lateral force versus relative displacement of all tests with a 2-in. (50 mm) haunch.*

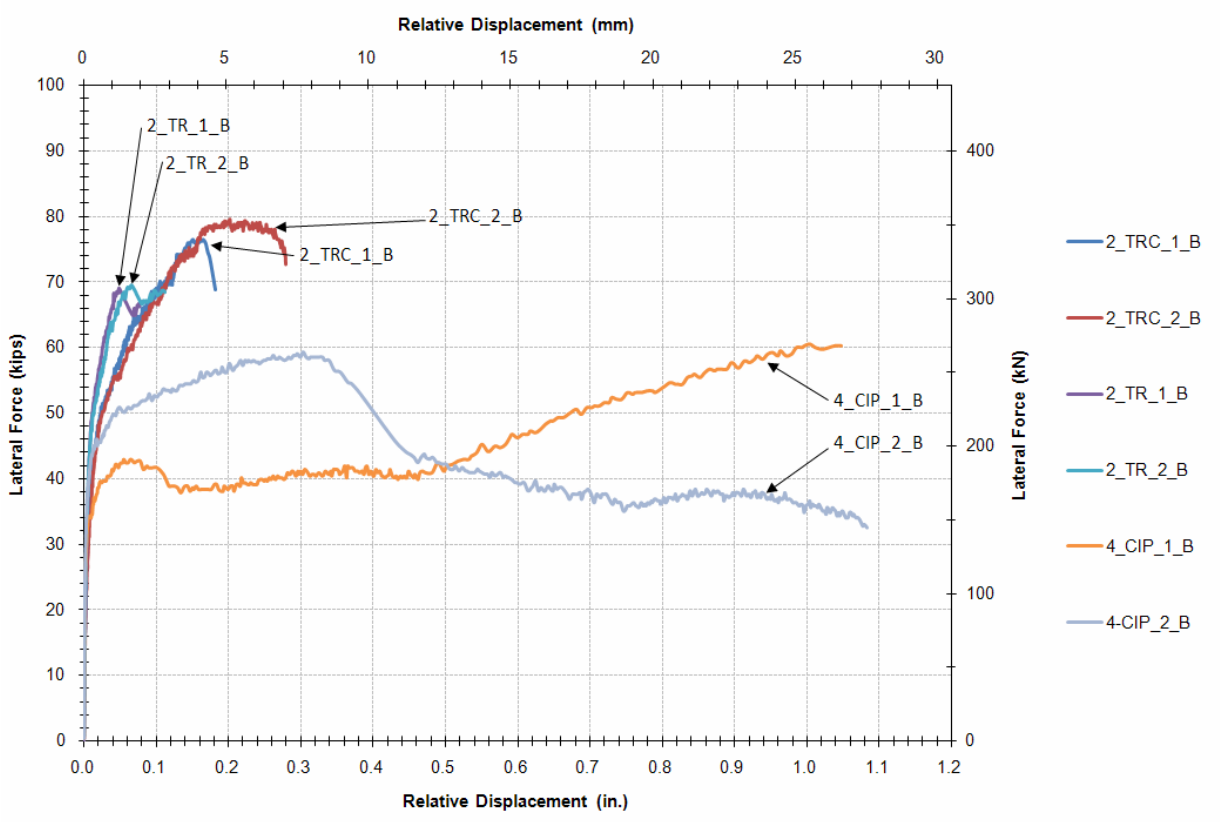

Figure 3.15 *Lateral force versus relative displacement of all tests with a 3.5-in. (89 mm) haunch.*

3.10 Discussion on the Problem of Beam Failure

During the course of testing it became evident that there was an inherent weakness in the detailing of the pocket-fastener-to-beam details. The two threaded fasteners when yielding have a combined pull-out force capacity of 143 kips (634 kN). This large force imposes significant distress to the beam. Evidently, as the threaded rods become heavily strained, much of their anchorage is provided by the headed nut, which in turn imposes a large uplift force within the concrete beam. This force is restrained by strut action from the nearby beam hoops, as shown in Figure 3.16.

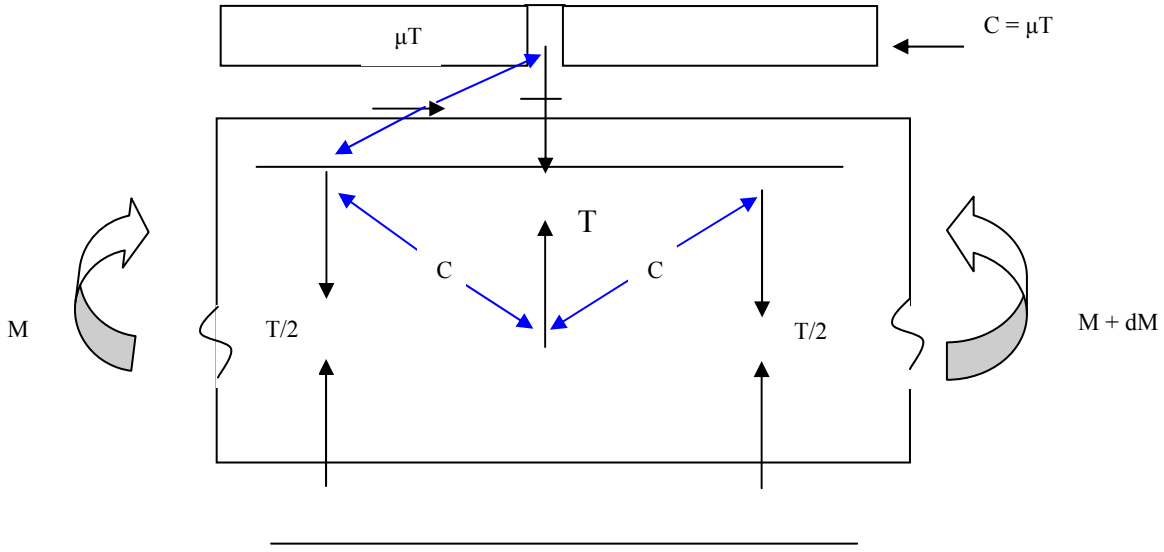

Figure 3.16 *Strut-and-tie mechanism within the beams tested.*

The tensile force that can be generated by the fasteners is restricted to the tensile capacity of the hoops that are sufficiently close to enable the strut forces to activate. Clearly, there were insufficient hoops for this purpose in some of the tests, particularly for the 3.5-in. (88 mm) haunch specimens. It is therefore suggested that the detailing of the hoops within the beam be altered accordingly. The dependable capacity of the hoops within one embedment length on either side of the fasteners should be not less than the maximum load to be sustained by the fasteners. More formally,

$$\phi n A_{sh} f_{yh} \geq \sum A_{sf} f_{su} \tag{3.6}$$

in which n = number of hoopsets required; A_{sh} = area of steel within one hoopset (typically two-legs of #4 [#13M] bars; f_{yh} = yield stress of hoop steel; ϕ = undercapacity factor suggested here to be 0.9; A_{sf} = area of threaded fasteners; and f_{su} = ultimate tensile stress of threaded fastener. For the present design with two threaded rod fasteners per pocket, this has the solution

$$n \geq \frac{2A_{sf} f_{su}}{\phi A_{sh} f_{sh}} = \frac{(2\times 0.52)(125)}{(0.9)(0.393)(60)} = \frac{130}{21} = 6.1 \tag{3.7}$$

Thus, at least *three* #4 (#13M) hoopsets should be grouped to either side of the fasteners.

If on the other hand the hoop bar size is increased and #5 (#13M) hoops are used:

$$n \geq \frac{2A_{sf} f_{su}}{\phi A_{sh} f_{sh}} = \frac{(2\times 0.52)(125)}{(0.9)(0.614)(60)} = \frac{130}{33} = 3.9 \tag{3.8}$$

This appears to be a more manageable solution; therefore, *two* #5 (#16M) hoopsets should be grouped as close as practicable on both sides of the fasteners, as shown in Figure 3.17.

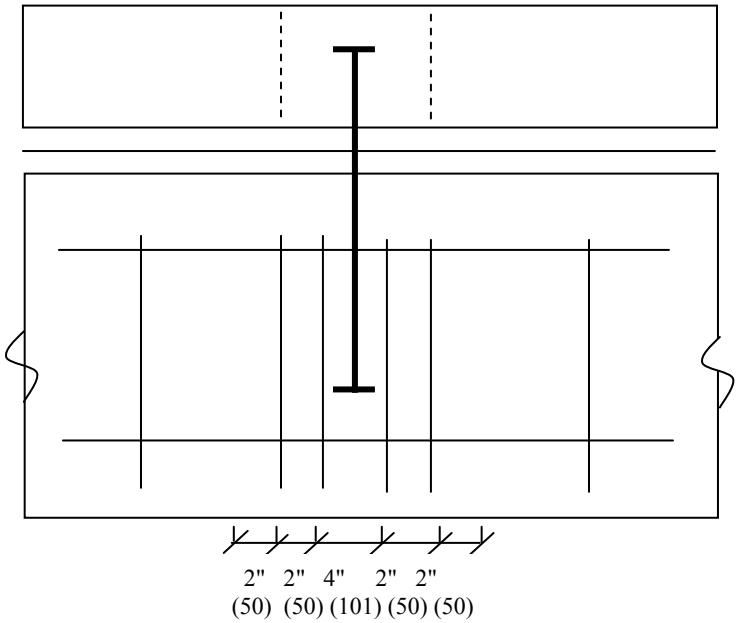

Figure 3.17 *Hoopsets grouped on either side of the fasteners.*

3.11 Summary

Based on the shear tests conducted in this investigation, the following summary is provided:

- The interface shear capacity of the existing R-bar system used in present practice is sound. From the tests, the inferred coefficient of interface friction between cracked concrete-concrete interfaces that exist within the haunch of a prestressed concrete slab-on-girder bridge is at least 1.0.
- The apparent coefficient of sliding friction in the cracked grout-bed that exists between the precast concrete slab and concrete girder, based on the present test data, should not exceed 0.4. This result is lower than expected; it is attributed to the relatively smooth shear interface between the soffit of the precast panels and the grout in the haunch.
- Based on two threaded-rods per pocket, as tested, the interface shear system to connect precast concrete slabs to concrete girders via a grout bed, as proposed by TxDOT engineers in collaboration with the research team, *does not* have sufficient capacity as expected by the initial design.

The relatively meager resistance provided by the interface shear using the haunch can be improved by using more pockets and fasteners. This design will increase the number of pockets for the three panels at the end of the girders to seven, and all other panels will require four pockets.

CHAPTER 4. MATERIALS

This section of the report presents findings from the testing of grout materials and haunch forming materials. The grout research investigated the requirements for grout specifically for use in the haunch section of precast bridge deck systems. Flow and strength characteristics were evaluated for different types of mixtures. The haunch form materials research investigated the characteristics of foam materials and how these materials resist lateral loads from grout pressures.

4.1 Haunch Grout Material

4.1.1 Experimental Plan

The purpose of this material testing program is to identify a grout that can be used to connect together bridge panels with bridge girders for precast overhang bridge construction. The mixtures tested used SikaGrout 212^{TM} high performance grout (herein referred to as Sika) and sand, and were evaluated based on both their fresh and hardened characteristics.

4.1.1.1 Mixing Variables

Conditions of bridge construction requires that the grout be mixed on site; hence, a simple mix proportion accompanied by straightforward performance tests are required. To provide a more economical grout mix, a test matrix consisting of different water to Sika powder ratios (herein referred to as w/p) and varying sand contents were evaluated to identify an optimized mixture. Table 4.1 shows the experimental plan used in this research, where the mixtures have been identified based on the following labeling system: “w/p_sand content.”

Table 4.1 Test matrix of Sika mix designs.

w/p	0%	10%	20%
0.17	17_ 0	17_10	17_20
0.185	185_ 0	185_10	185_20
0.20	20_0	20_10	20_20
0.25	25_0	25_10	25_20

4.1.1.2 Design Considerations and Testing

Grout for precast overhang systems needs to be cast through panel pockets into the underlying haunch, where the grout should flow freely through the haunch until full. This requires the grout to be sufficiently fluid to flow through the haunch while maintaining dimensional stability and later attaining sufficient strength. Obtaining both of these criteria can have conflicting effects. To evaluate these characteristics the flowability, segregation, bleeding, early age dimensional stability, fresh density, and strength were evaluated. The research investigating these characteristics is discussed in the following sections.

4.1.1.3 Flowability

Flowability is a composite characteristic that can be described by the grout's cohesiveness and consistency. Cohesiveness is a measure of the grout's stability and its ability to withstand segregation and bleeding. Cohesiveness considers the yield stress required to break the interparticle forces within the grout through shear. Once broken, the plastic viscosity defines the ease of flow of the grout, which is described by the consistency.

An optimum level of flowability is required for precast panel construction, as a high plastic viscosity is required to allow the grout to freely flow and consolidate within the haunch. However, the grout mixture must be cohesive enough to maintain a homogenous profile while moving through the haunch zone.

The consistency can be indirectly measured using an efflux cone apparatus in accordance with Tex-437-A, *Test for Flow of Grout Mixtures (Flow Cone Method 2)*, a modified version of ASTM C939-02, *Flow of Grout for Preplaced-Aggregate Concrete*. This test is used to provide an indirect measure of the grout's consistency by measuring the time for 33.8 fl oz. (1000 mL) of fresh grout material to pass through a defined opening. Figure 4.1 shows the apparatus used to evaluate the grout consistency. To put this test into perspective, the efflux time of water is three seconds, whereas syrup has an efflux time of 15 seconds.

Figure 4.1 *Efflux cone test.*

Another test used to indirectly measure both consistency and cohesiveness is the flow cone test. This is a scaled-down version of a slump cone test; however, due to the fluid nature of grout, the diameter of the grout circle after removal of the cone is measured as opposed to height drop (as in slump). The testing procedure has been modified from ASTM C230/C 230M-98, *Flow Table for Use in Tests of Hydraulic Cement,* as the original test requires the use of a flow table. However, for practical issues of onsite field testing, this drop table has been excluded from the test procedure. Figure 4.2 shows the three-step procedure to carrying out this modified test.

Step 1	Step 2	Step 3
		
• Lay a flat steel sheet of metal measuring no less then 15x15 in. (375x375 mm) on the ground so that it is level in both planes. • Wet and clean the flow cone approximately 1 minute before use and allow to stand and dry • Wipe down the metal surface with a damp cloth approximately 30 seconds prior to use and place the flow cone in the center. • Place cone on flat sheet.	• Fill the cone with grout so that it is flush with the top of the cone and strike off any excess grout with a flat surface. • Ensure that the area around the flow cone is clean.	• Swiftly lift the cone vertically and hold slightly above the flowing grout to allow any excess to drip while the grout spreads in a circular pancake-like shape. • Once the grout has stopped flowing, take two perpendicular readings of the circle's diameter to the closest .25 in. (6 mm). • If grout continues to spread, this is an indication that either the grout has not been properly mixed because there is free water present, or that the w/p is too high.

Figure 4.2 *Testing procedure for flow cone test.*

To obtain the loss of flowability with time relationship, a mix was batched and divided evenly into 5 buckets and left to set in a room of known temperature and humidity. Each sample was left undisturbed until the time of testing, and then it was promptly mixed for ten seconds and tested. Readings were taken at 15-minute intervals and the grouts were discarded after use.

4.1.1.4 Segregation

Segregation control is the ability to maintain dimensional stability without having the individual components segregate under gravity or flow. Segregation in mixes is more easily observed than measured while the grout is in its fresh state, where free water and grout paste separate. Mixtures that are susceptible to segregation will separate into two layers when

performing a flow cone test; the sand and grout will be deposited in the center of the circle while the free water will flow freely at the edge of the grout circle, as shown in Figure 4.3.

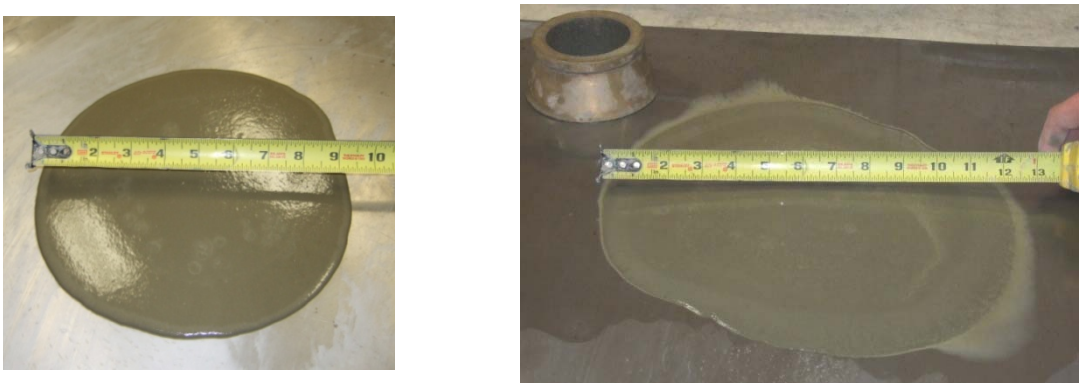

(a) Flow cone displaying good consistency *(b) Flow cone showing signs of segregation*

Figure 4.3 *Examples of good and bad flow cone tests.*

4.1.1.5 Bleeding

Bleeding is a form of segregation that is defined by the process of water rising (bleeding) to the surface after the grout has been placed and consolidated, but before it has set. Bleed water needs to be minimized due to the enclosed space the grout is occupying in the haunch. Bleed water can become trapped on the underside of the panel and result in unwanted voids. Generally speaking, mixtures with lower w/p are less likely to bleed, as they have minimal amounts of free water.

Take, for example, a precast overhang system bridge that is 120-ft. (36.6 m) long with a 4 percent grade, where it is assumed that the entire haunch is to be poured in one cast and all the bleed water is to accumulate at the top end of the bridge. If a bleed water percentage of 0.1 percent by volume of grout is specified, then this will result in a void forming that is 0.5-in. (13 mm) deep and stretches 16 in. (406 mm) longitudinally at the top of the haunch. Given the size of the bridge in comparison, and the unlikelihood of this occurrence since the voids will be dispersed over the span of the bridge, this is an allowable tolerance to specify for the grout.

ASTM C940-03, *Expansion and Bleeding of Freshly Mixed Grouts for Preplaced-Aggregate Concrete in the Laboratory*, can be used to determine the level of bleed water produced by the grout.

4.1.1.6 Expansion/Subsidence

It is reported that Sika contains shrinkage compensating characteristics by which the grout undergoes an initial expansive volume change during the very early stages of curing. This reaction then compensates for subsidence that takes place during setting due to shrinkage. Mixtures with expansive tendencies will increase the lateral pressure applied to the foam walls of the haunch, whereas mixtures that suffer from shrinkage will result in a loss of bond to the panel interface.

The level of expansion/subsidence can be measured using the provisional test method, AASHTO Designation: X 10, *Evaluating the Subsidence of Controlled Low-Strength Materials,* (Folliard et al. 2008).

4.1.1.7 Fresh Density

The fresh density of the grout is an easy way to verify mix proportioning and w/p. The fresh density can be determined using the Baroid Mud Balance test; however, as Sika is more granular than the materials this test was designed for, a proper seal of the lid is challenging to achieve. For this reason the test method has been modified by turning the lid over when sealing the mud balance, then scaling the obtained reading with a modification factor on the specific gravity of water. For example, the factor for the specific gravity of water is 1.1 when using this modified method. Therefore, readings obtained with grout and the inverted lid need to be scaled by a factor of 1.1 to define the actual specific gravity.

4.1.1.8 Strength

The design compressive strength of the concrete deck is 4000 psi (28 MPa); thus, the grout must be proportioned to achieve at least this strength. Other factors may require higher strength and these will be assessed as required. ASTM C942-99 (2004), *Compressive Strength of Grouts for Preplaced-Aggregate Concrete in the Laboratory*, can be used to determine the strength of the grout at 1, 3, 7, 28, and 56 days with a sample size of three cubes per test.

4.1.2 Materials

The research team evaluated literature for several grout types and from several manufactures. Based on this review, Sika High Performance grout was selected for further evaluation in this program. Other non-proprietary grouts are being evaluated as part of this research program. However, this research is still underway and this report will only include recommendations based on Sika test results.

4.1.2.1 SikaGrout™ 212 High Performance Grout

SikaGrout 212 is a non-shrink, cementitious grout that is recommended for structural applications and is versatile for high flow applications. Refer to Appendix B for the material data sheet.

Based on the material recommendations a 500 rpm mechanical drill mixer was used with a circular paddle mixer. The mixing procedure consisted of batching the materials to an accuracy of 0.1 pounds (0.045 kg). The grout powder was gradually added to the water in 3 to 4 stages with short bursts of mixing between each to prevent balling of the grout. Mixing continued for 5 minutes from the time of water addition, ensuring that the grout was well mixed and homogenous.

4.1.2.2 Sand

Testing of the sand for absorption capacity and specific gravity was carried out in accordance with ASTM C128–04a, *Density, Relative Density (Specific Gravity), and Absorption of Fine Aggregate*. The determination of the fineness modulus and sieve analysis for the sand was carried out in accordance with ASTM C136–05, *Sieve Analysis of fine and Coarse Aggregates*. Table 4.2 shows the values obtained based on these tests.

Table 4.2 Characteristics of sand.

Absorption Capacity	Oven Dry Specific Gravity	Saturated Surface Dry Specific Gravity	Fineness Modulus
1.23	2.57	2.60	2.40

The sand gradation curve (Figure 4.4) was determined based on an average of three tests. Results indicate that the particle sizes passing through the #30 sieve (0.6 mm) were slightly higher than the grading limits for fine aggregates recommended by ASTM C 33-03, *Concrete Aggregates*.

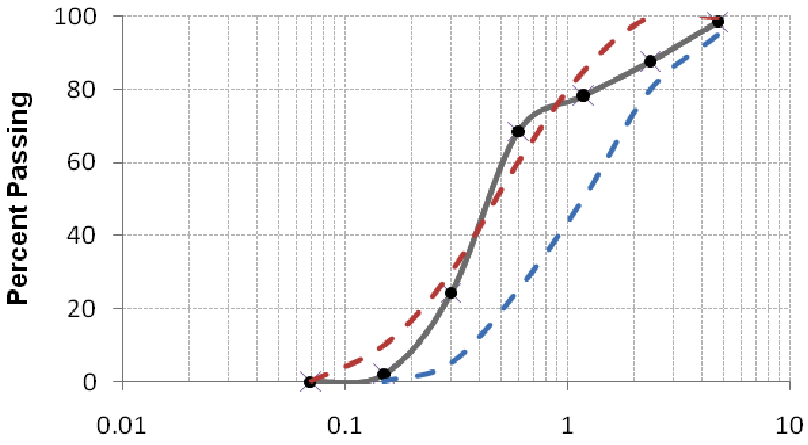

Figure 4.4 *Sand particle size distribution curve (dashed lines are minimum and maximum limits fir ASTM C33).*

4.1.3 Results & Analysis

Testing has been performed over the last 5 months in order to develop an appropriate grout to meet the design criteria of the precast overhang bridge system. Following are the results from the grout testing program.

4.1.3.1 Flowability

It is desirable for the grout efflux time to be less than twenty seconds based on typical grout requirements. Figure 4.5 (a) shows the efflux times directly after mixing and 30 minutes after mixing. As expected, decreases in the w/p and/or the addition of sand results in a loss of workability; however, Figure 4.5 (b) illustrates that lower w/p are affected more severely by increasing the sand content.

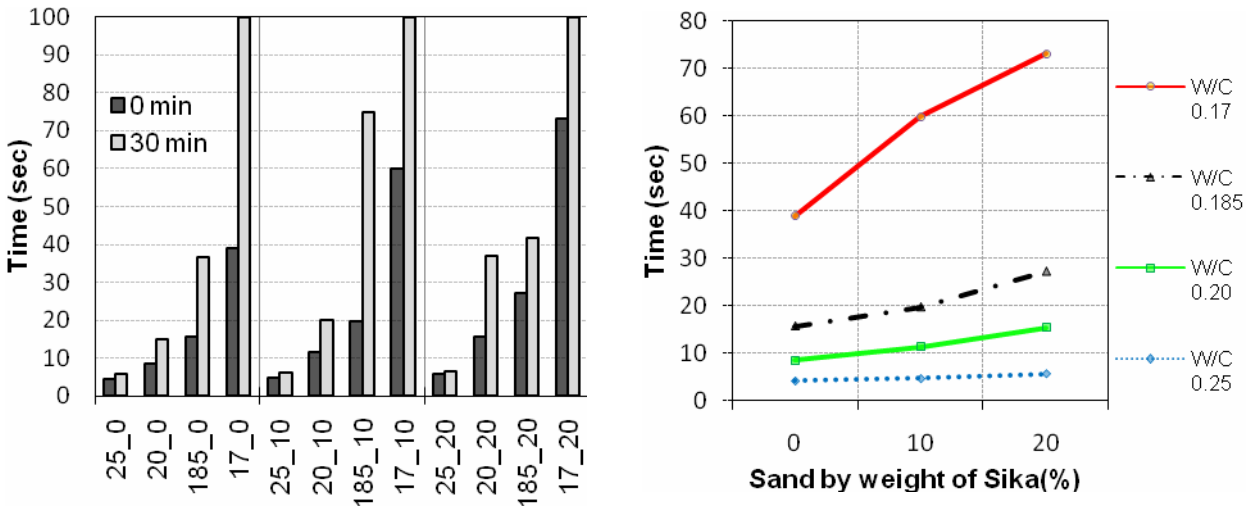

(a) Initial and 30 minute efflux times *(b) Influence of sand content on efflux time*

Figure 4.5 *Influence of time and sand content on efflux time.*

A relationship between efflux time and the flow cone results can be derived when plotted against one another. As shown in Figure 4.6 (a), a linear relationship is evident between the two test results.

Figure 4.6 (b) shows the decrease in flow and the increase in efflux time as a function of time after mixing. Samples were mixed and tested in a room with a temperature of 87°F (30.6°C) and 55 percent relative humidity. It can be observed that the efflux time approximately doubles after 30 minutes while the flow cone loses approximately 1 in. (75 mm) in diameter after the same period. These results indicate that once mixed, the grout needs to be placed as soon as possible (within the first 15 minutes ideally) to ensure good flowability while being placed into the haunch.

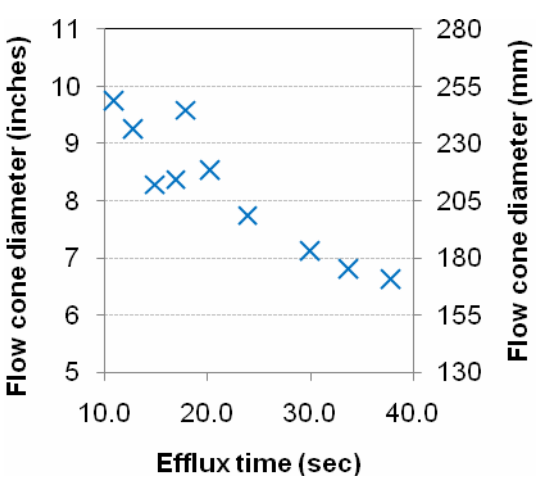

(a) Flow cone diameters plotted with corresponding efflux times

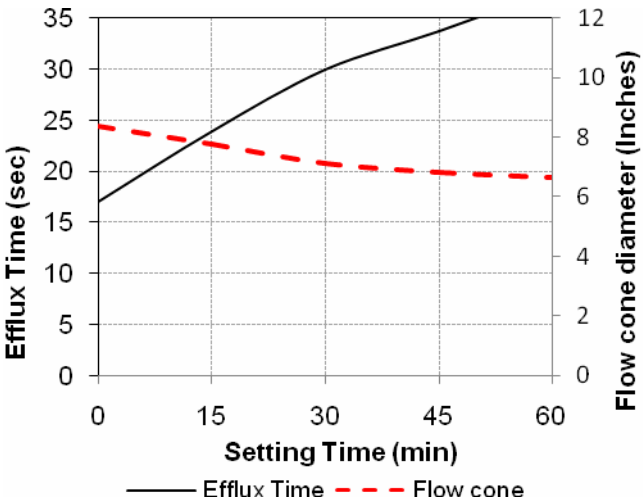

(b) Loss of flowability with time for a mix with w/p = 0.185

Figure 4.6 *Efflux time and flow cone results.*

4.1.3.2 Bleeding

Results from bleed water testing did not present any reasonable trends, as shown in Figure 4.7. The percentage of bleed water is shown for increasing sand contents. To derive more reliable relationships between the varying bleed water percentages, more tests would be required to find the averages. However, from these results it can be concluded that the lower w/p values provide better bleed control. Lower values of w/p should be specified and used in order to minimize bleeding.

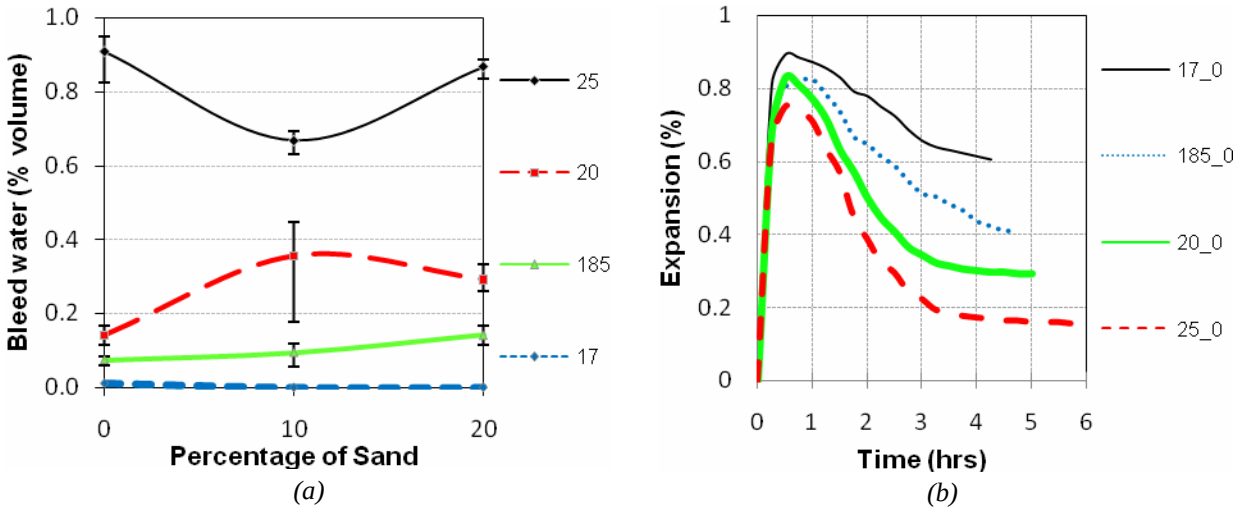

Figure 4.7 *(a) Bleed water percentages for increasing sand contents; (b) Expansion/Subsidence profile of Sika mixtures.*

4.1.3.3 Expansion/Subsidence

Figure 4.8 shows the expansion and subsidence of grout where expansion and subsidence are in the positive and negative directions, respectively. It can be observed that higher w/p values result in lower levels of expansion. Initial set times are shown by the end points of the curves. Figure 4.8 shows the volumetric change in profile of individual w/p value with varying sand contents. A common trend shows that the increase of sand reduces the initial expansion and overall subsidence of the grout.

The repercussions of having a grout that subsides could result in the loss of bond between the top of the haunch and bottom of the bridge deck panel interface, possibly reducing the overall shear capacity of the bridge-beam connection. For this reason, sand is not recommended to be used as a supplementary material with Sika grout.

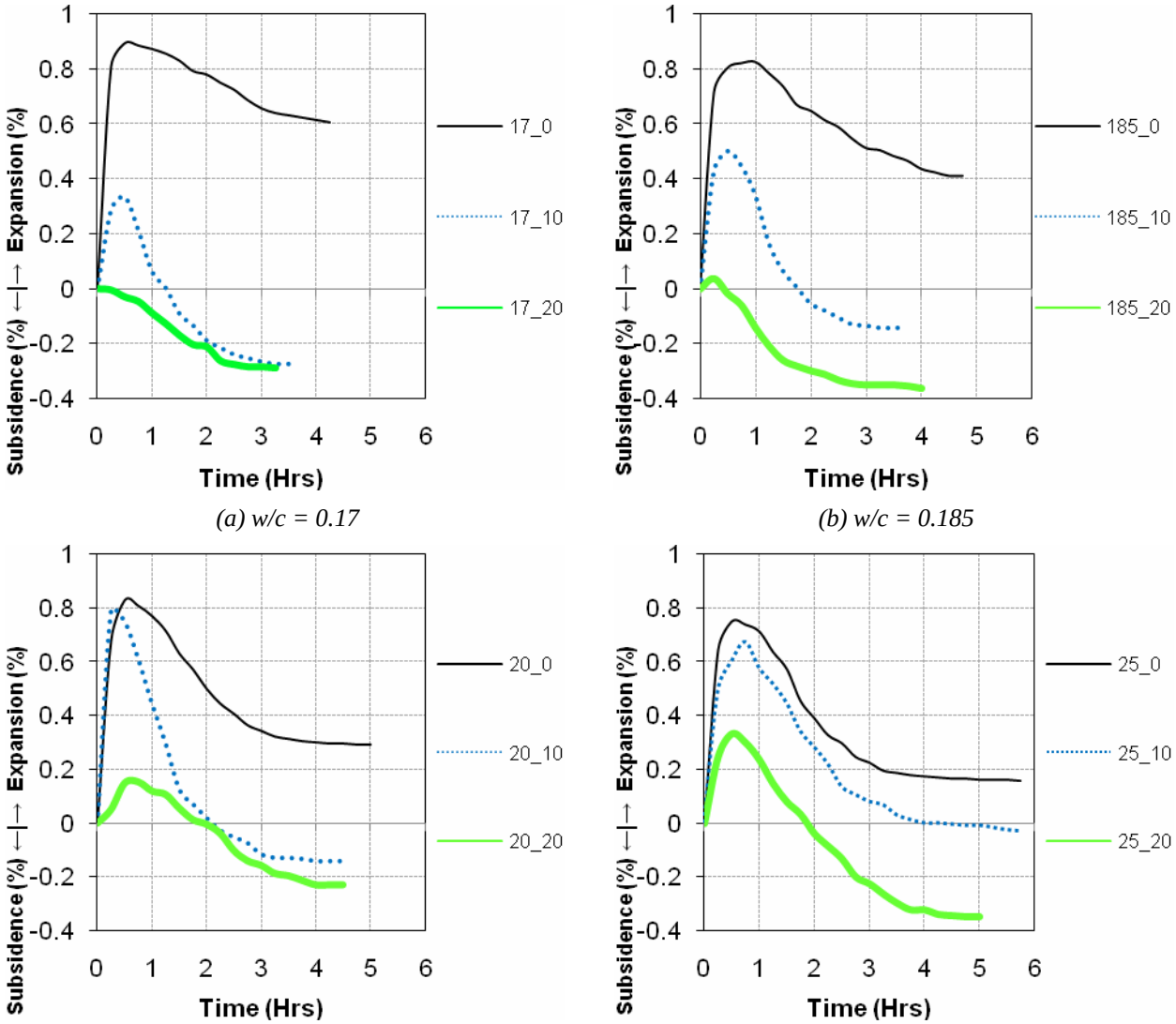

(a) w/c = 0.17 *(b) w/c = 0.185*

(c) w/c = 0.20 *(d) w/c = 0.25*

Figure 4.8 *Volume change profiles of mixes with varying sand percentages.*

4.1.3.4 Strength

The results from this testing are shown in Figure 4.9 for each w/p with varying sand contents. These results confirm that all the mixes below a w/p of 0.20 will obtain and exceed the required 4000 psi (28 MPa) compressive strength within the first 7 days. This concludes that strength is not one of the limiting factors for this design, provided the w/p is less than 0.20.

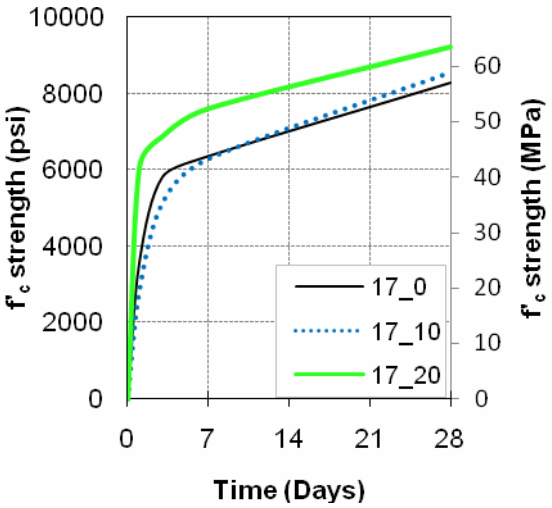

(a) w/c = 0.17

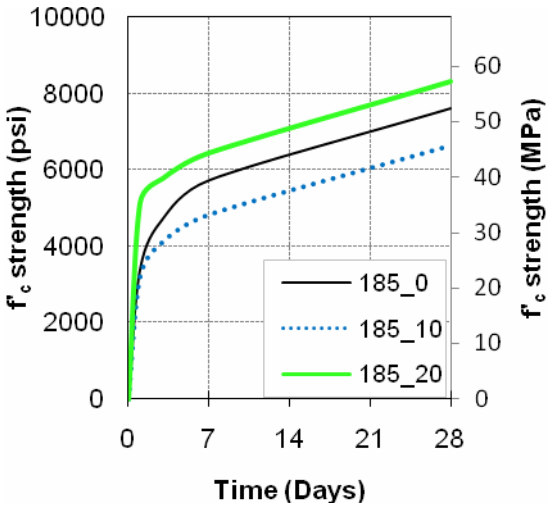

(b) w/c = 0.185

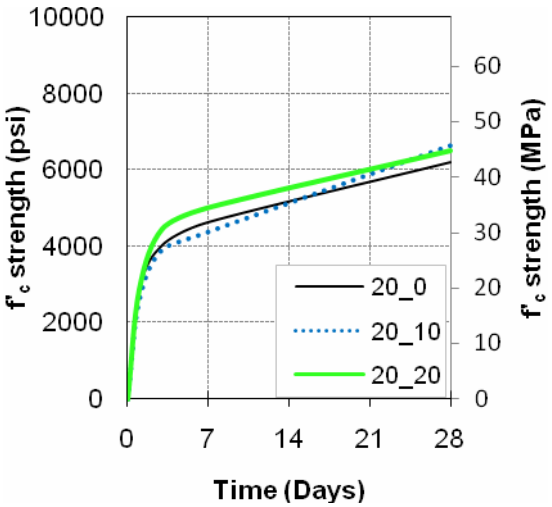

(c) w/c = 0.20

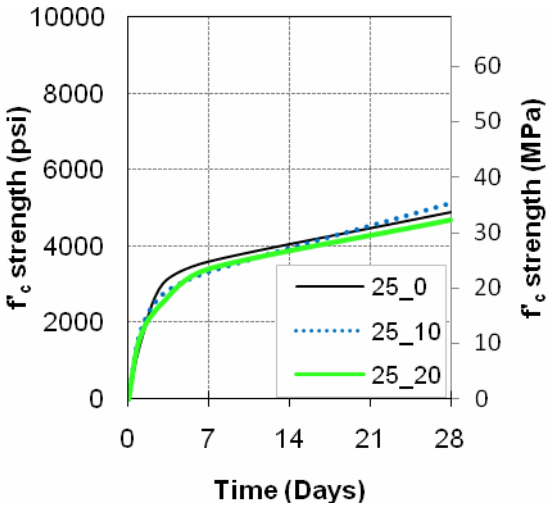

(d) w/c = 0.25

Figure 4.9 *Strength development curves for different w/p.*

4.1.3.5 Comparisons

From the findings of this grout testing program, strength versus efflux time can be graphed against each other to find the ideal mix based on the criteria that a strength greater than 4000 psi (28 MPa) and an efflux time less than 20 seconds is required. This is shown in Figure 4.10. Subsequently, from the expansion/subsidence and bleed results it was determined that mixes

containing sand are unsound and that lower w/p values result in less bleed water. Thus, a w/p of 0.185 is recommended for the Sika.

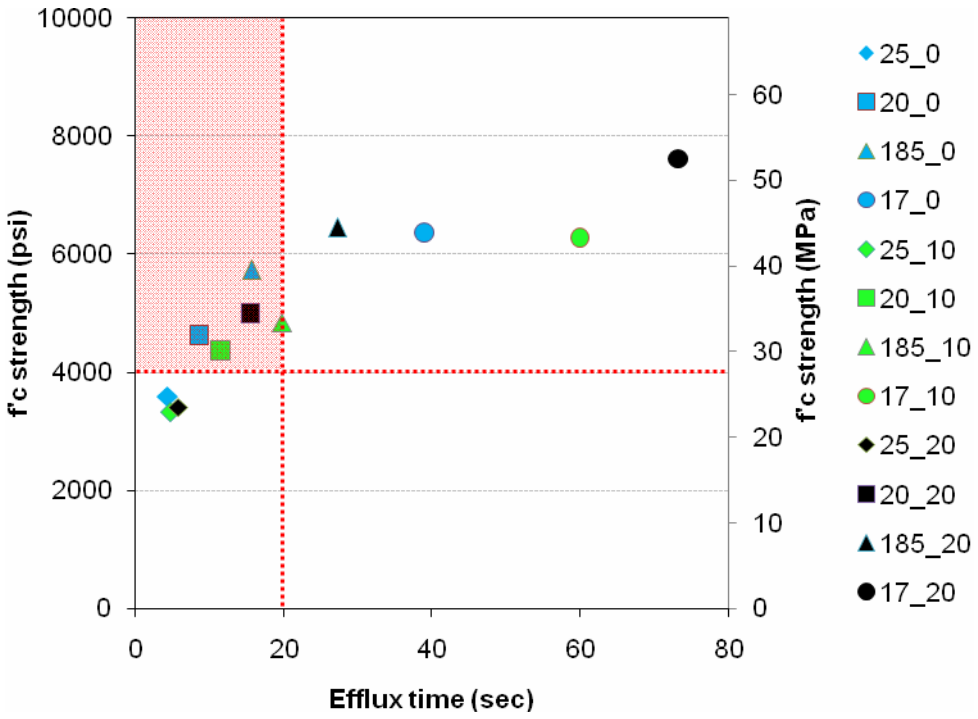

Figure 4.10 *Comparison of strength vs efflux time.*

4.1.4 Constructability and Proposed Special Specifications

The following section provides a general description of the recommended installation procedure for the haunch grout materials. The procedure is recommended to prevent the collection and formation of voids in the haunch zone. In general, grout materials should be placed from the lowest elevation to higher elevations. To prevent leakage of the grout during installation, all haunch form materials shall be well connected to the girders (or other elements when necessary) and the bottom of the panels (or other surfaces as necessary).

4.1.4.1 Construction Sequence for Haunch of the Partial Full-Depth Precast Overhang System

Grouting of the haunch involves a 5-step approach using the Sika product batched with a w/p of 0.185, and tested in accordance with Special Specification XXX; Structural Grout for Haunch. Table 4.3 provides a general procedure for placing grout on the Rock Creek Bridge.

Table 4.3 *Grout placement procedure.*

Step 1: Begin placing from the lowest pocket and continue filling until the pocket is full.	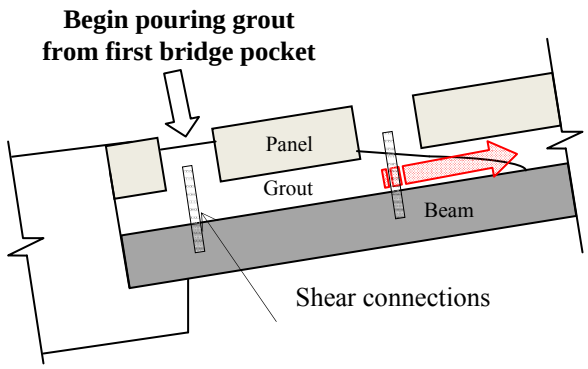
Step 2: Use a pocket cover to force grout down until the grout is at the correct level. The pocket cover will need to be built to prevent leakage of grout, as well as to have a method of securing it to the shear connectors.	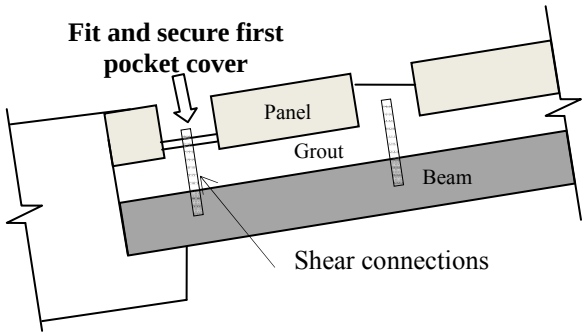

Table 4.4*(continued)Grout placement procedure.*

Step 3: Continue working up the bridge by blocking off pockets that are full by using pocket covers.	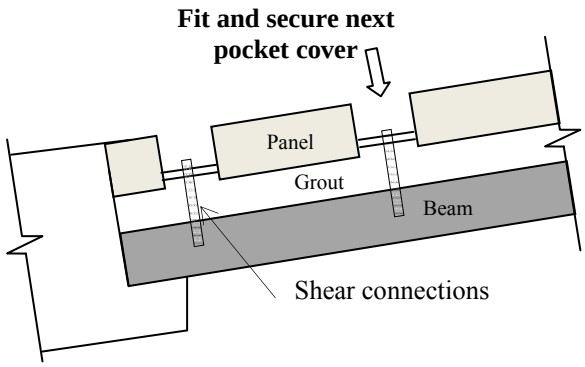
Step 4: The last pocket that has a full haunch now becomes the next pocket to pour into in order to continue filling the haunch. This ensures that no grout is able to flow downhill, as this creates entrapped air under the panel.	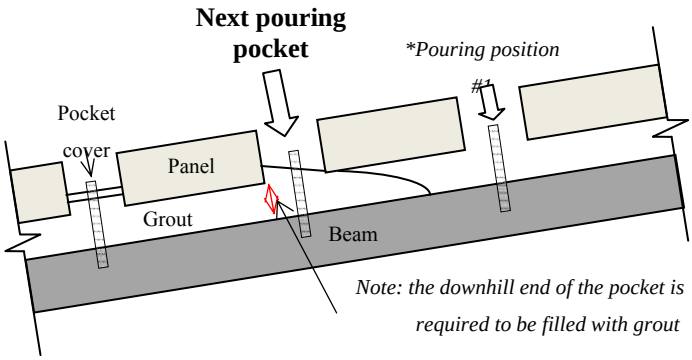
To illustrate the consequences of pouring grout downhill, a test was conducted, and the results clearly showed a circular volume of entrapped air voids at the interface where the new grout came into contact with the grout that had already been placed.	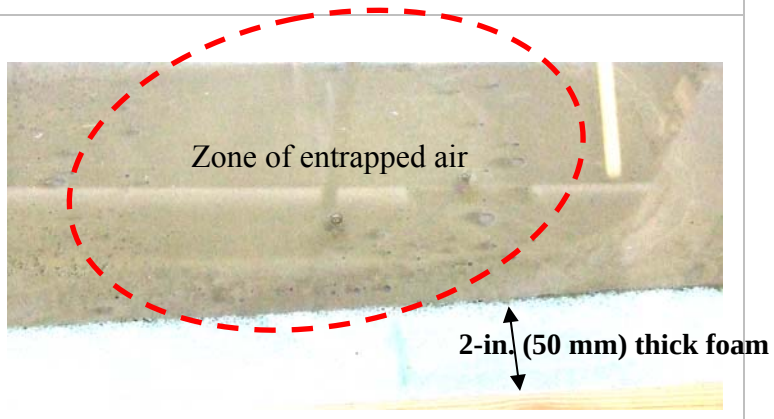
Step 5: Repeat steps 1 through 4 until the entire haunch has been filled.	

Table 4.4 *Laboratory Model*

A full-scale model of the bridge haunch for two panels (16 ft. [4.9 m] in length) was built to illustrate the recommended placement method of steps 1 to 3 for a precast bridge with a 4% grade. This testing confirmed that the recommended Sika mixture is flowable through both a 0.5- and 3.5- in. (13 and 88 mm) haunch height.	
Step 1: Place grout into first pocket.	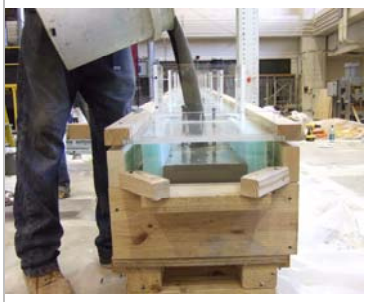 
Step 2: Fit and secure pocket cover to first pocket.	 
Step 3: Fit and secure pocket covers to the remaining pockets.	

4.1.4.2 Special Specification

The following is a recommended special specification for the haunch grout on the Rock Creek Bridge.

200X Specifications CSJ XXX-XX-XXX

SPECIAL SPECIFICATION
XXX

Structural Grout for Haunch

1. **Description.** Furnish, mix, place, and cure prepackaged, non-shrink, cementitious grout for precast bridge construction.
2. **Materials.** Provide prepackaged, non-shrink, cementitious grout that conforms to the following requirements:
   (a) General. SikaGrout™ 212 is to be used for the grout in the haunch zone with a water to Sika powder ratio of 0.185. SikaGrout™ 212 should not be cast in the overhang pockets. A minimum of 3 in. (75 mm) of deck concrete shall be placed in the pockets after the SikaGrout has achieved its final set.
   (b) Mechanical. Minimum compressive strength of ASTM C942-99 (2004) 2-in. (50 mm) cubes per Table 1.

Table 1

Minimum Grout Strengths

Age	Compressive Strength, psi (MPa)
1 day	2,000 (14)
3 days	3,200 (22)
7 days	4,000 (28)
28 days	4,600 (32)

   (c) Constructability
      1) Flowability: 8- to 18-second fluid consistency efflux time per Tex-437-A, Test for Flow of Grout Mixtures (Efflux Cone Method 2).
      2) Consistency: 8.5- to 11-in. (215 to 280 mm) average diameter circle per modified method of ASTM C230/C 230M-98, Flow Table for Use in Tests of Hydraulic Cement1.

3. **Equipment.** Provide clean mechanical mortar mixer for batching grout. Use appropriate hardware to block off bottom of panel pockets to prevent grout from hardening in pockets.
4. **Construction.** Mix and place grout in accordance with manufacturer recommendations with the exception of requirements in this special provision. The requirements of this special provision supersede the manufacturer's requirements.

[1] Refer to Section 4.2.3.1 Flow ability for test method procedure

(a) Trial Batching. A trial grout mixture of a simple mock-up connection will be required at least two weeks in advance of the grout placement. The trial grouting will demonstrate the reliability of the Contractor's grout mixing and testing procedures, confirm the grout placement procedure in the haunch, and familiarize the Contractor with the grout placement process.

(b) Grout Mixing and Placement. Grout shall be mixed in accordance with this provision. Manufacturer recommendations, including requirements for expiration date, grout mixing, outside air temperatures, and mixing durations shall be followed. The grout shall be placed in one uninterrupted placement unless otherwise approved by the Engineer. A placement procedure has been recommended in Section 4.1.4.1 of this report. Variation from this procedure will require approval from the Engineer.

Quality control of each batch mixed is required before placement as per test methods in "2.C. Constructability" of this provision.

(c) Job Sampling. Quality control of grouting in construction will include tests for flowability, consistency, fresh density, and compressive strength.

1) **Flowability:** A minimum of one test per mixture batched is required and must obtain an efflux time within the range of 8 to 18 seconds per "Tex-437-A, (Efflux Cone Method 2)."
2) **Consistency:** A minimum of one test per mixture batched is required and must obtain an average diameter circle of 8.5 to 11 in. (215 to 280 mm) based from a minimum of two readings per modified ASTM C230/C 230M-98; "Flow Table for Use in Tests of Hydraulic Cement."[1]
3) **Fresh Density:** A minimum of one test per mixture batched is required and must obtain a specific gravity within the range of 2.37 to 2.47 per modified Baroid Mud Balance.

5. **Measurement.** This Item will be measured by the cubic foot (cubic meter) of neat lines from the top of the girder to the bottom of the panel, from the inside edge of the haunch forms, over the span length. The average distance between the top of the girder and the bottom of the panel will be determined by measuring this distance at each pocket, summing these values, and dividing summation by the number of pockets.
6. **Payment.** The work performed and materials furnished in accordance with this Item and measured as provided under "Measurement" will be paid for at the unit price bid for "Structural Grout." This price is full compensation for furnishing and placing grout and for all labor, tools, equipment and incidentals necessary to complete the work. The preparation of trial batches described will not be paid for directly and shall be considered subsidiary to this bid item.

4.1.5 Summary of Grout Testing

The purpose of this material testing program was to identify a grout that can be used in the haunch zone between bridge panels with bridge girders for precast overhang bridge construction based on the fresh and hardened state characteristics of the grout. SikaGrout™ 212 was evaluated, and it was determined that the optimum mixture design most suited for the project was a w/p of 0.185 without sand. A proposed special provision for the Rock Creek Bridge has been provided.

4.2 Haunch Form Materials

The haunch, the space between the beam and the bridge deck, plays an important role in the construction of bridges. This area may need to be adjusted significantly in the field to ensure that the correct roadway profile and bridge deck thickness is provided. Determining the height of the haunch can become especially challenging when prestressed concrete beams are used, as the camber can be quite variable between beams of the same design (Kelly et al. 1987).

There have been several precast bridge deck systems developed in the last 10 years and implemented by various SHAs that have demonstrated that a precast bridge deck system needs to have the ability to be adjustable to meet construction and grading tolerances. However, previously developed systems have largely ignored the importance of the haunch and often require workers to go back under the bridge once the geometry is established to manually complete the forming of the haunch (Badie et al. 2006; Sullivan 2007). While these approaches appear to have been satisfactory for past projects, the performance of precast deck systems can be improved if a forming system is used that provides the strength needed to resist the lateral pressure from the fluid cementitious material filling the haunch, allows for an easy adjustment of the system, and does not require workers under the bridge deck for either installation or removal.

During an early meeting with TxDOT personnel, the research team proposed investigating low-density packing foam for this application instead of a spring loaded form system. The suggestion was approved and four different foams and three different adhesives were investigated for their ability to resist lateral pressure, direct tension, and a combination of tension and lateral pressure. These tests were designed to best simulate the performance of the glue and adhesives in different phases of the construction.

4.2.1 Experimental Plan

In the following tests, different combinations of foams and adhesives were investigated at different ages. In all of the tests, the initial specimen preparation was performed in the following manner:

- Adhesive is applied to thoroughly cover the concrete beam (dimensions 18 x 3 x 3 in. [450 x 75 x 75 mm]).

- A foam plank (dimensions 10.5 x 3 x 1.5 in. [263 x 75 x 38 mm]) is then placed on the glue-covered surface of the beam.
- The top surface of the foam is then thoroughly covered with the adhesive.
- The formed surface of the concrete beam is then placed on top of the foam.
- The glue is then allowed to gain strength while being supported with a jig under gravity loads.

In this testing program it was important to ensure that a surface was used on the concrete blocks that would be similar to the surface used in the actual structure. For this reason the foam was glued to a trowel-finished concrete that represented the top surface of the precast beam and to a formed surface of a beam that represents the bottom of the precast panel. A brief summary is provided on the lateral pressure, tension, and tension and lateral pressure in the following sections.

4.2.1.1 Lateral Pressure

This test examines the capacity of a foam and adhesive combination from lateral pressure by using an inflated air bag to simulate the lateral pressure from a fluid grout or concrete. In this test the air bag is monitored with a pressure gauge, and adjustments in pressure are made with a regulator valve. The specimens are supported on their side on a wooden table, and the concrete blocks are fixed to the table using pipe clamps. The air bag is then placed between the foam and the table. The test setup is shown in Figure 4.11. Care must be taken to ensure that the air bag applies pressure uniformly on the foam. Deflection gages were used in the test to measure the deflection at the edge and center of the specimen.

Figure 4.11 *Experimental setup for the lateral pressure test.*

The specimens were measured at regular intervals starting at 1.5 psi (10 kPa) and increasing by 1 psi (7 kPa) until a maximum pressure of 6.5 psi (45 kPa) was reached. At each pressure interval the loading is paused for 1 minute to allow the deflection of the system to stabilize. The value of 6.5 psi (45 kPa) was chosen because it was the capacity of the air bag equipment used in the testing and is also a reasonable upper bound on the amount of pressure that one might see from a gravity placement of concrete or grout. This would roughly correspond to 6.5 ft. (2 m) of concrete head. An example of a failed specimen is shown in Figure 4.12.

Figure 4.12 *A lateral pressure test specimen at failure.*

4.2.1.2 Tension

This test focuses on the capacity of foam and glue in tension when it is pulled apart at 10 lb/minute (44 N/minute). This test provides information about the amount of elongation that can occur before the specimen fails. This simulates a situation that may occur if the precast overhang panel is glued to the foam and then the height is adjusted.

For the loading in this testing, a universal testing machine was used. Specimens were prepared as described previously and then clamped to steel plates that were bolted to the load heads of the machine. A level was used to ensure that the specimen was attached with minimal eccentricities. During the testing, deflection gages were also used to monitor the deflection of the specimen. The test assembly is shown in Figure 4.13.

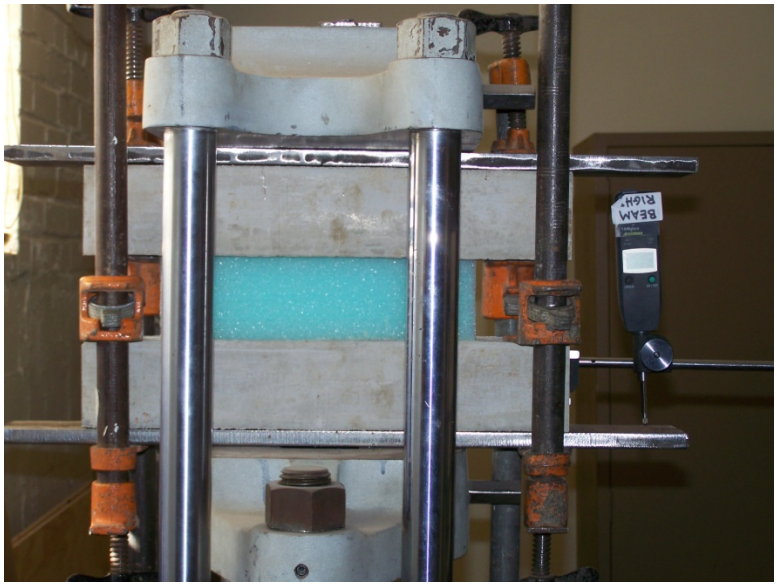

Figure 4.13 *Experimental setup for the tension test.*

Tension was applied to the specimen at a rate of 10 lb/min (44 N/min). The specimen was loaded until a tear, wide enough for grout to pass through, was observed in the specimen. Failure was defined when grout was observed passing through the tear in the haunch foam. The load was then stopped, and the deflection readings on the gages were recorded.

4.2.1.3 Tension and Lateral Pressure

This test evaluated the lateral pressure capacity of the foam and adhesive after the specimen was elongated 0.25 in. (6 mm). This combination of elongation on the foam and then subsequent lateral pressure can occur if a panel is first glued to the foam, the height is then adjusted, and then a subsequent lateral load is placed on the foam. The value of 0.25 in. (6 mm) was chosen from the tension results described in the previous section.

First, the specimen was prepared and placed on the wooden table as described previously. Next, small screw jacks were used to elongate the specimen by 0.25 in. (6 mm). The specimen was then clamped to the wooden table and a lateral pressure was applied with an air bag system. Gages were then used to measure the deflection of the specimen from the lateral pressure. The specimens were measured at regular intervals starting at 1.5 psi (10 kPa) and increasing by 1 psi

(7 kPa) until 6.5 psi (45 kPa) was reached. At each pressure interval the loading was paused for 1 minute to allow the deflection of the system to stabilize.

4.2.2 Materials

For this testing a large number of foam samples were investigated. However, after discussions with representatives in the foam industry, it was decided to narrow the investigation to either polyethylene or cross-link foams. These foams were chosen for their economy, availability, durability, and water tightness. A summary of the foam properties included in the study is provided in Table 4.4. Foams 1 through 3 are polyethylene foams, and foam 4 is a cross- link material. Typically, as a foam's density increases so does the modulus and tearing resistance.

Table 4.5 *Summary of the manufacturer reported foam properties.*

Property	Foam Number				Test Method
	1	2	3	4	
Density, psf (Pa)	1 (48)	1.2 (57)	1.7 (81)	2.0 (96)	ASTM D-3575 Suffix W
Force required to give a given deflection, psi (kPa):					ASTM D-3575 Suffix D
25%	3 (21)	5 (34)	5.5 (38)	5 (34)	
50%	6 (41)	10 (69)	12.5 (86)	14 (96)	
Percent increase in the sustained load:					ASTM D-3575 Suffix B
2 hours	30	30	34	Not tested	
24 hours	24	24	20	Not tested	
Percent increase in deflection at 1 psi (7 kPa)	12%	5%	3%	Not tested	ASTM D-3575 Suffix BB
Tensile strength, psi (kPa)	20 (138)	38 (262)	26 (179)	54.5 (376)	ASTM D412
Elongation, %	75	75	59	237	ASTM D412

Adhesives were obtained that were compatible with both the concrete and foam. There were three main types of adhesives investigated. These included (A) synthetic elastomer liquid, (B) two part epoxy, and (C) aerosol adhesive. In the remainder of the report each adhesive will be referred to by its corresponding letter. Results for adhesive A and B are included in this document. The testing for adhesive C will be included in the final report, but it was realized

through preliminary testing that this adhesive did not perform as well as the other two and is quite costly.

4.2.3 Results and Analysis

The results from the previously described tests are presented in Table 4.5. The average and standard deviation values are presented for three tests. The maximum pressure investigated in the lateral pressure and tension and lateral pressure tests was 6.5 psi (45 kPa). If a specimen exceeded this capacity, then the value was reported as 6.5 psi (45 kPa). If a standard deviation was reported as zero, then this means that all three specimens had the same value. Data were included in the table for a cure time of one and two days. This was done to evaluate how the strength of the foam changed with time.

Table 4.6 *Summary of the testing for the foams and adhesives investigated.*

Foam	Adhesive	Cure Time (days)	Lateral Pressure		Tension		Tension/Lateral Pressure*	
			psi (kPa)	St. Dev.	in. (mm)	St. Dev.	psi (kPa)	St. Dev.
1	A	1	5.5 (38)	0	0.91 (23)	0.13 (3)		
	A	2	6.5 (45)	0	0.89 (23)	0.09 (2)	6.5 (45)	0
2	A	1	4.8 (33)	0.58 (4)	0.36 (9)	0.05 (1)	3.5 (24)	0
	A	2	6.5 (45)	0	0.83 (21)	0.23 (3)		
3	A	1	6.1 (42)	0.55 (3.8)	0.36 (9)	0.02 (0.5)	6.5 (45)	0
	A	2	6.3 (43)	0	0.7 (18)	0.28 (7)	6.5 (45)	0
4	A	1	6.5 (45)	0	0.75 (19)	0.22 (6)	6.5 (45)	0
	A	2	Not tested		0.66 (17)	0.3 (8)		
2	A	1	4.8 (33)	0.58 (4)	0.36 (9.1)	0.05 (1)	3.5 (24)	0
	A	2	6.5 (45)	0	0.83 (21)	0.23 (6)		
2	B	1	4.5 (31)	0	0.32 (8)	0.15 (4)	3.5 (24)	1 (7)
	B	2	4.5 (31)	0	0.33 (8)	0.05 (1)		

**The maximum pressure investigated in the lateral pressure test is 6.5 psi (45 kPa). If the specimen exceeded this capacity then the result was reported as 6.5 psi (45 kPa).*

4.2.4 Discussion

Not all combinations of foam and adhesive were investigated for this testing. From preliminary testing, adhesive A appeared the most practical due to constructability and economy. For these reasons each of the foams were evaluated with this adhesive. In order to make a comparison between adhesives, foam 2 was investigated with both adhesives A and B to investigate the impact on the physical properties of the specimen. Adhesive B had very similar properties after the first day of curing to adhesive A; however, after the second day of curing adhesive A showed improved performance in the lateral pressure and tension test.

From Table 4.5 it can be seen that the minimum lateral pressure resistance for the foams was 4.5 psi (31 kPa) after one day of curing for all of the adhesives investigated. This would mean that the system could roughly resist 4.5 ft. (1.4 m) of head pressure from a concrete or grout pour (assuming that the unit weight of the concrete/grout was 144 pcf [2307 kg/cubic meter]). While this number is likely sufficient, in all cases where adhesive A was used the lateral pressure was at or exceeded 6.5 psi (45 kPa) or 6.5 ft. (2 m) of concrete/grout head pressure. This implies that adhesive A will be satisfactory for this application.

One parameter that is not quantified in the data in Table 4.5 but is implied in Table 4.4 is the compressive stiffness of the foam. This parameter is important for the use of these foams, as the foam needs to deflect under the weight of the precast overhang panels as needed. Foam 1 has the lowest compressive stiffness of the foams tested, so it would provide the most flexibility during construction.

Another parameter that is not considered in the data presented is the aesthetics of the foam, as it will be left in place in a visible location at the edge of the bridge. The foam manufacturer creates foam in a distinctive color so that the properties are represented by the color of the foam. The typical color for foam 1 is a gray that is similar to concrete.

For these reasons it is recommended to use a combination of foam 1 and adhesive A for future projects implementing the precast overhang system. A brief summary of the recommended construction methods are as follows:

- The surface of the precast beam where the foam is to be placed should be thoroughly covered in adhesive.
- The foam should be cut to height that is approximately 1 in. (25 mm) higher than the desired haunch.
- The foam should then be placed on the adhesive and held in place.

- Before the precast overhang panel is placed, the top of the foam should be thoroughly covered in adhesive.
- The grade bolts in the precast panels should be adjusted to provide a haunch depth that closely matches that required for the bridge deck.
- The panel should be placed and then allowed to cure for a day before adjusting. After the glue has cured, the height of the panel can still be lowered but should not be raised more than 0.25 in. (6 mm).

4.2.5 Summary for Haunch Form Materials

When foam 1 and adhesive A are used in combination the forming system used can be left in place, will provide sufficient lateral strength against gravity-fed concrete or grout placements, and does not provide an aesthetic issue in the final bridge. By implementing this system it minimizes the work needed under a bridge deck with precast overhang panel construction and possibly other precast bridge construction. This leads to an improvement in not only the constructability and economy but also the safety of the precast overhang or any other precast bridge deck system that requires an adjustable haunch.

CHAPTER 5. CONCLUSIONS AND RECOMMENDATIONS

The research performed in this project evaluated the overhang and shear capacity of a precast, prestressed full-depth bridge overhang system for possible use in the Rock Creek Bridge in Parker County, Texas. Research was also conducted to evaluate grout materials and haunch-forming materials for the bridge. The findings of the research team are as follows:

- SikaGrout™ 212 exhibits good early strength and adequate flow characteristics to fill the haunch when using a w/p of less than 0.20. Bleeding is low when the w/p is 0.185 or lower.
- A combination of a flexible polyethylene foam and an adhesive can be used to produce an adjustable haunch form that is able to resist the lateral pressure from the gravity-fed concrete and grout used to construct the precast overhang system.
- In the present research four overhangs were tested: two overhangs were based on a proposed new, full-depth, precast system where the panels were manufactured in a precasting plant with a two-stage pour. Performance of these two overhang specimens was compared with a specimen that had standard CIP construction.
- The concept of using conventional precast, prestressed panels to construct an overhang was verified. Current TxDOT bridge capacities have sufficient reserve strength over the required AASHTO loads. The full-depth precast panels also showed sufficient strength in both interior bays and overhangs.
- The stiffness of the full-depth precast, prestressed panels was comparable to the conventional CIP deck. Overhang failure loads were made critical by loading at the edge of the panel and seam joint. It is evident that the introduction of the seam decreases the overall strength, but only the bottom longitudinal steel is discontinuous. Nevertheless, some positive (and negative) moment strength is still provided due to the CIP panel-to-panel joint that has a single layer of link bars. Although this is weaker than the full-depth overhang, overall the reduction of load carrying capacity is only in the order of 14 percent. It should be noted that the overhang systems evaluated in this research did not contain barriers.
- A sufficient factor of safety was provided against the design wheel load of 16 kips (71 kN) for all 3-ft. (0.9 m) overhangs tested on this project.

- The interface shear capacity of the existing R-bar system used in present practice is sound. From the tests the inferred coefficient of interface friction between cracked concrete-concrete interfaces that exist within the haunch of a prestressed concrete slab-on-girder bridge is at least 1.0.
- The apparent coefficient of sliding friction in the cracked grout-bed that exists between the precast concrete slab and concrete girder, based on the present test data, has a dependable coefficient of friction of 0.4. This result is lower than expected and is believed to be attributed to the relatively smooth shear interface between the soffit of the precast panels and the grout in the haunch.
- Based on two threaded-rods per pocket, as tested, the interface shear system to connect precast concrete slabs to concrete girders via a grout bed, as proposed by TxDOT engineers in collaboration with the research team, *does not* have sufficient capacity as expected by the *initial* design.
- The relatively low resistance provided by the interface shear using the haunch can be improved by using more pockets and fasteners.

Based on these findings, the following recommendations are made:

- SikaGrout^{TM} 212 should be used for the haunch on the Rock Creek Bridge.
- Class S deck concrete should be used to fill the pockets on the Rock Creek Bridge.
- Use low density gray Polyethylene 1.0# density from Pregis and 3M Scotch Grip 4693 adhesive for the haunch forms
- The panels initially designed for the project require modification. The three panels closest to the ends of the bridge should contain 7 pockets and at least 2 connectors per pocket. The other panels should contain 4 pockets with at least 2 connectors per pocket. Drawings are provided in the appendix.
- The capacity of the precast, prestressed overhang system tested exhibits sufficient capacity to safely carry AASHTO loads.

It should be noted that the overhang system has significant potential to increase economy and safety of bridge construction in Texas. Additional research is needed to optimize the design and construction. The research team makes the following recommendations:

- Surface roughness. Concrete codes typically recommend roughening of interfaces to improve the friction coefficient for sliding interface shear. For example, if the surface is intentionally roughened, providing an amplitude of more than 0.2 in. (5 mm), a friction coefficient of 1.4 can be assumed, by design. Lesser values are recommended for smoother surfaces, such as 1.0 and 0.7 for a roughness amplitude of > 0.08 in. (2 mm) and laitance-free non-roughened surfaces, respectively. Several tests need to be conducted to explore the optimal trade-off between constructability and surface roughness.

- Optimization of the pocket details. Continue to use additional pockets, but instead of using expensive threaded fasteners, use conventional extended R-bars into the pocket zone. Only two, or at most three, #5 R-bars may be necessary for the most adverse cases. Several tests need to be conducted to investigate the efficacy of R-bars in multiple pockets. If seven pockets per panel are used, then there is little need for expensive and relatively difficult-to-place grout. Instead, conventional concrete with 6-in. (150 mm) slump and a maximum aggregate size of .375 in. (10 mm) may be sufficient. This class of concrete is commonly used for filling concrete block masonry. It is likely that such a material will have rougher cracked interface surfaces, possibly leading to a higher coefficient of sliding friction.
- Grouping effects of connectors. The summary of these results included tests for only 2 connectors within a pocket; however, it is known that there can be grouping effects, especially when having more connectors in a pocket. While this would increase the shear resistance capacity, additional shear reinforcement provided by R-bars may also be needed.
- Effect of haunch height. Longer beams with sufficient capacity provided by hoops are needed to test additional specimens to assess the effect of a variable haunch height such that beam failure does not prematurely occur as a result of distressing the beam. More data can be obtained to make more conclusive remarks on the effect of the haunch height on the deck-haunch-beam system.

REFERENCES

AASHTO LRFD Design Manual (2007).

Badie, S., Tadros, M., and Girgis, A. "Full-Depth, Precast-Concrete Bridge Deck Panel Systems," NCHRP 12-65, 2006.

Folliard, K. J., Du, L, Trejo, D., Halmen, C., Sabol, S., and Leshchinsky, D., Development of a Recommended Practice for Use of Controlled Low-Strength Material in Highway Construction, NCHRP Report 597, Transportation research Board, Washington D.C., 2008

Kelly, D.J., Bradberry, T.E., and Breen, J.E. "Time Dependent Deflections of Pretensioned Beams." Research Report CTR 381-1, Center for Transportation Research – The University of Texas at Austin, 1987.

Sullivan, S. "Construction and Behavior of Precast Bridge Deck Panel Systems," Dissertation, Virginia Polytechnic Institute and State University, 2007.

APPENDICES

This analysis is to be evaluate the shear interface stress between the bridge deck and a 120 ft. Type IV girder with 6 ft. beam spacing. The shear connectors should only have to resist the live loads from an HL93 Truck. No dead load needs to be transferred from the deck by the couplers as the girder will resist all of the weight of the fresh concrete.
This analysis will also only focus on the exterior beams.
As per Table 4.6.2.2.3b-1 for case cast-in-place concrete on concrete girder in AASHTO LRFD 2007.

1 Design Lane

Lever rule

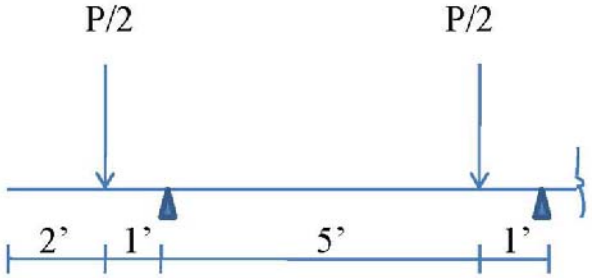

$0 = -6R + (P/2)*1 + (P/2)*7$

$R = 0.67 * 1.2 = 0.8$ DF

↑ Mult. Pres factor

2 or More

$g = e\, g_{INT} : e = 0.6 + (d_e/10)$

$g_{INT} = 0.2 + (5/12) - (5/35)^2$

$g_{INT} = 0.2 + (6/12) - (6/35)^2$

$g_{INT} = 0.67$

$e = 0.6 + ((3-1)/10) = 0.8$

$g_{EXT} = 0.8*(0.67) = 0.54$

<u>0.8 DF Controls</u>.

*Assumes 1 ft. rail width and tire load 1 ft. from rail.

Find I

I for type IV = 260403
$Y_B = 24.75$”
$Y_T = 29.25$”
A = 788.4

Properties from TxDOT Bridge Design Guide

$I_{SLAB} = (1/12)*6*12*8^3 = 3072\ in^4$
$A_{SLAB} = 8*6*12 = 576\ in^2$

$I_{HAUNCH} = (1/12)*20*2^3 = 13.33\ in^4$
$A_{HAUNCH} = 2*20 = 20\ in^2$

$\bar{y} = (\sum A_Y / \sum A)$
$\bar{y} = ((788.4* 24.75) + (40*(54+1)) + (6*12*8*(54+2+4)) / (788.4 + 40 +576)$
$\bar{y} = 40$” from bottom

$I_{COMP} = I + A*\bar{y}^2$
$= 260403 + 3072 + 13.3 + (788.4*(40-24.75)^2)+ (40*(40-55)^2) + (576*(54+2+4-40)^2)$
$= 686241\ in^4$

$Q = 576*(54+2+4-40)$
$= 11520\ in^3$

Loading:

Lane load:

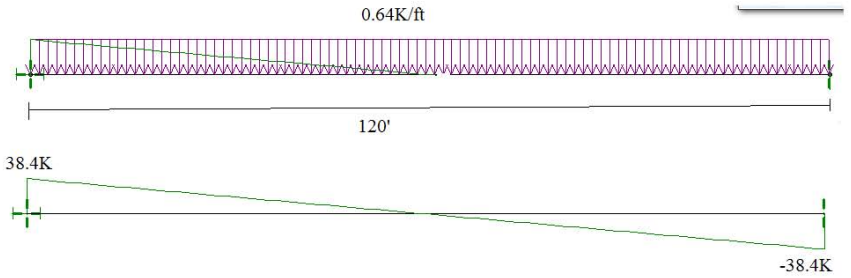

Truck load:

Maximum V @ center:

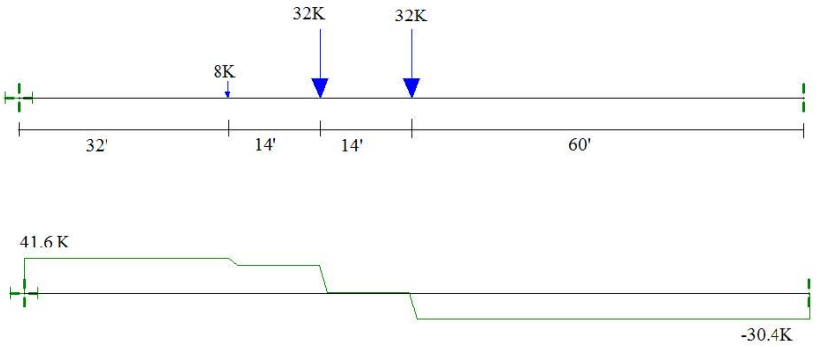

Maximum V @ edge of the slab:

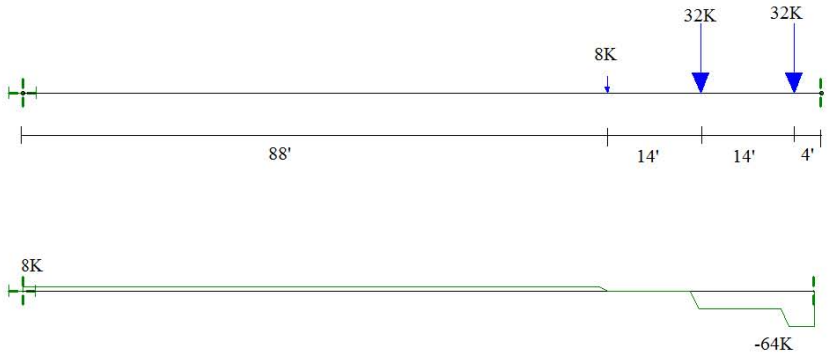

Look @ V @ 2nd panel:

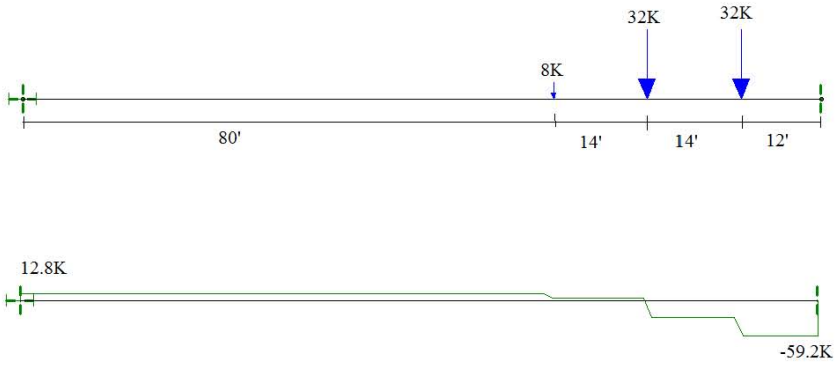

Look @ V @ 3rd panel:

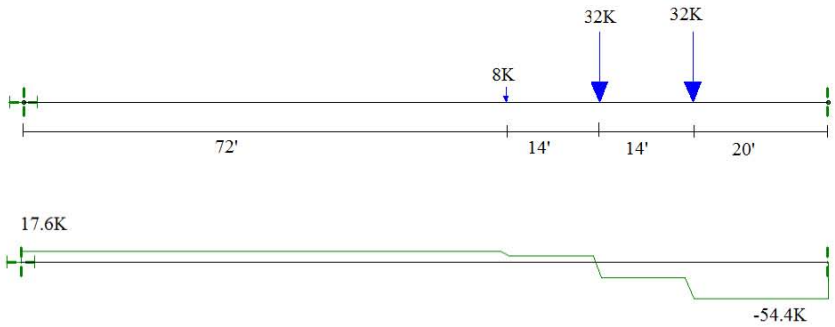

Look @ V @ 4th panel:

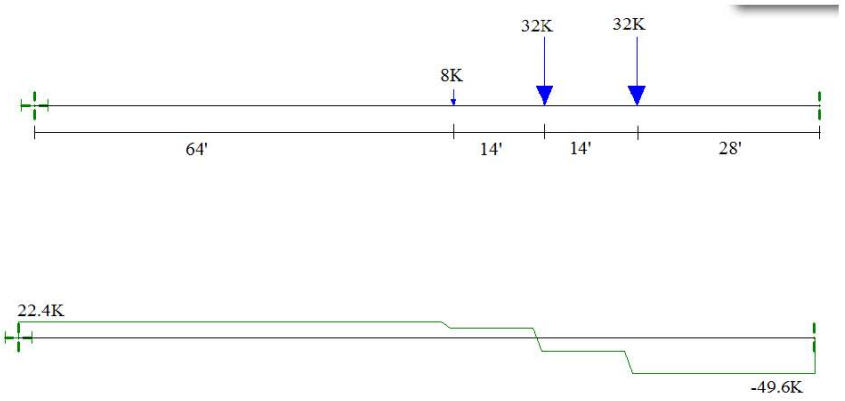

For every panel increase truck shear reduces by 4.8K.

Design Shear = 1.75 DF (LL +1.33 LL Truck)

Lane Impact

@ End

Design V = 1.75*0.8*((38.4*(54/60)) + (1.33*64)) = 167.55 K

q = (VQ)/I = ((167.55*11520)/686241) = 2.81 K/in *8*12 = 270 K

Number of fasteners = 270 K / (45 K / pair) = 6 pair Use 7 pair to make spacing equal

@ Middle

Design V = 1.75*0.8*(0 + (1.33*30.4)) = 56.60 K

q = (VQ)/I = ((56.60*11520)/686241) = 0.95 K/in *8*12 = 91.21 K

Number of fasteners = 91.21 K / (45 K / pair) = 2.03 pair

@ 2nd panel

Design V = 1.75*0.8*((38.4*(48/60)) + (1.33*59.2)) = 153.24 K

q = (VQ)/I = ((153.24*11520)/686241) = 2.57 K/in *8*12 = 246.96 K

Number of fasteners = 246.96 K / (45 K / pair) = 5.48 pair

Continue on spread sheet…..

Panel	Lane Shear	Truck Shear	Design Shear	q (k/in)	number of required fasteners	number to use
1	35.8	64.0	169.3	2.8	6.1	7
2	30.7	59.2	153.2	2.6	5.5	7
3	25.6	54.4	137.1	2.3	4.9	7
4	20.5	49.6	121.0	2.0	4.3	7
5	15.4	44.8	104.9	1.8	3.8	4
6	10.2	40.0	88.8	1.5	3.2	4
7	5.1	35.2	72.7	1.2	2.6	4
8	0	30.4	56.6	1.0	2.0	4

7 fasteners are used to keep the spacing of the pockets at a regular spacing.

Appendix B – Proposed Plan Sheets

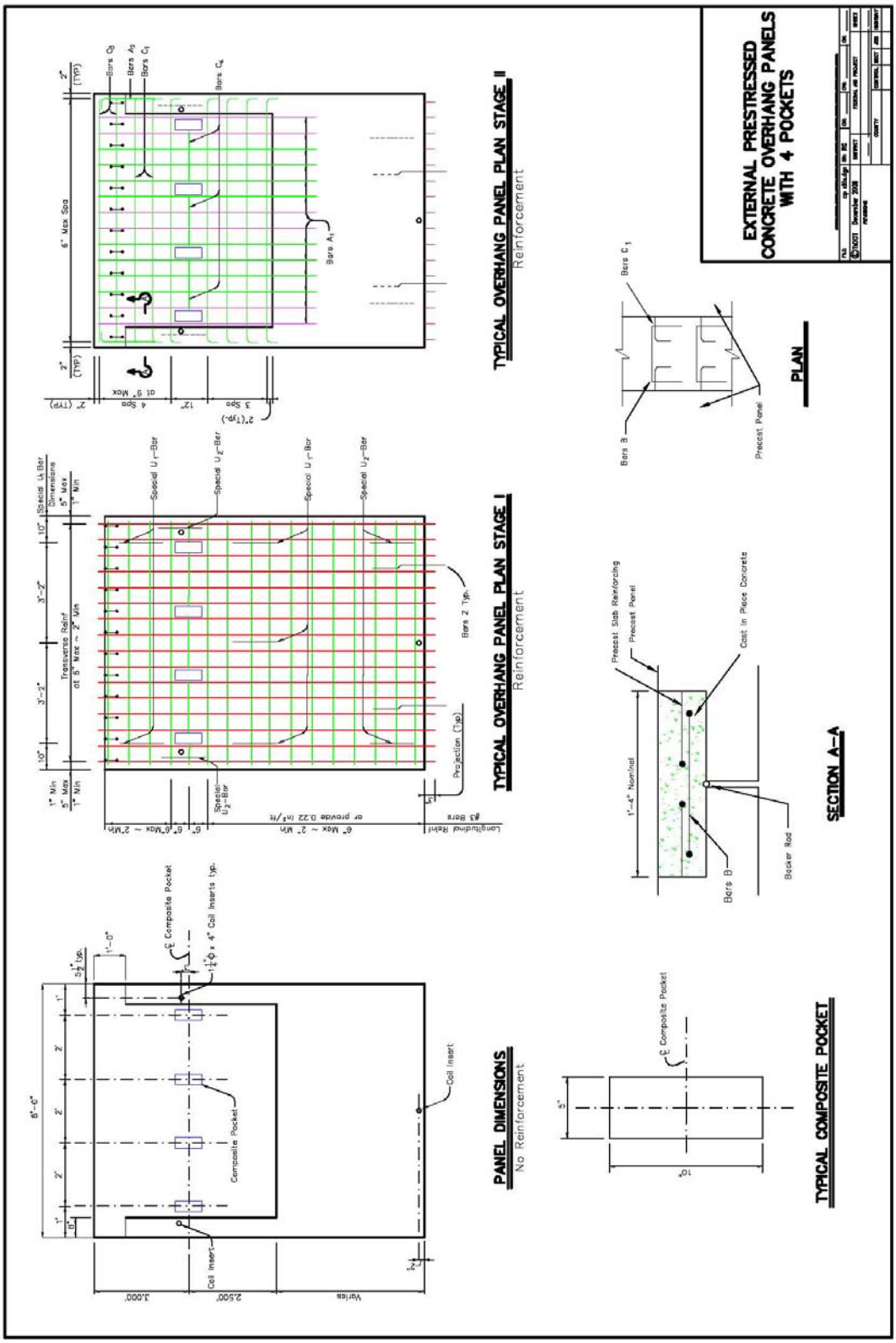

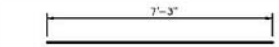

BARS A_1 (#5)

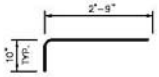

BARS A_2 (#5)

BARS B (#4)

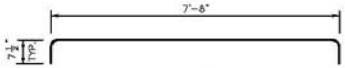

BARS C_1 (#4)

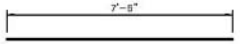

BARS C_3 (#4)

BARS C_4 (#4)

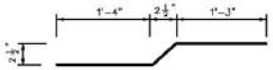

BARS Z (#4)

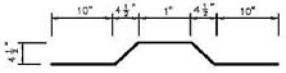

SPECIAL U_1 AND U_2–BAR (#4)

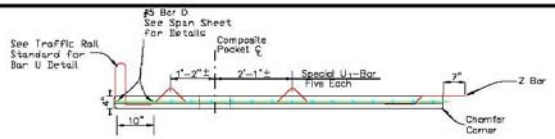

Typical Section–Stage I

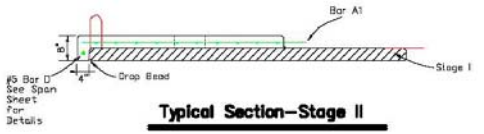

Typical Section–Stage II

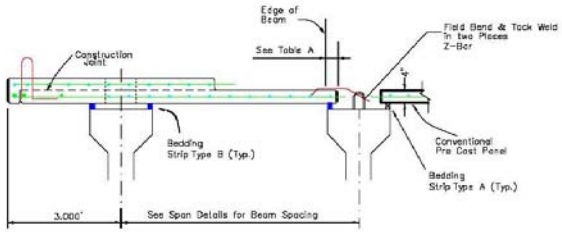

Completed Typical Section

FABRICATION NOTES:

All concrete for panels is to be Class H. Use Class H (HPC) concrete for panels if required elsewhere in plans. Release strength f'_{ci}=4000 psi. Minimum 28 day strength f'_{cm}=5000 psi.

Remove laitance from top panel surface.

A minimum of 80 percent of the top surface area shall have the required broom finish.

Shop drawings for the fabrication of panels will not require the Engineer's approval if fabrication is in accordance with the details shown on this standard.

A panel layout which identifies location of each panel shall be developed by the fabricator. Permanently mark each panel in accordance with the panel layout. A copy of the layout is to be provided to the Engineer.

TRANSVERSE PANEL REINFORCEMENT:

For panel widths over 5', use ½" or ⅝" Dia (270k) prestressing strands with an initial tension of 16.1 kips per strand.

For panel widths over 3'-6" up to and including 5', use ½" or ⅝" Dia (270k) prestressing strands with an initial tension of 16.1 kip per strand. Optionally, #4 Grade 60 reinforcing bars may be used in lieu of prestressed strands.

For panel widths up to 3'-6", use #4 Grade 60 reinforcing bars (prestressed strands are not allowed).

Place transverse panel reinforcement at panel centroid and space at 6" Max.

LONGITUDINAL PANEL REINFORCEMENT:

Any of the following options may be used for longitudinal panel reinforcement:

1. (#3) Grade 60 reinforcing steel at 6" Max Spacing. No splices allowed.
2. ⅜" Dia prestressing strands at 4 ⅜" Max Spacing (unstressed). No splices allowed.
3. ⅜" Dia prestressing strands at 6" Max Spacing (unstressed). No splices allowed.
4. Deformed Welded Wire Reinforcement (WWR) (ASTM A497) providing 0.22 sq in per foot of panel width. Wires larger than D11 not permitted. Provide transverse wires to ensure proper handling of reinforcing. One splice per panel is allowed. See WWR Splice Detail.

No combination of longitudinal reinforcement options in a panel is allowed.

Place longitudinal panel reinforcement above transverse panel reinforcement.

GENERAL NOTES:

Cover per PCP standards sheets, including overhang details (typical clear cover is 1–2", except A1 and A2 bars 2", clear to top surface, and underside overhang has 1–½" clear cover.

Use additional steel as necessary to ensure placement of #5 bar D in Stage II.

Prestressing strands intersecting the blockouts shall be removed prior to shipping.

The interface between stage I & II shall be cleaned of laitance W/A light water blast before placement of stage II.

All chamfers 3/4".

The location of Special Bars U_1 to be determined by the contractor to provide a balanced lift.

TABLE A

Beam Type	Normal (in.)	Min (in.)	Max (in.)
A	3	2 ½	3 ½
B	3	2 ½	3 ½
C	4	3	4 ½
IV	5	4	7 ½
VI	6 ½	4 ½	8 ½
U40	5 ½	5 ½	7
U54	5 ½	5 ½	7

EXTERNAL PRESTRESSED CONCRETE OVERHANG PANELS WITH 4 POCKETS

FILE:	cp sht.dgn	dn: RC	ck:	ck:	ck:	
©TxDOT December 2008		DISTRICT	FEDERAL AID PROJECT			SHEET
REVISIONS						
		COUNTY		CONTROL	SECT	JOB	HIGHWAY

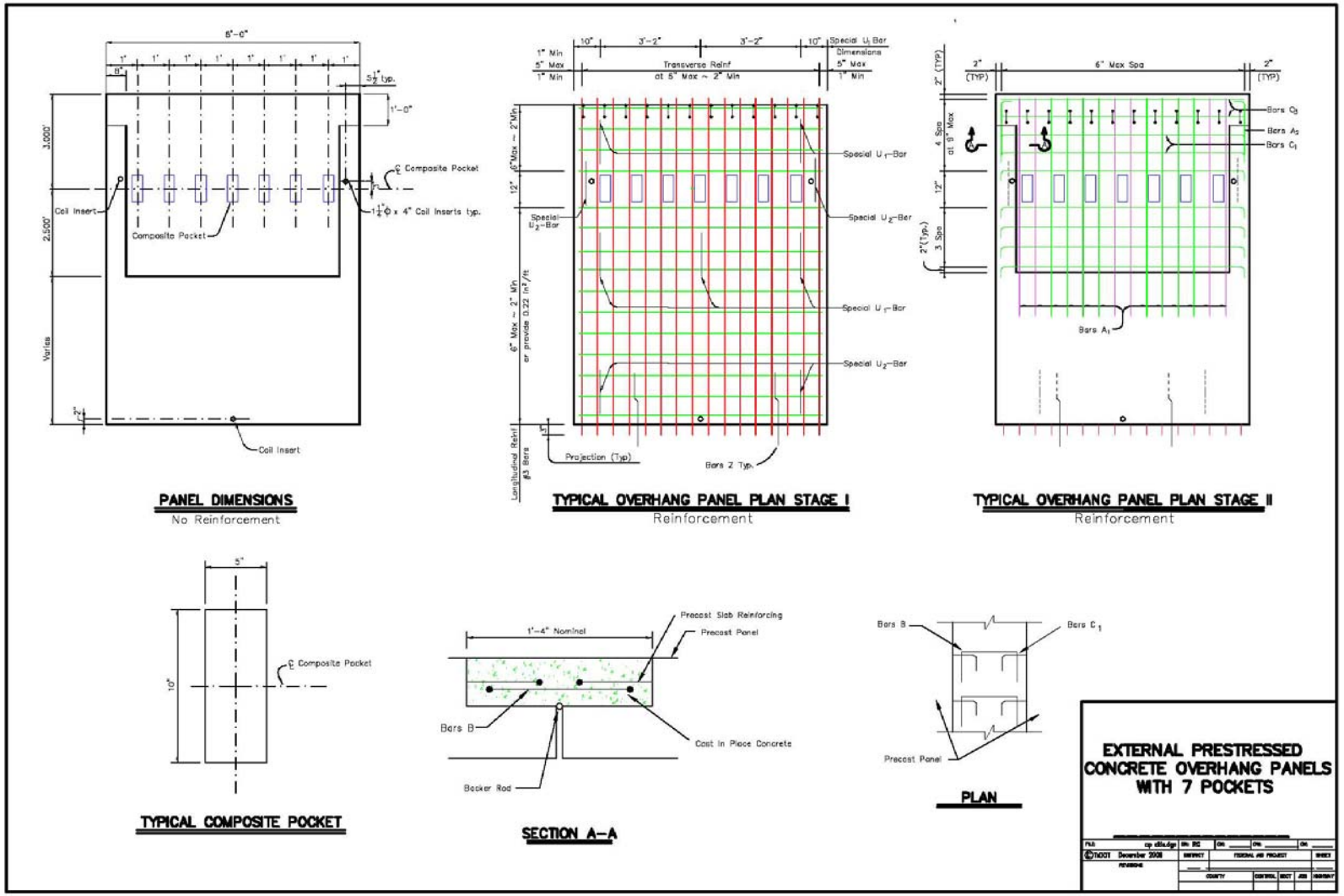
PANEL DIMENSIONS
No Reinforcement
TYPICAL OVERHANG PANEL PLAN STAGE I
Reinforcement
TYPICAL OVERHANG PANEL PLAN STAGE II
Reinforcement
TYPICAL COMPOSITE POCKET
SECTION A–A
PLAN
EXTERNAL PRESTRESSED CONCRETE OVERHANG PANELS WITH 7 POCKETS
Coil Insert
Composite Pocket
Special U1–Bar
Special U2–Bar
Bars A1
Bars B
Bars C1
Precast Slab Reinforcing
Precast Panel
Cast In Place Concrete
Backer Rod
Projection (Typ)
Bars Z Typ.
Transverse Reinf at 6" Max ~ 2" Min
6" Max Spa
Longitudinal Reinf #3 Bars
1'–4" Nominal

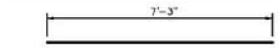

BARS A_1 (#5)

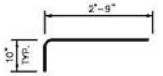

BARS A_2 (#5)

BARS B (#4)

BARS C_1 (#4)

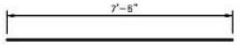

BARS C_3 (#4)

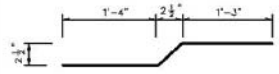

BARS Z (#4)

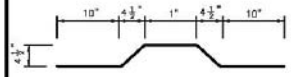

SPECIAL U_1 AND U_2–BAR (#4)

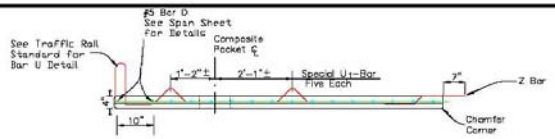

Typical Section–Stage I

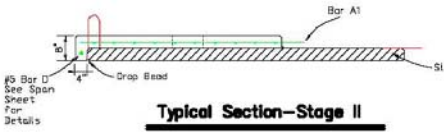

Typical Section–Stage II

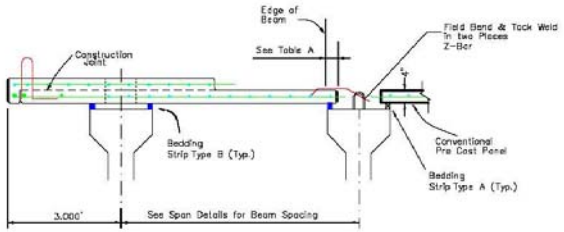

Completed Typical Section

FABRICATION NOTES:

All concrete for panels is to be Class H. Use Class H (HPC) concrete for panels if required elsewhere in plans. Release strength f'_{ci}=4000 psi. Minimum 28 day strength f'_{cm}=5000 psi.

Remove laitance from top panel surface.

A minimum of 90 percent of the top surface area shall have the required broom finish.

Shop drawings for the fabrication of panels will not require the Engineer's approval if fabrication is in accordance with the details shown on this standard.

A panel layout which identifies location of each panel shall be developed by the fabricator. Permanently mark each panel in accordance with the panel layout. A copy of the layout is to be provided to the Engineer.

TRANSVERSE PANEL REINFORCEMENT:

For panel widths over 5', use ½" or ⅝" Dia (270k) prestressing strands with an initial tension of 16.1 kips per strand.

For panel widths over 3'-6" up to and including 5', use ½" or ⅝" Dia (270k) prestressing strands with an initial tension of 16.1 kip per strand. Optionally, #4 Grade 60 reinforcing bars may be used in lieu of prestressed strands.

For panel widths up to 3'-6", use #4 Grade 60 reinforcing bars (prestressed strands are not allowed).

Place transverse panel reinforcement at panel centroid and space at 6" Max.

LONGITUDINAL PANEL REINFORCEMENT:

Any of the following options may be used for longitudinal panel reinforcement:

1. (#3) Grade 60 reinforcing steel at 6" Max Spacing. No splices allowed.
2. ½" Dia prestressing strands at 4 ⅜" Max Spacing (unstressed). No splices allowed.
3. ⅜" Dia prestressing strands at 6" Max Spacing (unstressed). No splices allowed.
4. Deformed Welded Wire Reinforcement (WWR) (ASTM A497) providing 0.22 sq in per foot of panel width. Wires larger than D11 not permitted. Provide transverse wires to ensure proper handling of reinforcing. One splice per panel is allowed. See WWR Splice Detail.

No combination of longitudinal reinforcement options in a panel is allowed.

Place longitudinal panel reinforcement above transverse panel reinforcement.

GENERAL NOTES:

Cover per PCP standards sheets, including overhang details (typical clear cover is 1–3", except A1 and A2 bars 2", clear to top surface, and underside overhang has 1–¾" clear cover.

Use additional steel as necessary to ensure placement of #5 bar D in Stage II.

Prestressing strands intersecting the blockouts shall be removed prior to shipping.

The interface between stage I & II shall be cleaned of laitance W/A light water blast before placement of stage II.

All chamfers 3/4".

The location of Special Bars U_1 to be determined by the contractor to provide a balanced lift.

TABLE A			
Beam Type	Normal (in.)	Min (in.)	Max (in.)
A	3	2 ⅜	3 ⅜
B	3	2 ⅜	3 ⅜
C	4	3	4 ⅜
IV	5	4	7 ⅜
VI	6 ⅜	4 ⅜	8 ⅜
U40	5 ⅜	5 ⅜	7
U54	5 ⅜	5 ⅜	7

EXTERNAL PRESTRESSED CONCRETE OVERHANG PANELS WITH 7 POCKETS

FILE: cp sta.dgn | dn: PC | ck: | dw: | ck:

©TxDOT December 2008 | DISTRICT | FEDERAL AID PROJECT | SHEET

REVISIONS | COUNTY | CONTROL | SECT | JOB | HIGHWAY

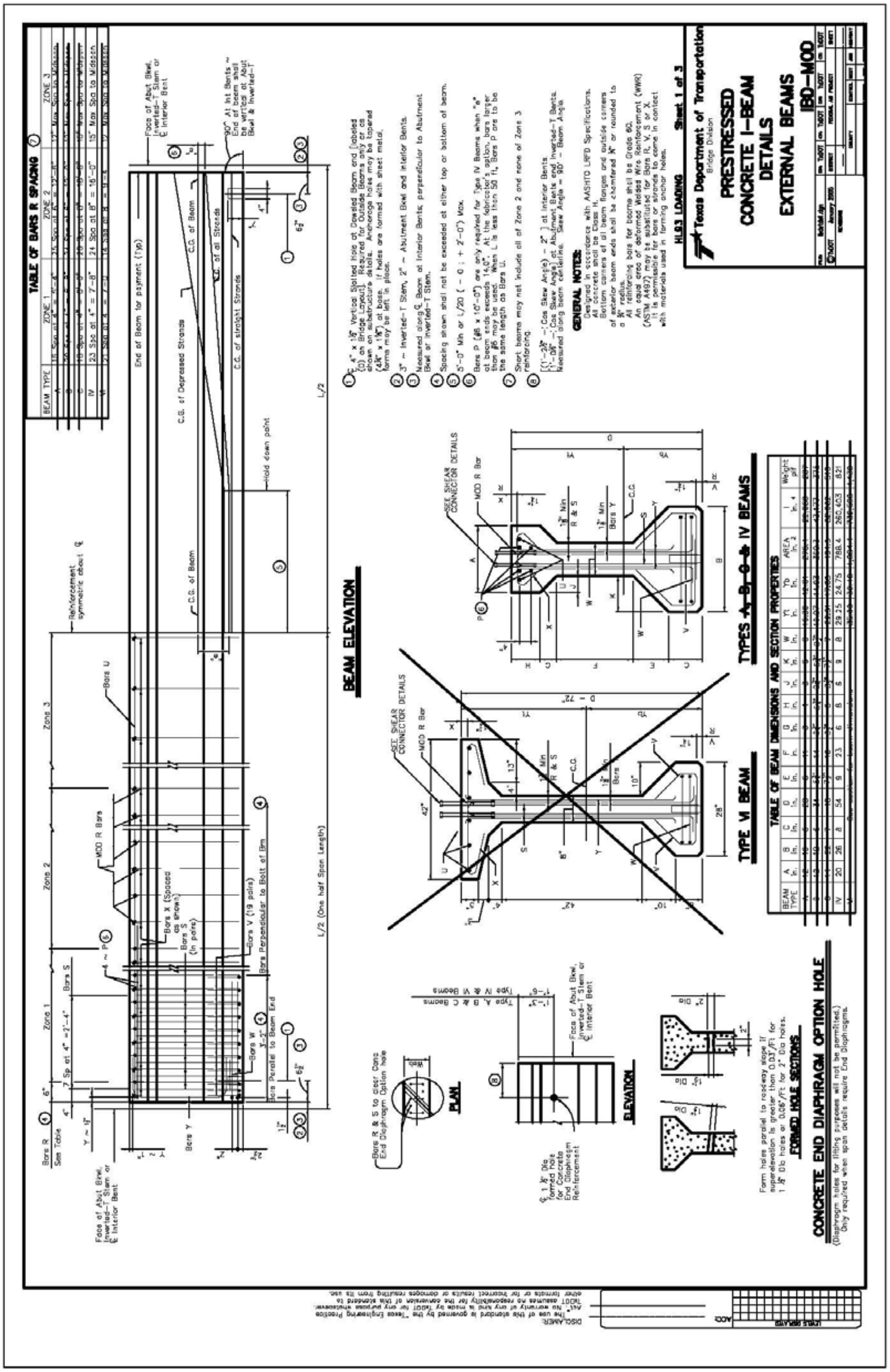
TABLE OF BARS R SPACING
BEAM ELEVATION
TYPE VI BEAM
TYPES A, B, C & IV BEAMS
TABLE OF BEAM DIMENSIONS AND SECTION PROPERTIES
GENERAL NOTES:
PLAN
ELEVATION
FORMED HOLE SECTIONS
CONCRETE END DIAPHRAGM OPTION HOLE
HL93 LOADING
Sheet 1 of 3
Texas Department of Transportation
Bridge Division
PRESTRESSED
CONCRETE I-BEAM
DETAILS
EXTERNAL BEAMS
IBD-MOD

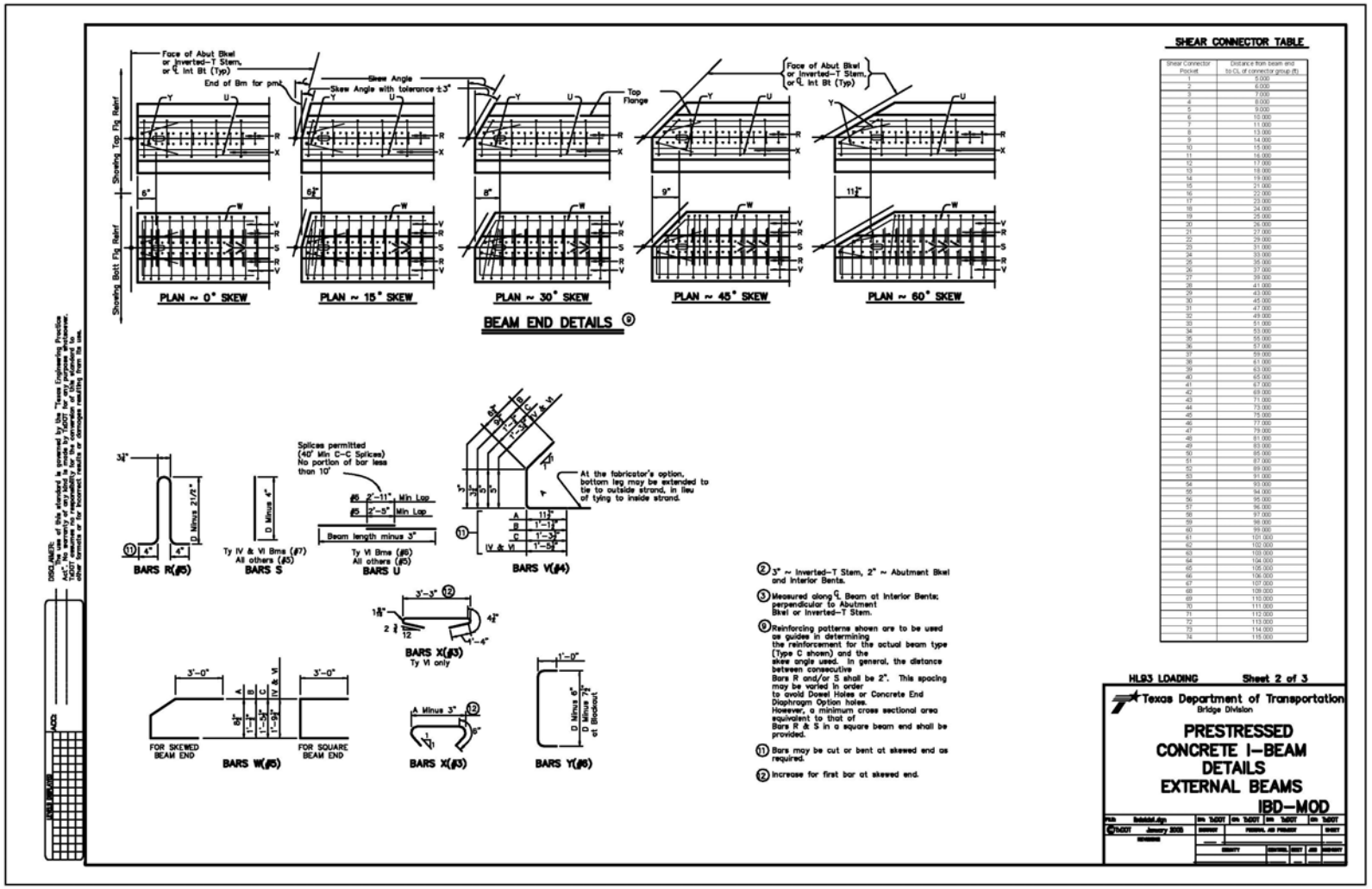

② 3" ~ Inverted–T Stem, 2" ~ Abutment Bkwl and Interior Bents.

③ Measured along ℄ Beam at Interior Bents; perpendicular to Abutment Bkwl or Inverted–T Stem.

⑨ Reinforcing patterns shown are to be used as guides in determining the reinforcement for the actual beam type (Type C shown) and the skew angle used. In general, the distance between consecutive Bars R and/or S shall be 2". This spacing may be varied in order to avoid Dowel Holes or Concrete End Diaphragm Option holes. However, a minimum cross sectional area equivalent to that of Bars R & S in a square beam end shall be provided.

⑪ Bars may be cut or bent at skewed end as required.

⑫ Increase for first bar at skewed end.

SHEAR CONNECTOR TABLE

Shear Connector Pocket	Distance from beam end to CL of connector group (ft)
1	5.000
2	6.000
3	7.000
4	8.000
5	9.000
6	10.000
7	11.000
8	13.000
9	14.000
10	15.000
11	16.000
12	17.000
13	18.000
14	19.000
15	21.000
16	22.000
17	23.000
18	24.000
19	25.000
20	26.000
21	27.000
22	29.000
23	31.000
24	33.000
25	35.000
26	37.000
27	39.000
28	41.000
29	43.000
30	45.000
31	47.000
32	49.000
33	51.000
34	53.000
35	55.000
36	57.000
37	59.000
38	61.000
39	63.000
40	65.000
41	67.000
42	69.000
43	71.000
44	73.000
45	75.000
46	77.000
47	79.000
48	81.000
49	83.000
50	85.000
51	87.000
52	89.000
53	91.000
54	93.000
55	94.000
56	95.000
57	96.000
58	97.000
59	98.000
60	99.000
61	101.000
62	102.000
63	103.000
64	104.000
65	105.000
66	106.000
67	107.000
68	109.000
69	110.000
70	111.000
71	112.000
72	113.000
73	114.000
74	115.000

HL93 LOADING Sheet 2 of 3

Texas Department of Transportation
Bridge Division

PRESTRESSED CONCRETE I–BEAM DETAILS EXTERNAL BEAMS

IBD–MOD

File: ibdetail.dgn	DN: TxDOT	CK: TxDOT	DW: TxDOT	CK: TxDOT
©TxDOT January 2005	CONT	FEDERAL AID PROJECT		SHEET
REVISIONS				
	DISTRICT	COUNTY	CONTROL	SECT	JOB	HIGHWAY

DISCLAIMER:
The use of this standard is governed by the "Texas Engineering Practice Act". No warranty of any kind is made by TxDOT for any purpose whatsoever. TxDOT assumes no responsibility for the further use of this standard for other formats or for incorrect results or damages resulting from its use.

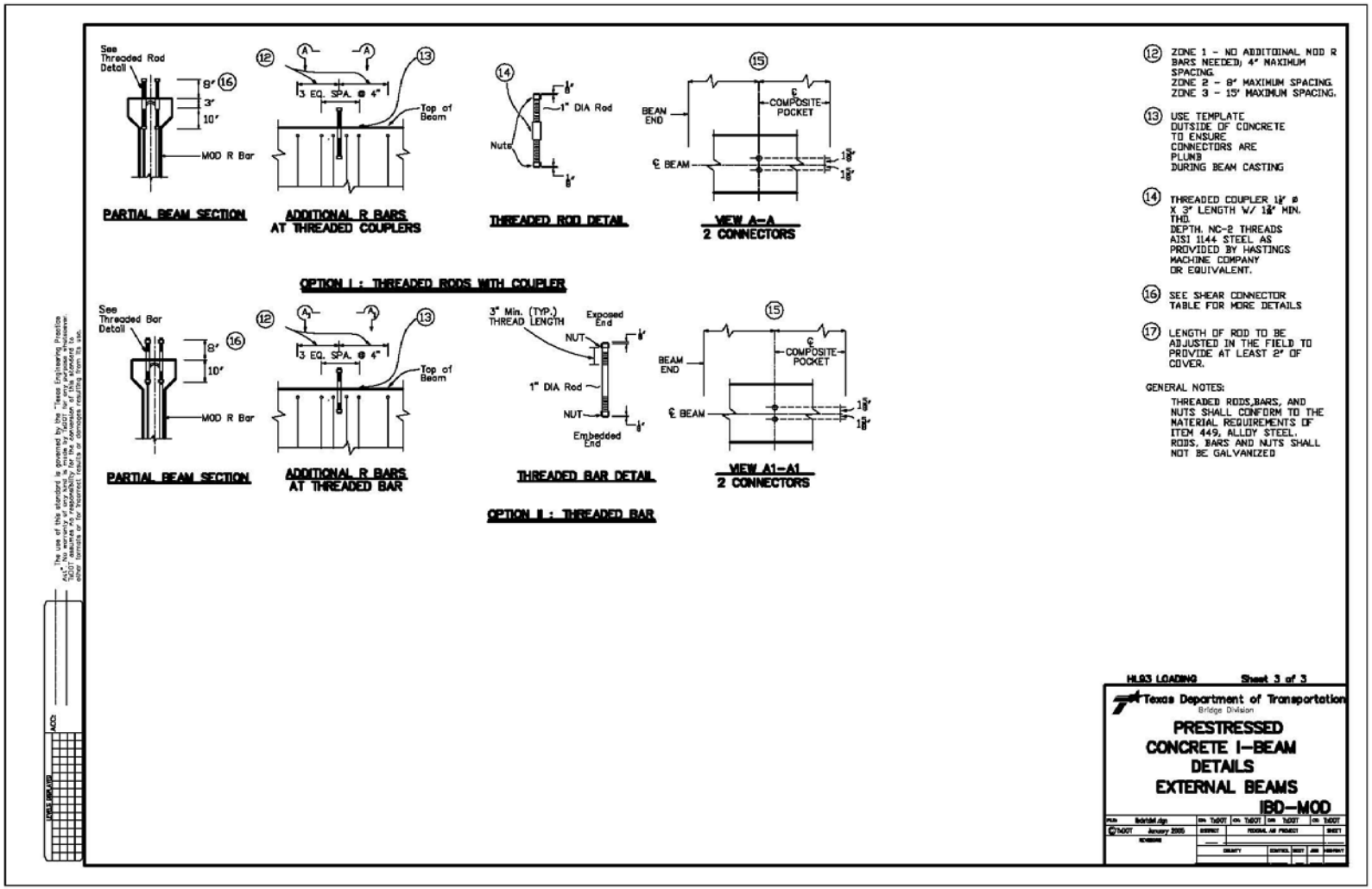
See Threaded Rod Detail
8"
3"
10"
MOD R Bar
PARTIAL BEAM SECTION
3 EQ. SPA. @ 4"
Top of Beam
ADDITIONAL R BARS AT THREADED COUPLERS
1" DIA Rod
Nuts
THREADED ROD DETAIL
BEAM END
℄ COMPOSITE POCKET
℄ BEAM
VIEW A-A
2 CONNECTORS
OPTION I : THREADED RODS WITH COUPLER
See Threaded Bar Detail
PARTIAL BEAM SECTION
ADDITIONAL R BARS AT THREADED BAR
3" Min. (TYP.) THREAD LENGTH
Exposed End
NUT
1" DIA Rod
Embedded End
THREADED BAR DETAIL
VIEW A1-A1
2 CONNECTORS
OPTION II : THREADED BAR
(12) ZONE 1 - NO ADDITIONAL MOD R BARS NEEDED, 4" MAXIMUM SPACING.
ZONE 2 - 8" MAXIMUM SPACING.
ZONE 3 - 15" MAXIMUM SPACING.
(13) USE TEMPLATE OUTSIDE OF CONCRETE TO ENSURE CONNECTORS ARE PLUMB DURING BEAM CASTING
(14) THREADED COUPLER 1⅛" ø X 3" LENGTH W/ 1⅛" MIN. THD. DEPTH, NC-2 THREADS AISI 1144 STEEL AS PROVIDED BY HASTINGS MACHINE COMPANY OR EQUIVALENT.
(16) SEE SHEAR CONNECTOR TABLE FOR MORE DETAILS
(17) LENGTH OF ROD TO BE ADJUSTED IN THE FIELD TO PROVIDE AT LEAST 2" OF COVER.
GENERAL NOTES:
THREADED RODS,BARS, AND NUTS SHALL CONFORM TO THE MATERIAL REQUIREMENTS OF ITEM 449, ALLOY STEEL. RODS, BARS AND NUTS SHALL NOT BE GALVANIZED
The use of this standard is governed by the "Texas Engineering Practice Act". No liability of any kind is assumed by the Texas Department of Transportation for any damages resulting from its use.
HL93 LOADING
Sheet 3 of 3
Texas Department of Transportation
Bridge Division
PRESTRESSED CONCRETE I-BEAM DETAILS EXTERNAL BEAMS
IBD-MOD
bdridet.dgn
©TxDOT January 2005

Construction

Product Data Sheet
Edition 6.2003
Identification no. 525-501
SikaGrout 212

SikaGrout® 212

High performance, cementitious grout

Description	SikaGrout 212 is a non-shrink, cementitious grout with a unique 2-stage shrinkage compensating mechanism. It is non-metallic and contains no chloride. With a special blend of shrinkage-reducing and plasticizing/water-reducing agents, SikaGrout 212 compensates for shrinkage in both the plastic and hardened states. A structural grout, SikaGrout 212 provides the advantage of multiple fluidity with a single component. SikaGrout 212 meets Corps of Engineers' Specification CRD C-621 and ASTM C-1107 (Grade C).
Where to Use	▪ Use for structural grouting of column base plates, machine base plates, anchor rods, bearing plates, etc. ▪ Use on grade, above and below grade, indoors and out. ▪ Multiple fluidity allows ease of placement: ram in place as a dry pack, trowel-apply as a medium flow, pour or pump as high flow.
Advantages	▪ Easy to use...just add water. ▪ Multiple fluidity with one material. ▪ Non-metallic, will not stain or rust. ▪ Low bleed. ▪ Low heat build-up. ▪ Excellent for pumping: Does not segregate...even at high flow. No build-up on equipment hopper. ▪ Non-corrosive, does not contain chlorides. ▪ Superior freeze/thaw resistance. ▪ Resistant to oil and water. ▪ Meets CRD C-621. ▪ Meets ASTM C-1107 (Grade C). ▪ Shows positive expansion when tested in accordance with ASTM C-827. ▪ SikaGrout 212 is USDA-approved.
Coverage	Approximately 0.44 cu. ft./bag at high flow.
Packaging	6 lb. pail, 6/case, 36/pallet; 50-lb. multi-wall bags; 36 bags/pallet.

Typical Data *(Material and curing conditions @ 73°F (23°C) and 50% R.H.)*

Shelf Life	One year in original, unopened bags.			
Storage Conditions	Store dry at 40°-95°F (4°-35°C). **Condition material to 65°-75°F before using.**			
Color	Concrete gray			
Flow Conditions		**Plastic[1]**	**Flowable[1]**	**Fluid[2]**
Typical Water Requirements:		6 pt.+	6.5 pt.	8.5 pt.
Set Time (ASTM C-266):	**Initial**	3.5-4.5 hr.	4.0-5.0 hr.	4.5-6.5 hr.
	Final	4.5-5.5 hr.	5.5-6.5 hr.	6.0-8.0 hr.
Tensile Splitting Strength, psi (ASTM C-496)				
28 day		600 (4.1 MPa)	575 (3.9 MPa)	500 (3.4 MPa)
Flexural Strength, psi (ASTM C-293)				
28 day		1,400 (9.6 MPa)	1,200 (8.2 MPa)	1,000 (6.8 MPa)
Bond Strength, psi (ASTM C-882 modified): Hardened concrete to plastic grout				
28 day		2,000 (13.7 MPa)	1,900(13.1 MPa)	1,900 (13.1 MPa)
Expansion % (CRD C-621)	**28 day**	+0.021%	+0.056%	+0.027%
Compressive Strength, psi (CRD C-621)				
1 day		4,500 (31.0 MPa)	3,500 (24.1 MPa)	2,700 (18.6 MPa)
7 day		6,100 (42.0 MPa)	5,700 (39.3 MPa)	5,500 (37.9 MPa)
28 day		7,500 (51.7 MPa)	6,200 (42.7 MPa)	5,800 (40.0 MPa)

[1]CRD C-227: 100-124% (plastic), 124-145% (flowable)
[2]CRD C-611: 10-30 sec efflux time.

Construction

How to Use

Surface Preparation	Remove all dirt, oil, grease, and other bond-inhibiting materials by mechanical means. Anchor bolts to be grouted must be de-greased with suitable solvent. Concrete must be sound and roughened to promote mechanical adhesion. Prior to pouring, surface should be brought to a saturated surface-dry condition.
Forming	For pourable grout, construct forms to retain grout without leakage. Forms should be lined or coated with bond-breaker for easy removal. Forms should be sufficiently high to accommodate head of grout. Where grout-tight form is difficult to achieve, use SikaGrout 212 in dry pack consistency.
Mixing	Mix manually or mechanically. Mechanically mix with low-speed drill (400-600 rpm) and Sika mixing paddle or in appropriately sized mortar mixer. **Product Extension:** For deeper applications, SikaGrout 212 (plastic and flowable consistencies only) may be extended with 25 lbs. of 3/8" pea gravel. The aggregate must be non-reactive, clean, well-graded, saturated surface dry, have low absorption and high density, and comply with ASTM C33 size number 8 per Table 2. Add the pea gravel after the water and SikaGrout 212.
Mixing Procedure	Make sure all forming, mixing, placing, and clean-up materials are on hand. Add appropriate quantity of clean water to achieve desired flow. Add bag of powder to mixing vessel. Mix to a uniform consistency, minimum of 2 minutes. Ambient and material temperature should be as close as possible to 70°F If higher, use cold water; if colder, use warm water.
Application	Within 15 minutes after mixing, place grout into forms in normal manner to avoid air entrapment. Vibrate, pump, or ram grout as necessary to achieve flow or compaction. SikaGrout 212 must be confined in either the horizontal or vertical direction leaving minimum exposed surface. After grout has achieved final set, remove forms, trim or shape exposed grout shoulders to designed profile. SikaGrout 212 is an excellent grout for pumping, even at high flow. For pump recommendations, contact Technical Service. Wet cure for a minimum of 3 days or apply a curing compound which complies with ASTM C-309 on exposed surfaces.
Limitations	▪ Minimum ambient and substrate temperature 45°F and rising at time of application. ▪ Minimum application thickness: 1/2 in. ▪ Maximum application thickness (neat): 2 in. Deeper applications are possible, please contact Sika's technical services department. ▪ Do not use as a patching or overlay mortar or in unconfined areas. ▪ Material must be placed within 15 minutes of mixing. ▪ As with all cement based materials, avoid contact with aluminum to prevent adverse chemical reaction and possible product failure. Insulate potential areas of contact by coating aluminum bars, rails, posts etc. with an appropriate epoxy such as Sikadur Hi-Mod 32.

Caution

Irritant	Suspect carcinogen - contains portland cement and crystalline silica. Skin and eye irritant. Avoid breathing dust. Use only with adequate ventilation. May cause delayed lung injury (silicosis). IARC lists crystalline silica as having sufficient evidence of carcinogenicity in laboratory animals and limited evidence of carcinogenicity in humans. NTP also lists crystalline silica as a suspect carcinogen. Use of safety goggles and chemical resistant gloves is recommended. In case of high dust concentrations or exceedance of PELs, use an appropriate NIOSH approved respirator. Remove contaminated clothing.
First Aid	In case of skin contact, wash thoroughly with soap and water. For eye contact, flush immediately with plenty of water for at least 15 minutes; contact physician immediately. Wash clothing before re-use.
Clean Up	In case of spillage, ventilate area of spill, confine spill, vacuum or scoop into appropriate container. Dispose of in accordance with current applicable local, state and federal regulations. Uncured material can be removed with water. Cured material can only be removed mechanically.

KEEP CONTAINER TIGHTLY CLOSED — KEEP OUT OF REACH OF CHILDREN
NOT FOR INTERNAL CONSUMPTION — FOR INDUSTRIAL USE ONLY
CONSULT MATERIAL SAFETY DATA SHEET FOR MORE INFORMATION

Sika warrants this product for one year from date of installation to be free from manufacturing defects and to meet the technical properties on the current technical data sheet if used as directed within shelf life. User determines suitability of product for intended use and assumes all risks. Buyer's sole remedy shall be limited to the purchase price or replacement of product exclusive of labor or cost of labor.

NO OTHER WARRANTIES EXPRESS OR IMPLIED SHALL APPLY INCLUDING ANY WARRANTY OF MERCHANTABILITY OR FITNESS FOR A PARTICULAR PURPOSE. SIKA SHALL NOT BE LIABLE UNDER ANY LEGAL THEORY FOR SPECIAL OR CONSEQUENTIAL DAMAGES.

Visit our website at www.sikausa.com — **1-800-933-SIKA NATIONWIDE**

Regional Information and Sales Centers. For the location of your nearest Sika sales office, contact your regional center.

Sika Corporation
201 Polito Avenue
Lyndhurst, NJ 07071
Phone: 800-933-7452
Fax: 201-933-6225

Sika Canada Inc.
601 Delmar Avenue
Pointe Claire
Quebec H9R 4A9
Phone: 514-697-2610
Fax: 514-694-2792

Sika Mexicana S.A. de C.V.
Carretera Libre Celaya Km. 8.5
Corregidora, Queretaro
C.P. 76920 A.P. 136
Phone: 52 42 25 0122
Fax: 52 42 25 0537

QUALITY ISO 9001 9002 ACHIEVEMENT

Cement mill test report for cement used in the batching of the Sika tested

2580 Wald Road
New Braunfels, TX 78132
Telephone (210) 250-4100
FAX (210) 250-4044
Customer Service
Telephone (800) 492-9004
FAX (210) 250-4153

CEMENT MILL TEST REPORT

Cement Identified as: **Type I/II** **Date: 06/01/08**

Plant: Cemex Cement of Texas, LP
Location: New Braunfels, TX

Production Dates:
Beginning: May 1, 2008
Ending: May 31, 2008

STANDARD CHEMICAL REQUIREMENTS (ASTM C 114)	ASTM C 150 SPECIFICATIONS	TYPE I	TYPE II	TEST RESULTS
Silicon Dioxide (SiO_2), %		—	----	20.0
Aluminum Oxide (Al_2O_3), %	Maximum	—	6.0	4.5
Ferric Oxide (Fe_2O_3), %	Maximum	—	6.0	3.6
Calcium Oxide (CaO), %		—	----	63.5
Magnesium Oxide (MgO), %	Maximum	6.0	6.0	1.1
Sulfur Trioxide (SO_3), %	Maximum	3.0	3.0	2.7
Loss on Ignition (LOI), %	Maximum	3.0	3.0	2.7
Insoluble Residue, %	Maximum	0.75	0.75	0.28
Free Lime, %		—	----	2.0
Tricalcium Silicate (C3S), %		—	----	64
Tricalcium Aluminate (C3A), %	Maximum	—	8	6
Alkalies (Na_2O equivalent), %		—	----	0.61
PHYSICAL REQUIREMENTS				
(ASTM C 204) Blaine Fineness, m^2/kg	Minimum	280	280	391
(ASTM C 191) Time of Setting (Vicat)				
Initial Set, minutes	Minimum	45	45	120
(ASTM C 266) Time of Setting (Gillmore)				
Initial Set, minutes	Minimum	60	60	169
Final Set, minutes	Maximum	600	600	250
(ASTM C 185) Air Content, %	Maximum	12	12	8
(ASTM C 151) Autoclave Expansion, %	Maximum	0.80	0.80	0.02
(ASTM C 109) Compressive Strength, (psi)				
1 Day		—	----	2350
3 Day	Minimum	1740	1450	3970
7 Day	Minimum	2760	2470	4840
28 Day Previous		—	----	6350

WE HEREBY CERTIFY THAT THIS CEMENT COMPLIES WITH CURRENT ASTM C-150 SPECIFICATIONS.
THIS CEMENT CONTAINS PROCESSING ADDITIONS WHICH MEET THE REQUIREMENTS OF ASTM C-465.
COMPLIANCE DOCUMENTS FOR THESE PROCESSING ADDITIONS ARE AVAILABLE UPON REQUEST.
THE ABOVE DATA REPRESENTS THE AVERAGE OF REPRESENTATIVE SAMPLES FROM PRODUCTION.

By: _____
Quality Control Manager
CEMEX - Balcones Cement Plant